Assesment of Damages Caused by Alkali-Silica Reactions

Elgseter Bridge, Trondheim

Christine Elisabet Skogli

Department of Structural Engineering

Faculty of Engineering Science and Technology

NTNU- Norwegian University of Science and Technology

MASTER THESIS 2015

TITLE:
Assessment of Damages Caused by Alkali-Silica Reaction: Elgeseter Bridge, Trondheim Evaluering av skader grunnet alkali-silika reaksjoner i bjelker: Elgeseter bru i Trondheim.

BY:

Christine Elisabeth Rodriguez Skogli

SUMMARY:

Elgeseter Bridge was completed in 1951, and it is a main part of the infrastructure between the south side of Trondheim to the city centre. Early inspections showed signs of elongation of the bridge, but the cause for the elongation and expansion was not recognized at that point. The Alkali-Silica Reaction (ASR) that causes the expansion was not known at the time of construction. This thesis will present the theory of how the structure is affected. The structure is analysed both statically and theoretically, due to the expanding chemical reaction.

The expansive reaction is due to a reaction between the aggregate and the cement in the concrete mix- It causes stresses to occur in places the structure was not designed for. The thesis will consider mainly the two large vertical cracks, which are explained in the report from field inspections in 2012 by Aas-Jakobsen. Eurocodes and Handbooks from the Norwegian Public Road Administration (SVV) are the basis during calculation of the loads and capacities.

The bridge is 200 metres long, and is supported by eight column rows that are anchored in the foundations under the water surface of the river. Modelling of the bridge is done in the frame modelling software FAP, and the 3D modelling program Abaqus.

Modelling in Abaqus has shown that in order to create stresses in the lower edge of the inner beams, the expansion is occurring in both the bridge deck and outer beams. Calculations show that the spans affected by the large vertical cracks have formed plastic hinges in the weakest cross-section of the span. Further investigations must be performed to fully understand how much this affects the structure.

RESPONSIBLE TEACHER: Terje Kanstad

SUPERVISOR(S):   Terje Kanstad, NTNU. Hans Stemland, Sintef. Eva Rodum og Håvard Johansen, Statens vegvesen, Vegdirekroratet.

CARRIED OUT AT: Department of Structural Engineering

Preface

This thesis is carried out in the spring of 2015 at the Department of Structural Engineering, and is part of a 2-year master's degree at the Norwegian University of Science and Technology (NTNU). The task is written in the guidance of Terje Kanstad, as the internal supervisor at NTNU, and Hans Stemland at SINTEF. External suprevisors Eva Rodum and Håvard Johansen, from the Directorate of Public Roads at the NPRA, have been providing external guidance.

By working with this thesis, I have gained a great appreciation for the engineering of bridges, modelling in the framework programme FAP-2D and the three-dimensional analysis software Abaqus. I have gained knowledge about the general resistance and the specific effects ASR has on concrete structures, as well as some of its implications for the load carrying capacity. Literature used in the task is mainly taken from textbooks, reports, national and international standards, as well as received information from internal and external supervisors.

I would like to thank Professor Terje Kanstad at NTNU and Hans Stemland at Sintef for good guidance and discussions underway. Moreover, I would also like to thank Håvard Johansen and Eva Rodum, Public Roads, for professional information and guidance. Finally, I would also like to thank all fellow students at the Institute of Structural Engineering for professional and colorful discussions.

Trondheim, 10. juni 2015

Christine Elisabeth Rodriguez Skogli

Abstract

This thesis studies the condition and load carrying capacity for Elgeseter Bridge in Trondheim, Norway. Elgeseter Bridge is the main connection between the south side of Trondheim to the city-centre. The bridge is affected by a chemical reaction between the aggregates and the cement in the concrete mix. The chemical reaction that is occurring is the Alkali-Silica Reaction (ASR), where the alkali in the aggregate reacts with the silica in the cement This reaction causes the concrete to expand. The elongation of the bridge has been measured by measuring the dilation of the expansion joint on the northern end of the bridge. The expansion joint has been replaced several times over the years due to the elongation.

Elgeseter Bridge is two hundred metres long, with a total of nine spans. The longest span is 22.5 metres long. The bridge deck is cast-in-place with four beams carrying the bridge deck in longitudinal direction. The beams are then supported on eight column rows and the end supports. The beams are cast together with the reinforcement between the beams and columns to ensure continuous supports for the calculations.

The chemical reaction creates a gel that expands in accordance with the reactivity of the concrete mix. The global and local variations of the ASR is only possible to confirm with petrographic analyses of core samples. The reaction requires a large amount of moisture, and the parts with higher Relative Humidity (RH) are assumed to be more affected than parts with lower RH.

Elongation is assumed to cause extra stress on the construction. The last column rows are most affected by the elongation, and the three last column rows have been cut in order to regain verticality. Columns are the constructional parts more exposed to higher moisture level, but have been refurbished and are monitored by the Norwegian Public Road Administration. However, large vertical cracks has been observed in the inner beams, which are not explained by the elongation itself. Several relatively small cracks are also observed in the beams, which are explained by the expansion and curvature due to the ASR. This thesis will mainly focus on the two large vertical cracks in the two inner beams, how they have originated and their effect on the structure as such.

The 3D modelling program Abaqus is used to show how the constructional parts behave when the parts assumed with a higher RH expands. The structure is also modelled in a frame modelling program, FAP-2D, in order to see the statically effects on the structure due to self-

weight and relevant traffic loads. The structural effects by the ASR will also be modelled in the frame model.

The results from Abaqus show that when the bridge deck and the two outer beams expand together, the inner beams have an increase of stresses in the area that starts approximately from the edge between the bridge deck and the beams, and ends at the lower edge of the beam. Calculation show that the large vertical cracks are caused by the weakest cross-sectional area for bending moments reaches its yield-limit. When the yield-limit is reached, the cross-section can no longer carry bending moments. The redistribution of the forces can be critical for the bending moment over the supports. The strengthening of the cracks will not affect the static change when the yield-limit is reached.

Sammendrag

Abstract på norsk.

Denne masteroppgaven studerer tilstanden og bæreevnen for Elgeseter bru i Trondheim. Elgeseter bru er den viktigste forbindelsen mellom sørsiden av Trondheim og inn til sentrum. Konstruksjonen er påvirket av en kjemisk reaksjon mellom tilslaget og sementen i betongblandingen. Reaksjonen som finner sted er alkali-silika reaksjon (ASR), hvor alkalien i tilslaget reagerer med silika i sementmiksen. Denne reaksjonen vil føre til en lokal og global ekspansjon av betongn. Forlengelsen av brua har blitt målt ved flere anledninger, ved å måle utvidelsen av ekspansjonsfugen på den nordlige enden. Ekspansjonsfugen har i seg selv blitt erstattet flere ganger i løpet av årene på grunn av ekspansjonen.

Elgeseter bru er totalt tohundre meter lang, med i alt ni spenn. Den lengste spennet er 22,5 meter lang. Brudekket er plasstøpt med fire bjelker som bærer brudekket i lengderetningen. Bjelkene er så understøttet av åtte søylerader og endestøttene. Bjelkene er støpt sammen søylene, og armeringen mellom bjelker og søyler å sikre kontinuerlig overføring av krefter

Den kjemiske reaksjonen vil danne en gel som utvider seg i henhold til reaktiviteten av betongblandingen. Den globale og lokale forekomsten av ASR er kun mulig å bekrefte ved hjelp av petrografiske analyser av kjerneprøver. Reaksjonen krever en stor mengde fuktighet, hvor de deler av brua med høyere Relativ Fuktighet (RF) er antatt å være mer utsatt enn delene med lavere RF.

Forlengelsen av broen er antatt å føre til ekstra belastning på konstruksjonen. De siste søyleradene er mest berørt av forlengelsen, og de tre siste søyleradene har blitt kuttet i toppen, for å gjenopprette vertikaliteten. Søylene er de konstruksjonsdelene som er utsatt for et høyere fuktighetsnivå, men har blitt renovert og er kontinuerlig etterfulgt av Statens vegvesen. Imidlertid har det blitt observert store vertikale sprekker i de ti midterste bjelkene, som ikke kan forklares av selve ekspansjonen. Flere relativt små sprekker er også observert i bjelkene, som er forklart av utvidelsen og kurvaturen som oppstår på grunn av ASR. Denne oppgaven vil i hovedsak fokusere på de to store vertikale sprekkene i de to midterste bjelkene, hvor de har sin opprinnelse og deres effekt på strukturen som sådan.

3D-modelleringsprogrammet Abaqus brukes til å vise hvordan konstruksjonsdelene oppfører seg når delene som har en antatt høyere relativ fuktighet utvider seg. Konstruksjonen er også modellert i et to-dimensjonalt modelleringsprogram, FAP-2D, for å se den statiske effekten på

konstruksjonen på grunn av egenvekt og relevante traffikklaster. Den strukturelle effekten fra ASR vil også bli modellert i ramme-modellen i FAP-2D.

Resultatene fra Abaqus viser at når brobanen og de to ytterste bjelkene ekspanderer sammen, så vil de midterste bjelkene har en økning av spenning i området som starte fra overgangen mellom steget og flensen og som ender i underkant av bjelken. Beregninger viser at de store vertikale sprekkene oppstår i det tverrsnittet med lavest bøyemomentkapasitet. Når flytegrensen er nådd i tverrsnittet, kan det ikke lenger bære flere bøyemomenter. Omfordelingen av de kreftene som påføres kan være kritisk for bøyemomentet over støttene. Reparasjon og evt forsterkning av sprekkene vil ikke påvirke den statiske endringen som har skjedd når flytegrensen er nådd.

Table of Contents:

List of figures

List of tables

Abbreviations

ASR	Alkali-Silica Reaction
DEF	Delayed Ettringite Formation
EC	Eurocode
EU	European Union
EFTA	European Free Trade Association
LC	Load Combination
LM	Load Model
NA	National Annex
NCAL	Norwegian Concrete and Aggregate Laboratory Ltd.
NGU	Norwegian Geological Survey
NPRA	Norwegian Public Road Administration
NS	Norwegian Standard
NTNU	Norwegian University of Science and Technology
FAP	Frame Analysis Program
RH	Relative Humidity
SINTEF	The Foundation for Scientific and Industrial Research
SLS	Service Limit State
ULS	Ultimate Limit State

1 Introduction

1.1 Case study of Elgeseter Bridge

This thesis considers the case study of the damaged caused by the expanding constructional
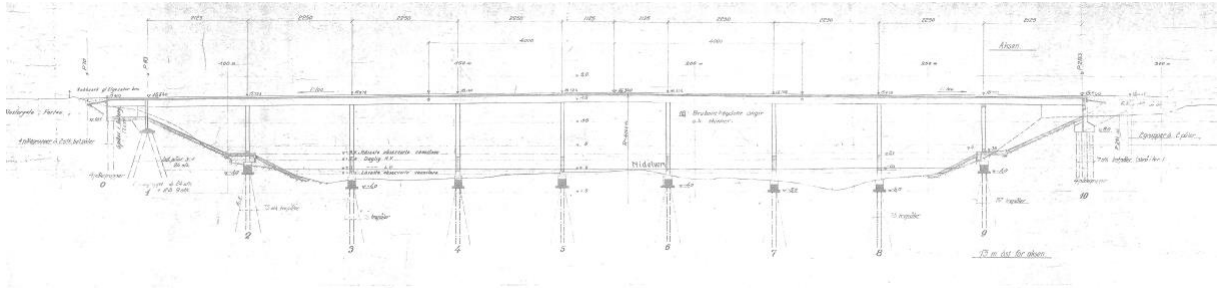
Figure 1.1: Elgeseter Bridge, seen from the side, according to drawings from the NPRA.

elements of Elgeseter Bridge. The expansion is mainly caused by a chemical reaction between the cement and aggregate in the concrete mix. Cracks, spalling and other damages has been seen on the bridge for several years. Inspections and reports have been made in order to grasp the cause of the cracks. The analysis in a 3D modelling program should grant some hints on how the expansion of the different constructional elements affects the behaviour of the entire structure.

1.2 Material properties

The Portland concrete mix was made specifically for the Elgeseter Bridge by the concrete factory. In comparison with most concrete mixes from that time, the mix for Elgeseter did not contain any marine aggregates. This was to prevent and reduce the risk for corrosion in the reinforcement bars.

The columns and the bridge deck were made from two separate mixes. The concrete mix for the beam measured slightly stronger compressive strength than for the bridge deck. The compressive strength considered for the concrete in the bridge deck is 31.9 N/mm². This will be more thoroughly described in *Chapter 4.5*.

The inspections of Elgeseter Bridge showed signs of expanding reactions in the concrete as early as the 1980s. The international science and research of the Alkali reactions in the concrete did not receive proper acceptance from the Norwegian associations that early. Early inspections created a theory assuming a serious carbonization process, which would cause serious damage to the bridge. Further inspections, and increasing information about the alkaline reactions, concluded that there was a serious expansion of the bridge in longitudinal

direction. The main suspect of the troubles now shifted to the alkaline reactions with the expansive gel, which could create such an expansion.

1.3 Reactive Aggregates

Alkali-Aggregate Reactions, AAR in short, are chemical reactions between the aggregate and the alkaline pore water in the cement paste. The reaction requires sufficient moisture to develop and creates a gel. The created gel can suck water and swell, which leads to an increase in volume. The characteristic crack pattern for this swelling is map cracking on the concrete surface. This reaction may take several years to form and develop, and may not show any signs of the reaction for over 10 years. The "RAW triangle" describes the conditions needed for AAR to develop.
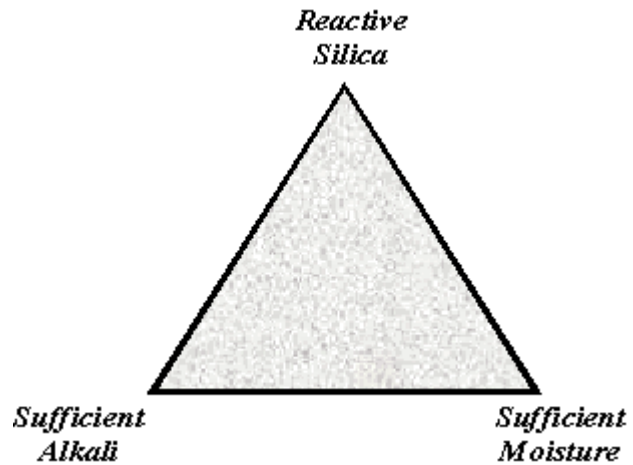
Figure 1.2: The RAW triangle describing the conditions for Alkali-Aggregate Reaction.

First in the late 80s, it was publicly accepted that some of the Norwegian aggregates were alkali-reactive, and that Norwegian concrete structures could possibly be damaged by it.

In the aggregate, all rocks that contain quartz minerals are potentially alkali-reactive rocks. Most Norwegian rocks do contain some quartz minerals, but not all has shown to be alkali-reactive. The reactivity depends on particle size, degree of deformation and the microstructure of the rock types. A research project in Norway concluded that the rock types containing microcrystalline quartz are those that mainly cause problems. [1]

There has been several research projects, including one project that listed rock types defined as "risk rock types", evaluated by SINTEF in cooperation with NGU. Another project's objective was to determine better test methods to ascertain the alkali-reactivity for aggregates.

According to the research project, following methods were concluded as most suitable, for Norwegian conditions[1]:

1) Petrographic analysis with thin section:
   Any aggregate is firstly tested by this method. Measurements by counting aggregates in thin sections, in order to evaluate the alkali-reactivity.

2

2) The mortar bar method:

Measurements of the expansion of mortar bars.

3) Concrete prism method:

Measurements of the expansion of concrete prisms.

Petrographic analysis are best when used to compare samples of the same construction. This analysis of core samples is one of the test methods quite frequently used for the Elgeseter Bridge.

1.3 Fundamental aspects in designing Elgeseter Bridge

As early as in the planning stage, there were decisions to maintain stable conditions for the bridge. The requirements for the aggregate, in order to minimize the corrosion in the reinforcement bars is one example of the steps taken for the endurance and longer life span of the bridge. At the time of design, as the local public transportation was dependent on the tramway, tracks for the tramway were placed in the centre of the bridge. When these tracks were removed, the width for traffic-lanes were not decreased although the footpaths were widened.

When it became clear that the bridge was being damaged, the municipality, who owned the bridge at that point, ordered inspections and reports of work needed. In later years, the NPRA has had the responsibility for maintaining and repairing the bridge. Earlier and current conservation includes core test taken regularly, as well as inspections and research projects.

Considering that this crossing is one of the city's most important bridges, the amount of total traffic weight has most likely increased from the building year, even without the added weight of the tramway. The design of the bridge includes slender beams with a rather slender bridge deck, which has proved durable with the increased traffic loads. The engineering of the bridge is impressive, given the resilient design, which would have been even more durable had the ASR not occurred.

2 Eurocodes and regulations

Rules and regulations for designing a bridge are determined internationally by the Eurocode regulations. Nationally by the Eurocodes National Annex and regulations from the relevant national authorities, NPRA.

2.1 Eurocodes

In 1989, the Commission of the European Community decided, in collaboration with the member states of the EU and EFTA, that the European Committee for Standardization (CEN) should be responsible for preparation and publication of Eurocodes, in the attempt to provide the Eurocodes a future status of European Standards. The European Standards are to be supplemented by the National Annexes, NA, and shall be used as national standards. The NA should contain national determined parameters, which enables the European Standards the possibilities of national diversity. Conflicting national standards should be withdrawn after a certain time after the publication of the correlating Eurocode.

Figure 2.1: Front page of NS-EN 1990. Basis of structural design.

Eurocodes are numbered in the values 0-9, when referred to as EC. When referred to as the national norm, which for Norway would be NS (Norwegian Standard), it is named "NS-EN 199X", where the X denotes the numbering as previously mentioned. The second Eurocode, the Eurocode for concrete, then becomes respectively *EC2* or *NS-EN 1992*. The Eurocodes are named in the general field of application, and are supplemented in parts by several specific fields. Which implies e.g. for concrete that the EC2 defines the design of concrete structures, the EC2-1-1 is for designing concrete structures in general, while EC2-2 is for concrete bridges.

Relevant Eurocodes for this thesis includes the EC0, EC1 and the EC2, respectively by NS-EN 1990-1, NS-EN 1991-1-1, NS-EN 1991-2 and NS-EN 1992-1-1:

- NS-EN 1990: Basis of structural design
- NS-EN 1991-1-1: Action on structures, Part 1-1: General Actions. Densities, self-weight, imposed loads for buildings.
- NS-EN 1991-2: Action on structures, Part 2: Traffic loads on bridges.
- NS-EN 1992-1-1: Design of concrete structures, Part 1-1: General rules and rules for buildings.

2.2 Handbooks

The Norwegian Public Roads Administration provides Handbooks, in cooperation with the Directorate for Public Roads. There are two levels of handbooks, where Level 1 contains norms and manuals and Level 2 contains guidelines. The Directorate for Public Roads are responsible for preparing and updating the norms and manuals, but the superior authority must approve the norms and manuals.

The most important Handbooks from the NPRA (Norwegian Public Roads Administration) are the norms and manuals, since these are used as regulations. Norms are regulations for every public road or street, while manuals are regulations for the Norwegian highways and for consultants and entrepreneurs working for the NPRA. The guidelines are assisting aids to the norms and regulations, meant to elaborate on the subjects written in the norms and regulations.

Figure 2.2: Cover page of handbook N400

2.2.1 Bridge designing

Handbook N400, Norm for Bridge Designing, is a norm for regulating the structural designing, control and authorisation of bridges, ferry docks and other constructions carrying load in or around public roads. The norm contains additional regulations where the standards are insufficient or unspecific. These regulations are assumed relevant throughout the whole design, construction period and service life, as well as during any repairs or maintenance

work that will affect the constructions load carrying ability. The norm also gives requirements for safety in temporary bridges, formwork constructions, scaffoldings and other aiding structures.

In June 2014, the NPRA's handbooks received revisited, numbers for a better structure over the different topics. The 10 main topics have their own 3-digit series, which begins with the topic-number. In this case, the handbook *Bridge Designing* was renumbered from 185 to N400, under the topic bridges and ferry docks. The former handbook 185's original edition is dated back to 2009. With the Eurocodes and modifications from the NPRA, a new version has been sent to a formal hearing, currently not approved as the formal edition. The handbook used for this thesis will be N400, the updated and EC-compatible version dated 2015. [2]

2.2.2 Classification of bridges

Bridges are classified to regulate the allowed, and assumed, type and intensity of traffic loads. For existing bridges, the classification determines the maximum allowed load from traffic. The classification is determined by drawings, documented capacities and the condition of the bridge. We find the regulations for this classification in handbook R412 *Classification of Bridges.* [3]

Formerly, there was a handbook containing supplements to the classification of bridges, that contains regulations and norms for public roads and bridges from 1912-1958. Until the year of 1973, the correct way of dimensioning and controlling loads was to look at the actual occurring stresses in a given part of the construction, and comparing these to a given value for allowable stress. These allowable stresses has changed over the years. The material utilization has also increased in modern times. These factors, described by the old handbook, are now implemented in handbooks N400 and R412.

Handbook R412 contains the given loads for each classification that can be loaded on
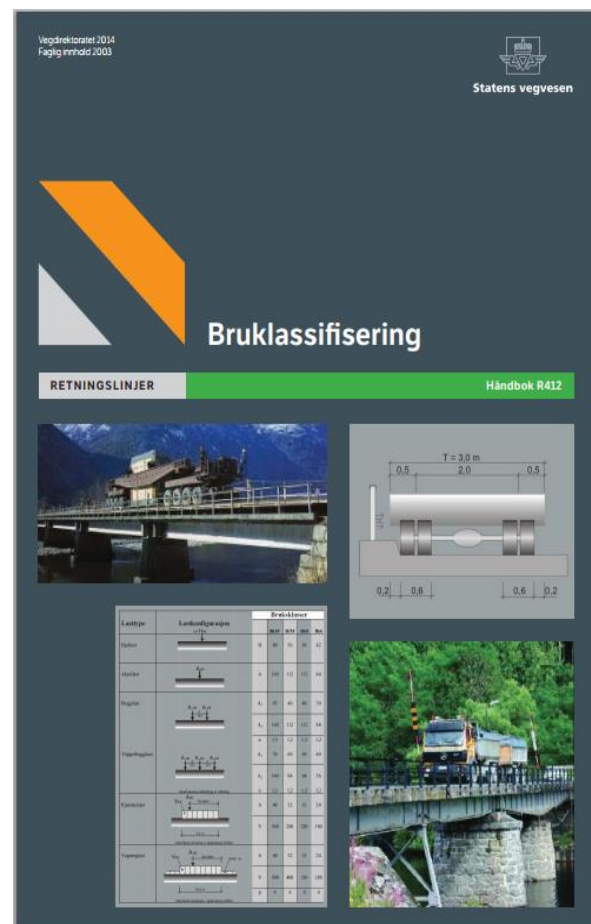
Figure 2.3: Cover page of handbook R412.

public roads, and denotes it as imposed load. This imposed load is then classified by either total load or axle load. The classification is often denoted "Bk" and followed by a number, where the number represents the highest allowed axle load, e.g. Bk10 for the highest axle load of 160kN. The handbook also contains an appendix providing material strength as well as safety factors for loads and materials.

3 ASR – Alkali-Silica Reaction

There are three forms of alkali-aggregate reactions, where ASR (Alkali-Silica Reaction) is the predominant form. The other two forms are alkali-carbonate reaction and alkali-silicate reaction, which will not be addressed in this thesis. The chemical reaction in ASRs occur when alkalis are combined with certain types of silica when moisture is present. The reaction produces a gel (alkali-silica gel) that can absorb water and expand. This expansion may cause cracking and disruption of the concrete.

3.1 Requirements for the reaction

For the expansion of the alkali-silica gel, due to ASR, to be damaging, we need three contributions:

- A sufficiently strong alkaline pore solution
- A portion of reactive silica in the aggregate – lying within the sensitive rate
- A sufficient moist state in the concrete

When ASR occurs, it may interact with any other form of structural or non-structural cracking for exposed areas, such as corrosion or frost. The high cement content of a concrete pore solution tends to associate with ASR, therefore cracking from early thermal effect and shrinkage often interacts with the ASR.

The vulnerability of a structure depends on the structural type, quality of detailing and the environment. For new structures, the considerations for ASR are useful to take into account for each of these conditions.

3.1.1 Alkali

Alkalis, which are usually predominantly from the cement, creates an alkaline environment in the concrete, useful to protect the reinforcement steel from corrosion. The alkalis in the free water in the pores of the concrete maintains the high pH. However, the alkali amount in concrete is also dependent on the total amount of cementitious material in the mix. Alkali in the mix may originate from cement, "fly ash", admixtures, water, sodium chloride in aggregates and other soluble sodium and potassium in aggregates.

Cement mixtures with high amount of alkalis do not provide a significantly better resistance to corrosion than those with low amount. This is because the reference to high or low relates to the Na_2O equivalent, whereas the reaction dominating the corrosion resistance is dependent on the $Ca(OH)_2$ hydration product. Moisture movement in the concrete may cause the

concentration of alkalis so that the reaction occurs in parts of the concrete pours that originally contained low amount of alkalis. In addition, the alkalis can leach out of the concrete when immersed in water.

3.1.2 Silica

In order for there to be a significant reaction between the alkalis in the concrete and the silica, the silica must have a distorted structure and/or fine particle size. Particle size, type and proportion of silica determines the rate and severity of the reaction, which increases when the proportion of reactive silica in the total amount of aggregate in the mix increases up to the 'pessimum'.

The pessimum is the proportion of reactive aggregate that will give the most adverse effect. When the proportion increases above the pessimum, the concentration of the hydroxide in solution is insufficient to maintain the reaction, thus the expansion decreases. A proportion on either side of the pessimum within the sensitive range of silica, which damage and creates expansion, differ for different types of silica.

The gel produced by such a reaction may vary its consistency from that of a heavy oil to polyethylene. With its characteristics varying with the chemical composition, temperature, moisture content and pressure. In many cases, the gel will only be visible in a petrographic examination of a core test.

3.1.3 Water

A sufficient supply of water is necessary for a damaging reaction, even though the reaction may occur and produce gel even in dry conditions. Best conditions for ASR are in environments with a RH (relative humidity) of 85% or more. Water providing sufficient high RH may not be only from external sources, such as weather or condensation, but also it can occur in sealed concrete parts or residual mix water in interior mass. For concrete parts kept consistently under a RH of 75%, the expansion is insignificant. Reducing the exposure to water may constraint or halt the reaction and expansion. However, the expansion will redevelop at a rapid pace when the concrete has retained the necessary RH. As mentioned before, the concrete parts immersed in water may leach alkalis to the surroundings. This will reduce expansion potential.

3.2 Effects on concrete structures

The chemical reaction creating the expanding alkali-silica gel developing in several locations in the concrete will create an overall expansion of the concrete. When the physical reaction of expansion is significant enough, the local effects are cracking, loss of strength and threats to serviceability. The expansions intensity may vary depending on distribution in the body of concrete, such as different types and quantity of reactive materials, and depending in the time scale of development. In addition, the expansion is dependent on water supply, where availability of water varies seasonally and may be prevented by effective drainage.

Even though the reaction causes an overall expansion of the concrete, the

Figure 3.2: Some structural effects and damages on Elgeseter Bridge.

expansion is not uniform throughout the entire concrete volume. Cracks may occur in between of expanding and non-expanding parts. Cracking of the outer layers can occur when there is differential expansion between core and surface. Micro-cracking can occur where there are a few or a cluster of reactive particles. The cracking will not be uniformly distributed either, since the cracking will be influenced by restraints and effects around the edges of the concrete. Where there are no restraints, the micro-cracking will be oriented randomly. Larger expansion in the interior of the concrete, plus the randomness of the expansion, results in tensile strain at the surface layer. Thus, macro-cracking may occur. Macro-cracks in unrestrained concrete occurs as intersecting and bifurcating cracks, referred to as map cracking. This pattern may also occur where there is differential expansion, shrinkage or where there are surfaces subjected to rapid cooling. The direction of restraints influences the cracks, since cracks are found to be parallel to the restraints.

To summarize the most usual physical effects the expansion brings, we have internal microcracking, surface macro-cracking, overall dimensional changes, induced tensile stresses in reinforcement and compressive stresses in concrete, induced bond stresses between steel and concrete, and differential movements between separate pours of concrete expanding at different rates.

Restraints against the expansion due to ASR are mainly surrounding non-reactive concrete, applied stress or reinforcement in either direction. Since the expansion is inhibited by the restraint in the direction of the restraint, the dominating cracks will form in the direction parallel to the restraint. Restraining ASR will delay the start and slow down the rate of expansion, and the restraint causes effects on the net expansion and the induced stresses. Net expansion in the restrained case is reduced in comparison to the unrestrained case. The effect on reinforcement is tension, while the concrete experiences compression parallel to the reinforcement. The more reinforcement in a section, the less induced strain in the reinforcement due to the expansion. Thus, the strain in shear links are more likely to be higher than the strain in main, longitudinal, reinforcement.

3.3 ASR in combination

ASR damage can occur independently or simultaneously with other types of deterioration processes. ASR can also create states that increases the vulnerability for other deterioration processes to initiate. For instance, when map cracking or spalling occurs, the risk of penetration of water and other fluids is increased. Freeze-thaw cycles are easily combined with ASR, since it gives expansion when low temperatures, and moisture when the temperature rises. Several deterioration processes, which can be seen in combination with ASR on the bridge, are briefly described in *Chapter 3.3.1-3*.

3.3.1 ASR combined with corrosion of reinforcement

The columns of Elgeseter Bridge are quite heavily infected by ASR, and several columns have map cracking. The cracking introduces oxygen and moisture deeper into the concrete, where oxidation process and chloride ions initiate the corrosion of embedded reinforcement.

Figure 3.3: Refurbished column still shows sign of earlier combination of ASR and corrosion of reinforcement in the excess rust at the bottom.

3.3.2 ASR combined with freeze-thaw cycles

Sufficient air treatment of concrete will increase the resistance to freeze-thaw cycles, as explained in *Chapter 4.6*. However, ASR can reduce the resistance even when the concrete is air-entrained. ASR induce cracks in which the freezing water will propagate and widen the cracks. Horizontal surfaces, e.g. the bridge carriageway, are more vulnerable to this combination due to water laying on the surface.

3.3.3 ASR combined with delayed ettringite formation

Delayed ettringite formation (DEF) is also an expansive reaction in the concrete, due to the delayed formation of the ettringite mineral, which is a normal product of cement hydration. High temperatures in the early curing can prevent the creation of ettringite. The formation of ettringite is then delayed, but will occur at a later state as DEF. ASR reduces the pH in the pore solution, which can accelerate the DEF, thus rushing the release of sulphates. The sulphates that free to form ettringite increases the expansion and cracking already occurring due to ASR.

Figure 3.4: DEF and ASR occurring in Elgeseter Bridge.

3.4 Treatment of ASR

Treatments of Elgeseter Bridge are currently being made for both the bridge deck and columns. The current treatments are not a part of this thesis. However, the general methods of treating ASR is relevant, to fully understand the effects of ASR.

The columns have been treated with different types of compounds, during different research projects, to restrain or treat the chemical reaction. Some columns have been cut in the joint between column and bridge deck, in order to regain the verticality. Thus, the built up stress

from the bridge deck expanding is released. Columns have been treated and are currently under surveillance.

The construction can never be cured of ASR, but the chemical reaction that drives ASR can be either prohibited or restrained. When it comes to ASR, it is common to consider two categories of mitigation:

1. Treating or removing the symptoms of ASR
2. Treating or addressing the cause of ASR

When treating the symptoms of ASR, the effects will be only temporary unless the cause of ASR is treated simultaneously. Treating the symptoms of ASR can include crack filling, restraining or stress relieving actions. Crack filling can be for aesthetic purposes, but also works as a sealant for external moisture or chloride ions. Restraining the structure or structural elements is in order to prevent further expansion, or to strengthen or stabilize the structural element. Cutting joints or slot cutting relieves stress, where the elongation affects the structural elements either by creating curvature or by skewing.

Treating the cause of ASR is the most long-lasting solution, but can be time-consuming or difficult to implement on a standing construction. In order to make the chemical expanding reaction to stop, it is necessary to remove one of the driving factors of the reaction, i.e. alkali, silica or water. Chemical treatments or injections, such as e.g. lithium compounds, can alter the chemical balance in the concrete. In order to decrease the supply of water it is necessary to control the moisture levels. Sealants, cladding or improved drainage are required.

Elgeseter Bridge has been treated in both categories. The symptoms have been treated by cutting joints in order to relieve the stress. Due to the elongation of the bridge deck, the three last column rows have experienced extra loading due to the eccentricities. Therefore, their joints at the top of the columns have been cut. In addition, columns have been treated chemically, and restrained. The wear layer of the bridge deck has been altered at several occasions. Sealants and improved drainage have been integrated for the bridge deck, to hopefully reduce the relative humidity of the concrete.

4 Elgeseter Bridge

Elgeseter Bridge is a crossing of the local river *Nidelva* in Trondheim, connecting the south part of the city with the city-centre. The bridge is on the road E6, a part of the International E-road network. In 1982, the bridge was classified as a Class-A road with the load class *Bk10*.

4.1 Historical

The location of this bridge is the oldest know crossing for the river *Nidelva*. The original bridge was built to give the monks on the south side of the river an easier access to the church and the archbishop's palace. The first mentioning of this bridge is in connection with a historic battle between King Sverre Sigurdsson and Erling Skakke, in the year of 1179. This bridge was the only crossing of the river, until the year of 1685, when the city planner Johan Caspar de Cicignon designed a new crossing now referred to as *Gamle Bybro*. With the new crossing more adapted to the movements in the city centre, the historical *Elgeseter Bru* deteriorated. The next bridge to cross where Elgeseter Bru is now standing was originally a railway-bridge for a local railway route, built in the year of 1864.[4]

Figure 4.1: Sign at the southern abutment of Elgeseter Bridge.

The city council in Trondheim decided in 1949 that it was due for a new and larger bridge, and announced an architectural competition for the design. The build of the new bridge was in 1950, with the opening of it in 1951.

In 2004, the Norwegian Concrete association awarded the bridge for its slenderness, and it was decided preserved by the Directorate of Cultural Heritage in 2008.

The original bridge from 1951 had tracks for trams in the mid-lane, which was removed in 1985. The pedestrian lane was then widened, still having four lanes for traffic across the

bridge. Thus, the current bridge has in each direction 2 lanes for traffic, one bicycle lane and a wide pavement for pedestrians. The total width of the bridge is 23.5 metres, where the road width is 16.5 metres. Total length of the bridge is 200 meters, with eight rows of pillars crossing the river, each row containing four pillars.

The southern side of the bridge is structurally pinned while the northern side is a roller connection with an expansion joint. The slab is cast-in-place with four beams connected with each column-row in the longitudinal direction.

4.2 Structural Design

Elgeseter Bridge is a continuous, multi-spanned and simply supported bridge. *Figure 4.2* shows a simplified model of the bridge. From the simplified figure, we see the southern side of the bridge is pinned while the northern side is roller-supported with an expansion joint. Four longitudinal beams carry the bridge deck, and four columns in turn support the beams. There are eight column rows across the entire length, each row containing four columns, one column at each beam.
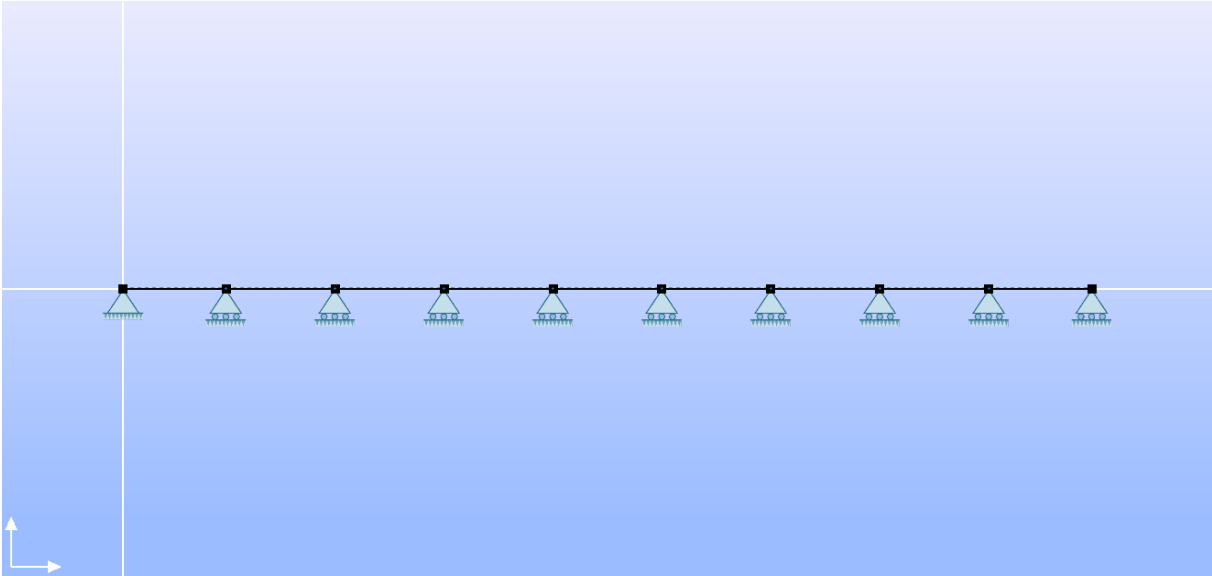
Figure 4.2: Simplified statistical system for Elgeseter Bridge.

Total length of the bridge structure is 200 metres, consisting of nine spans. The first and last span have a length of 21.25 metres, while the rest spans are equal to 22.50 metres each. Total width is 23.50 metres, where total road-width is 16.50 metres and the remaining 7 metres are sidewalks, 3.50 metres on each side. Furthermore, the bridge is oriented with longitudinal direction in North-South, divided in ten zones. The first zone is the southern abutment and the last zone on the north end, while the eight zones in the span contains one column-row each.

Numbering of the columns goes from 1-4 in the direction of west to east. Figure 4.3 shows the cross-sectional view of the bridge with the bridge deck and beams.
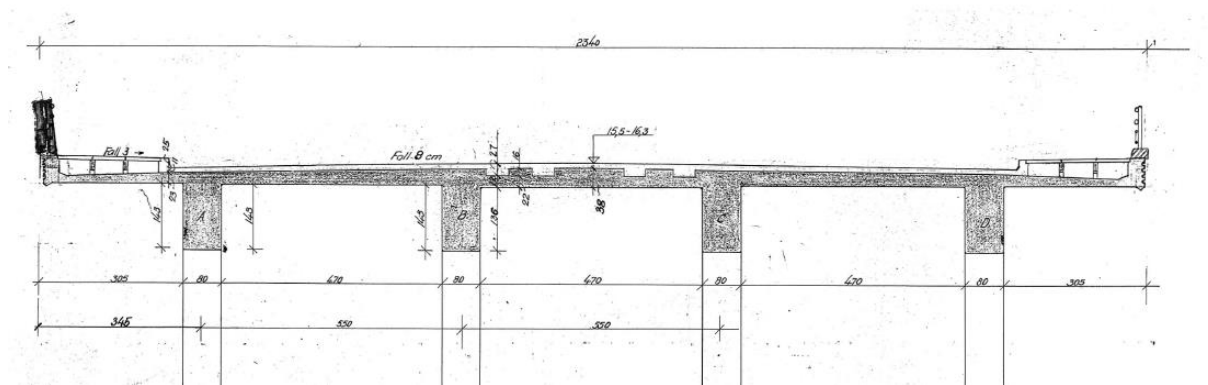
Figure 4.3: Design drawings showing the cross-section of Elgeseter Bridge, with four beams.

The foundations are all cast together in a slab under the water surface of the river. The slab is supported by numerous poles anchored a sufficient distance below the surface. The foundation is not anchored to solid soil, so it is possible that the soil condition might have changed slightly. However, the foundations will not be considered in this thesis since the ASR is not likely to have the same effects under water, since the alkalis may leach into the water and reduce the risk of reacting.

4.3 The state of Elgeseter Bridge

The bridge has a long history of inspections and measurements since its completion in 1951, with the first inspection and repair in 1985 when changing the expansion joint. The expansion joint needed to be replaced because of an expansion in the bridge so great that the joint closed itself.

Several parties have done inspections of the bridge over numerous occasions. The latest inspection was done by Aas-Jakobsen AS in 2012 [5], in which this chapter is primarily based on.

Early in the 90s, the prime suspect to the reactions in the bridge was the alkali-silica reactions. This was thought due to the expansion that lead to the replacement of the expansion joint, and measurements on the columns verticality. In addition, the cracks on the columns and their evolution is closely under observation.

Furthermore, Sintef has inspected the bridge at numerous occasion, as well as measured and run test programs over several years. Their core samples taken in 1990 and 1991 confirmed

that alkali-silica reactions had occurred or was occurring in the concrete. However, no alkali-silica reaction was confirmed occurring in the inner beams.

The expansion joint was replaced again in 1995, due to damages, and measurements of the expansion and opening of the joint were made in 2000 and 2004.

The columns of the bridge have been undergoing testing and measurements since 1995, by both Sintef, NPRA (Norwegian Public Road Administration) and NCAL (Norwegian Concrete and Aggregate Laboratory Ltd.). Cracks and crack patterns in the columns has been continuously monitored and repaired when needed. A test program by NORUT (Northern Research Institute Tromsø AS) included the use of carbon fiber products and extensometer measurements. Due to the extensive expansion of the bridge, the column tops of the three last column rows have been moved back to a vertical position. These results and other conclusions for the columns is not directly important for this thesis. However, conclusion made on the general basis for the Alkali-Silica reactions will be relevant for the conclusion on the bridge deck and beams. For instance, the report from NCAL [6] concludes that the external columns, which are more exposed to rain and water, were observed with several and larger cracks than the inner columns. Figure 4.4 shows the crack pattern occurring on one of the columns.

Figure 4.4: Pictures of the crack pattern, from NCAL's inspection and report on the columns.

Cracks in the bridge deck and beams were observed in 1991, with some signs of leaching and decalcification. The report from Sintef does not report any signs of overloading on the beams, but the report concludes that high loads might have caused some of the cracks on the bridge deck.

The reasons for the latest inspections have been large vertical cracks in the span of the inner beams, with crack widths as large as 6mm. There is only observed large cracks in two spans, with only one large crack in each span. The two cracks occur in each their inner beam, i.e. no large vertical cracks in the outer beams. One inner beam has the large crack in span 3-4, while the other beam has the crack in span 8-9. *Figure 4.4* shows the picture of one of the cracks, the picture is taken from Rambøll's report from field inspections in 2011. [7]

Figure 4.5: Picture of the vertical crack in span 8-9 from Rambøll's report from 2011.

Under the inspections there were also observed several smaller cracks, with crack widths rising up to 2 mm. These cracks are relatively small, width the average crack width to 0.5mm.

Findings from the last inspections, core samples and reports from Aas-Jakobsen confirms a larger alkali-silica reaction in the external beams and large expansion of the bridge deck. Large areas of high moisture levels were observed on the whole bridge deck on the top level, and on the underside from the outer parts of the deck to between the inner beams and external beams. Next to no signs of leaching or decalcification on the inner beams adds to the theory

of lower moisture level in the inner beams, and therefore less or no alkali-silica reactions have occurred.

Earlier repairs of the bridge include the repairs of the columns, and the cutting of column tops, but also some of the large cracks in the concrete beams have been repaired. The wear layer of the bridge deck has also been replaced on several occasions.

The expansion of the bridge deck, and the measurements of the dilation of the expansion joint have been covered by both Sintef and Aas-Jakobsen. As mentioned before, the expansion joint was replaced on several occasions, one time due to damages by the snowplough, but mostly because the expansion of the bridge deck. The dilation of the joint has been measured and monitored since the first replacement. The uncertainties for the measurements are the quality and accuracy of the temperature measurements, as well as the assumed coefficient of thermal expansion in concrete.

The report from Sintef [8] concludes with insignificant expansion in the years from 2004-2012. The report from Aas-Jakobsen [9] states that this may not be the case, and when looking at the structural consequences one should perhaps not consider the safest conclusion when it comes to the expansion. The figures for the expansion are taken from another report from Aas-Jakobsen [10], which shows expansion by the closure of the expansion joint. The smallest value concludes with an expansion of 150mm from 1950-2000, and the highest value yields 180mm expansion during the same time. These values are not necessarily caused by the expanding bridge deck alone, but also movement in the abutment can affect these readings and cause an overestimation of the values.

The bridge deck originally had two paved footpaths with the width of 2.35m, with two lanes for tram and two lanes for traffic. The bridge was overhauled in 1985 to hold four driving lanes (with two lanes for bicycles) and the footpaths were then widened to 3.5m on each side. *Figure 4.6* shows the sketches of both footpaths.
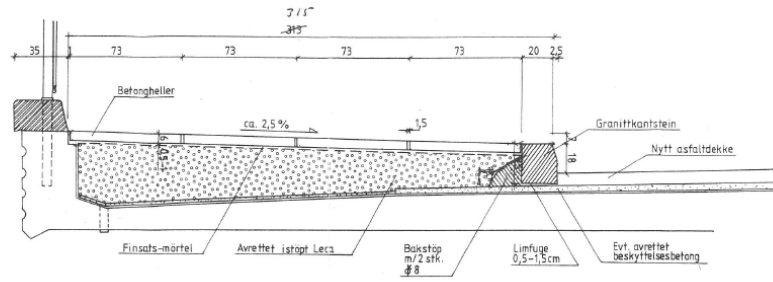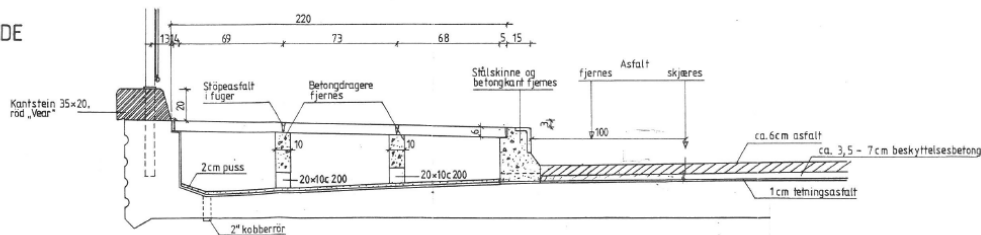
Figure 4.6: Original drawings showing the old footpaths and the new, widened footpaths.

The old footpaths were made out of very porous concrete, which would contribute to higher moisture levels over that part of the bridge deck. During the construction of the new footpath, the waterproof membrane over the bridge deck might have been injured or broken, which also would contribute to higher moisture levels. In addition, inspections revealed that the drainage systems was heavily blocked. This, in addition to heavy rain on the outer parts of the bridge, causes the moisture level to be higher on the bridge deck and outer beams. As described in *Chapter 3*, the alkali-silica reaction needs a high level of moisture in the concrete to create the gel, and thus the expansion.

Inspections show that the moisture level has been quite high on the bridge, which would mean that the probability of high relative humidity in the concrete is elevated for the discussed areas of the bridge, i.e. outer parts of bridge deck and beams.

Ongoing repairs on the bridge have decreased the excessive amount of asphalt, since the bridge was only designed with 11cm of wearing course, refurbishing the drainage system and footpaths. The bridge is continuously monitored when it comes to the expansion of the bridge deck and movements of the columns and beams.

4.4 General parameters relevant to the analysis

The total length of the bridge can be acknowledged to be longer than 200 metres, due to the abutments. However, the total length of any beam is 200 metres and therefore it is considered in this thesis that the bridge deck is considered equally long.

In the 3D modelling program, the bridge will be modelled as true to reality as possible. The bridge deck geometry is identical to the drawings provided by the NPRA (Norwegian Public Road Administration). The beams are modelled as a part of the bridge deck, with the possibility of having a different Young's Modulus in each beam. The columns are cast separately from the beams and bridge deck, but are casted with reinforcement to be a continuous joint. The joint between the columns and beams needs to be modelled so that the columns follow the movements of the beams.

The expansion of the bridge deck will affect the structure in all directions, and therefore the whole structure needs to be taken into account, even when symmetrical.

The analysis in 2D is not as exact, and does not have relevant load effects which would need the whole bridge deck to be modelled. Therefore, the bridge deck might be modelled with the relevant width, since it is symmetrical, depending on the load models. The total length of the structure still needs to be taken into account, even when symmetrical, due to the different loads on different locations on the length.

For the calculations of capacity and occurring load situations, the geometry of the cross section can be simplified to make a symmetrical t-beam in concrete. The total concrete area is the same in both the simplified and accurate model. The location and area of reinforcement is derived from the drawings and reports, to make a determination of the reinforcement as close to reality as possible.

The span lengths are modelled equal to the real span lengths, i.e. 21.25 m – 7x 22.5 m – 21.25 m. The column rows are assumed to have their centre in the location of the spans. The location of the centre node is the point where the connection is located. For the 3D modelling program, a single node in the beam and the surface of the top column determines the connection.

4.5 Concrete

As mentioned in Chapter 2, the Portland cement mix was made especially for this bridge, from the concrete factory. The aggregates were from local stone quarries, with the intention of not deteriorating early. The intent was that the concrete aggregates would not react with the reinforcement bars and cause corrosion, and therefore not marine deposits. At the time it was not known that the glaciofluvial aggregates that were used instead would react chemically with the cement. The combination of aggregates for the Elgeseter Bridge was as follows:

The combination of aggregates for Elgeseter Bridge is as follows [6]:

- Søberg glaciofluvial fine gravel; fraction 0-16mm.
- Klett glaciofluvial course gravel from the river Gaula, fraction 15-35mm.
- Trolla crushed rock; fraction 3-15mm, to compensate for the missing 4-16mm fraction of course gravel.

The ratio of aggregates for the concrete mix in the bridge deck and beams was different for the ratio of aggregates used in the columns, where the ratio for beam and bridge deck was slightly richer in stone.

The cement for this mix was also quite exceptional, and made in particular only for the construction of this bridge. This was because the Norwegian standard Portland cement, fabricated and tested at the two cement plants in Norway, showed less compressive strength compared to both Swedish and Danish cement. The difference between the new cement mix for the bridge and the old one was more fine-grained cement and more gypsum than standard cement mixes at that time. Both the amount of gypsum or alkali in the mix are unknown, but there is no doubt that the amount was sufficient to drive the chemical alkali-silica reactions. This new type of cement was called the "Standard-S".

When mixing the concrete mix, air entrainment is usually added to all concretes, where Elgeseter Bridge is no exception. This is because the air entrainment reduces the risk of separation and improves the frost resistance. Test results shows that concrete mixes with air entrainment of 4.2% air voids will be frost resistant even after 200 freeze-thaw cycles. However, the air entrainment reduces the compressive strength of the concrete. The reduction of strength could be compensated by lowering the water/cement ratio or by simply adding cement. The air volume added to Elgeseter Bridge was reduced to about 3% for the final mixes.

The compressive strength values given in NCAL's report [6] are 31.9 N/mm^2 for the beams and bridge deck and 39.6 N/mm^2 for the columns. The values are taken from control specimens during the construction period. The test specimens vary in both compressive strength, but also the cement/water ratio, which is also different for concrete mixes for beams, columns and foundations. The results from the test subjects for the bridge deck, beams and columns are shown *in table 4.1*.

Structural element	Compressive strength	Number of tests	Average comp. strength	Variation coefficient (%)
Bridge deck and beams	31.9 N/mm^2	37	34.2 N/mm^2	12.3
Columns	39.6 N/mm^2	22	40.8 N/mm^2	16.2

Table 4.1. Compressive strength for test specimens with 28 days curing

The compressive strength used for analysing the structure, in accordance with the Eurocodes, is the values derived in reports from Aas-Jakobsen [5]. The ratio 350 kg cement per m^3 for the bridge deck and beams is equivalent to the C25 concrete in the Eurocodes, which gives the compressive characteristic strength of 16.8 N/mm^2, and the design value of 12 N/mm^2. The columns contained 400 kg of cement for each m^3, which is the equivalent of the C30 concrete. Thus, the characteristic compressive strength is 20.3 N/mm^2 and design value of 14.5 N/mm^2. The Young's modulus for the concrete, derived from the Norwegian standards, is estimated in the reports from Aas-Jakobsen's report [5], and the former Norwegian standard NS 3473 [11], as follows:

$$E_{ck.beam} = 9500 \, (f_{cck.C25})^{0.3} = 9500 \cdot (20 \text{ N/mm}^2)^{0.3} = 23\,300 \text{ N/mm}^2 \qquad (Eq.\,4.1)$$

$$E_{ck.column} = 25\,000 \text{ N/mm}^2 \qquad (Eq.\,4.2)$$

4.6 Reinforcement

The reinforcement of the bridge is smooth steel mostly with the diameter, Ø, 32mm. The quality for the reinforcement is a Norwegian standard "*St. 52*" for the Ø32 reinforcement. All other reinforcement is classified as "*St. 37*". The report from Aas-Jakobsen[5] and the handbook R412[3] from the NRPA, predicts the characteristic yield strength for the St.37 to be 230 N/mm^2 and 340 N/mm^2 for St.52. The material parameter for the reinforcement depends on the year of construction. The design yield strength for the reinforcement is then 184 N/mm^2 and 272 N/mm^2 respectively. The material given the quality of St.52 is a very ductile material, which leads to the assumption that the reinforcement is most likely intact where there are cracks.

4.6.1 Sections

When looking at the capacity calculations, the specific reinforcement for the specific section under calculations is vital. The amount of longitudinal reinforcement changes throughout the total length of the structure. The amount of reinforcement in the top and bottom depends on whether the cross-section will experience tension or compression. For instance, over the supports there will be a negative bending moment, which causes tension in the top. Over the support, it will therefore be necessary to have longitudinal reinforcement in the top as well.
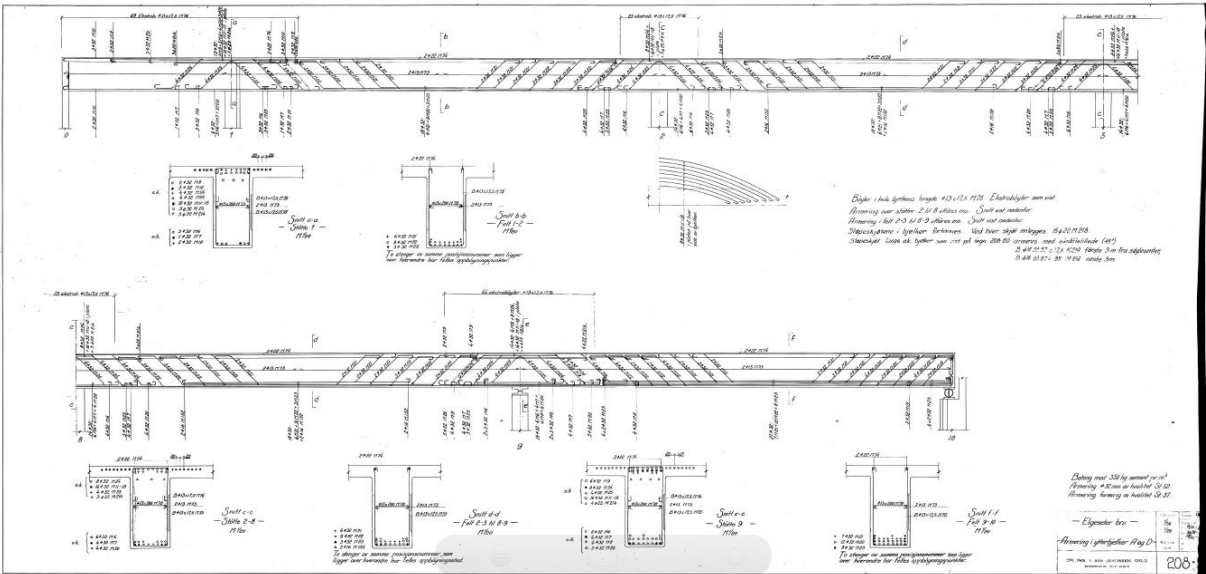
Figure 4.7: Drawings of both longitudinal and shear reinforcement for the beams.

Drawings produced when designing the bridge show the differing amount in both shear, and longitudinal reinforcement, as shown in *Figure 4.7*. Both longitudinal and shear reinforcement is mainly designed with diameter 32 or 22mm, Ø32 and Ø22. However, extra

reinforcement is added to several locations, where ties or stirrups of different diameters are used. The extra reinforcement has the same steel quality as the Ø22, i.e. st.37, with the same material parameters.

Relevant sections when designing limit states are those of maximum and minimum design values, from the loading. Bending moment will be highest either in the span or over the supports. Therefore, different sections for the span and supports are needed. The shear forces are most likely to be highest over the supports or abutments.

Capacities depend on the cross-sections, which are dependent on the effective width of the flanges. Effective width of the cross-section is dependent on the effective length of the relevant sections. To calculate the designing resistance of a cross-section it is necessary to also know the total height and width of the cross-sections, as well as loading, span width, supporting actions and reinforcement.

4.6.1.1 Span

The spans effective length and effective width is calculated from regulations in the Eurocode 2 [12]. The effective width in the span is slightly higher than the effective width over the support.
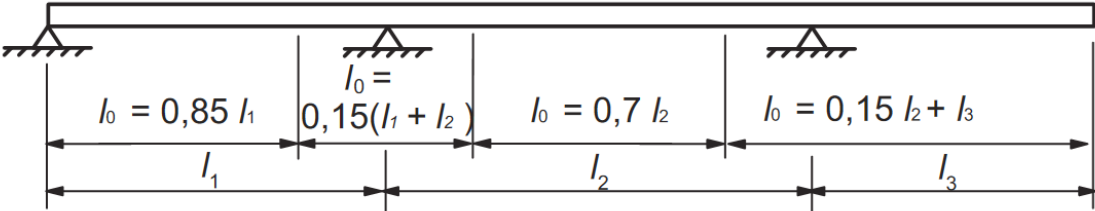
Figure 4.8: Effective length as described by the Eurocode 2 [12].

The first, and last, span is shorter than the other spans, and is most likely exposed to slightly higher bending moment. In the middle of the span shear reinforcement is barely present. No shear reinforcement is assumed in the centre of the spans. Due to variations in the reinforcement amounts, different sections are evaluated. Two sections are evaluated, one section for the first and last span and the other section for the spans in the middle.

4.6.1.2 Supports

The supports are designed for both high bending moments and shear force. Also here the cross sections have different amounts of longitudinal reinforcement. The last span may experience some higher effects due to the ASR and the traffic loads. Therefore, the calculations are made with two different sets of span, in order to correctly describe the capacities of the bridge.
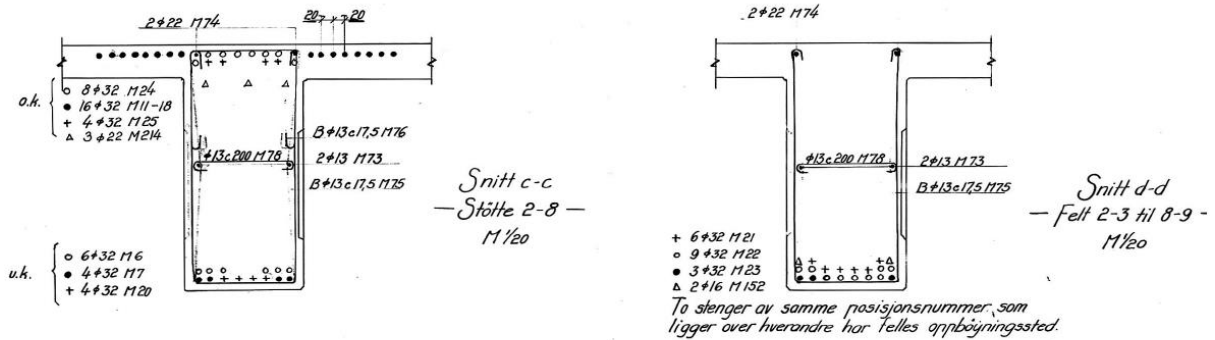
Figure 4.9: Design drawings showing reinforcement amounts for two sections along the outer beams.

5 Loads

This chapter presents the appropriate loads for the case of Elgeseter Bridge, with requirements and guidance given from the handbook N400 (and supplemented by handbook R412 where relevant). Loads are characterised into four categories, depending on time and the probability of occurring:

- Permanent loads
- Live loads
- Accidental loads
- Deformation loads: Considered either as a permanent or as live load.

5.1 Permanent loads

Loads considered as constant throughout the life span of the construction, i.e. weight of the construction as well as other permanent weights or equipment, as well as external pressure from water and soil. For the bridge-deck and columns, there is no water or lateral earth pressure. Therefore, they have no contribution to the permanent load. The permanent loads consist only of the self-weight for the concrete construction and contributions from the surface wear layer and additions for the footpath.

5.1.1 Self-weight

Density for the reinforced concrete construction, given by section 5.3.2.1.4 in N400 [2], is 25 kN/m^3. The wear layer and railings are not considered as self-weight since they are not a part of the constructional cross-section. They are still considered as a permanent load, evenly distributed. Wear layer and other concrete casts are also assumed to have the same self-weight, given the density of 25 kN/m^3 [2].

Self-weight for the construction is calculated from the density of the concrete and wear layer. Total self-weight is calculated to be 375 kN/m along the longitudinal direction. The handbook R412 [3] determines load caused by railings. That applies along the entire bridge length.

$$G_{concrete.k} = 25 \, kN/m^3 \cdot (A_{b.deck} + A_{beams} + A_{wear}) \qquad (Eq. 5.1)$$

$$G_{railing.k} = 0.5 \; kN/m \qquad (Eq. 5.2)$$

Added load for coatings are given in the handbook N400 [2] to bridges in accordance with the length of their longest span. The longer the span, the smaller the minimum requirement loading for coating. Minimum requirement for coating on Elgeseter Bridge is 3.5 kN/m^2 for

the carriageway, and 2.0 kN/m² for the pedestrian footpath. With the width of 16.5 metres on the carriageway, the line load to be added to the permanent load is equivalent to 445 kN/m.

For the carriageway:

$$G_{coating.1.k} = 3.5 \, kN/m^2 \cdot \omega_{carriageway} \qquad (Eq.5.3)$$

For the pedestrian footpath

$$G_{coating.2.k} = 2.0 \, kN/m^2 \cdot \omega_{footpath} \qquad (Eq.5.4)$$

To be on the safe side in calculations, the permanent load over pedestrian footpath is assumed to be the same as for the carriageway. The total line load on the structure, due to self-weight, is described in equation *(Equation 5.5)*.

$$G_{total.k} = G_{concrete.k} \cdot G_{railing.k} \cdot G_{coating.1.k} \qquad (Eq.5.5a)$$

$$G_{total.k} = 431 \, kN/m \qquad (Eq.5.5b)$$

5.1.2 Water and lateral earth pressure

Water pressure should be taken into account as external pressure for constructional parts immersed in water. Requirements are given by NS-EN 1997-1, as well as in part 5.5.5 in regulation V220 (from the NPRA). Lateral earth pressure for constructional parts where abutments or other constructional parts are in contact with earth that causes forces on the structure. Requirements are given in NS-EN 1997-1, as well as in regulation V220 (from the NPRA). [2]

Elgeseter Bridge has abutments in soil, and columns in water, thus the requirement must be in order with both the Eurocodes and the local regulations. However, since the effects of these loads are considered less significant than any other loads, these are not considered in this thesis. The columns are long and slender, and immersed with the depth approximately to 1 metre of river, the forces created by the stream will not be large enough that we need to consider them in this case.

5.2 Live loads

Live loads varies both in time and in duration. There are two types of live loads, divided by their origin.

- Traffic
- Nature

Traffic load depends on the classification of the bridge, with further explanation in *Chapter 6.2.1*. Natural loads are loads caused by wind, snow, ice, temperature, waves, currents or earthquakes.

Some temporary loads may be given in the calculations as live loads when considering the load cases, such as loads on the structure from i.e. equipment stored on the structure, or loads from transportation that is needed for the construction.

The live load relevant for this thesis are the loads caused by traffic, in both horizontal and vertical direction. The variety of live loads needed to assess when designing a bridge are also described later in this chapter.

5.2.1 Traffic load

Traffic load, load models and definitions are described and formulated both in the Eurocode1-2 [13] and in handbooks from the NPRA [2] [3]. The relevant load models in this thesis are added to the structure in the 2D analysis program.

Traffic loads are both horizontal and vertical loads on the structure, caused by normal and heavy vehicles, bicycles, pedestrians, and other effects caused by the loads. The centrifugal forces will not be considered, for the reason that Elgeseter Bridge is straight and will not undergo those forces. The norms describe the loading normally allowed on the bridge. Special (heavy) vehicles requires a dispensation in order to use the bridge.

The width of the bridge is a deciding factor when deriving the placement of the loads and load models. In accordance with the Eurocode 1-2 [13], the carriageway width is divided in to notional lanes (ω_i) with the width of 3 metres. This is corroborated by the Handbook N400 [2]. Notional lanes are to be loaded according to the load models. Carriageway width is the distance between kerbs or between the inner limits of vehicle restraint systems. The carriageway width for Elgeseter is 16.5 metres, which results in five notional lanes in addition to a remaining area of 1.5 metres. *Figure 5.1* shows the lane numbering for Elgeseter Bridge, in accordance with the Eurocode. The Handbooks decide the width of a heavy vehicle as 3

metres, but where there is only evenly distributed load, the width can be shortened to 2 metres. When calculating and analysing the loads, only the critical lane will be under consideration.

Figure 5.1: The total carriageway width of Elgeseter Bridge results in five notional lanes, and a remaining area, 6.

Traffic loads are defined by using equivalent forces to describe the effect of certain heavy weight vehicles surrounded by a mixture of light and or heavy vehicles. Load models are designed to cover all forces to occur from traffic, thus both horizontal, vertical, static and dynamic loads will occur depending on the load models. The location of the traffic load is to be where the load has the most unfavourable effect on the construction.

5.2.1.1 Vertical loads

The load models defined in the Eurocode 1-2 [13] is limited for road bridges with loaded lengths less than 200 metres. In practical use, the Eurocode defines load models up to loaded length of 200 metres. Loaded lengths greater than 200 metres are to be defined by the individual project or the National Annex. Elgeseter Bridge is 200 metres in total, thus the Eurocode values would be accurate for this case. However, the bridge is to be designed after the National Standards from the NPRA. The relevant Load Models are taken from the Handbook R412 [3].

Relevant load models for each bridge is decided by how they are classified. Elgeseter Bridge is classified as a *Bk10* bridge, i.e. the highest classification of Norwegian road bridges. With each classification, there follows a set of load classifications. Each load is placed in the longitudinal direction of the bridge in order to create the most unfavourable effect. The load models contains different amount and intensity of loads. Only one of the load models are to be taken into account. The load model taken into account should be the one creating the most unfavourable effect. Thus, both the placement creating the most unfavourable effect on bending moments as well as shear forces should be considered.

The special transportation load models for bridges, given in the Handbook [3], is not reviewed in this thesis. Relevant terms from the Eurocode [13] is used where the Handbook [3] utilizes the same notions.
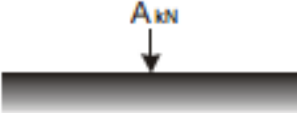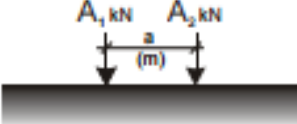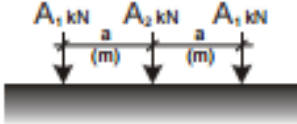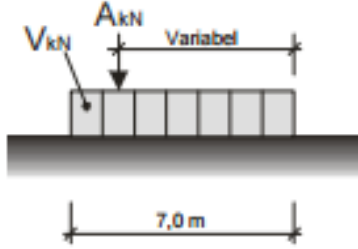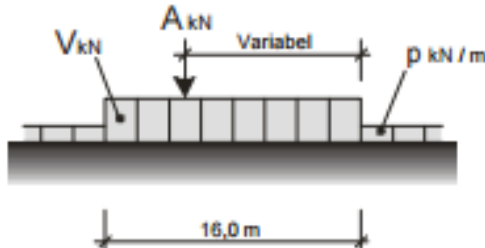
Load Models

Consists of both concentrated and uniformly distributed loads, meant to covers the wide spectrum of the effect from lorries and cars. This model is to be used for both general and local verifications. Each load model consists of either a wheel load (H), axial load (A), total load of a vehicle (V), an evenly distributed load (p), or a combination of the above. The load models are described in the Handbook [3] and are as follows:

- Wheel LM, consists of one wheel: H=80 kN
- Axial LM, consist of one axle: A=160 kN
- Bogie LM, consist of two axles: A_1=65 kN, A_2=160 kN
- Triple bogie LM, consists of three axles where the first and last axle have the same weight: A_1=A_3=70 kN, A_2=140 kN
- Vehicle LM, consists of a total load of a vehicle in combination with an axle load: V=300 kN over 7 metres, A=40 kN
- Lorrie LM, consists of a total load of a vehicle in combination with an axle load and an evenly distributed load outside of the vehicle: V=500 kN over 16 metres, A=40 kN, p=6 kN/m

The distance between the axles in the load models they are combined with each other, are 1.3 meters. Load models are described in *Figure 5.2*.

When positioning the forces on the notional lane, only one load model should occur in one lane.

Lasttype	Lastkonfigurasjon (*) H kN		Bruksklasser			
			Bk10	BkT8	Bk8	Bk6
Hjullast		H	80	56	56	42
Aksellast		A	160	112	112	84
Boggilast		A₁	65	40	40	30
		A₂	160	112	112	84
		a	1,3	1,2	1,2	1,2
Trippelboggilast		A₁	70	60	50	40
		A₂	140	84	84	56
	Aksellastenes rekkefølge er vilkårlig	a	1,3	1,2	1,2	1,2
Kjøretøylast		A	40	32	32	24
		V	300	280	220	180
	7,0 m — Aksellasten plasseres i ugunstigste stilling					
Vogntoglast		A	40	32	32	24
		V	500	400	320	280
	16,0 m — Aksellasten plasseres i ugunstigste stilling	p	6	6	6	6

(*) For lette brudekker (ståldekker, gitterrister etc.) skal det, uansett bruksklasse, kontrolleres for en hjullast på 35 kN fordelt på en 20x20 cm flate tilfeldig plassert i kjørebanen.

Figure 5.2: Load models as described by the NPRA's Handbook [3].

For the local verification, the effects of the axel load is distributed through axles with distance 1.3 metres in longitudinal direction, depending on which load model you are looking at. The wheel contact surface is described by a contact area of 0.6m x 0.2m.
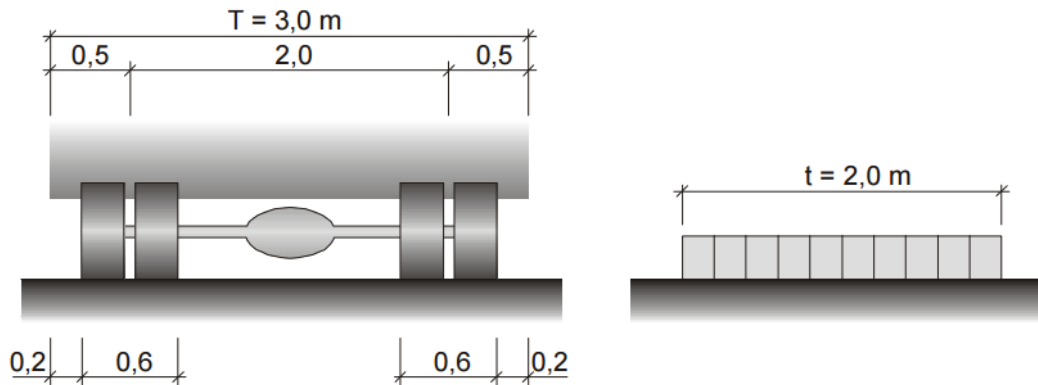
Figure 5.3: Details of tyre contact surface area, distance between tyres and distribution area for the uniformly distributed load.

Lorry Load Model

Consists of one single axle load applied within the vehicle area, one total load of a vehicle spread over 16 longitudinal meters, and an evenly distributed load outside the vehicle area. Any dynamic amplifications have been taken into consideration in the load models.

The axle load consists of a 40 kN point load. The vehicle load is described by a total weight and area of respectively 500 kN and 16 metres in longitudinal direction. Both the axle load and total vehicle load is assumed to work in the full width of the lane, i.e. 3 metres. The evenly distributed force, given on the area in front and after the vehicle, works on 2 metres of the width.

5.2.1.2 Horizontal and transversal forces

Horizontal loads on bridges are characterized by braking and acceleration forces, as well as centrifugal and lateral loads. These will only occur simultaneously with relevant vertical forces.

Braking forces from vehicles are to be taken into account as a horizontal concentrated point load acting at the surface level of the carriageway in the longitudinal direction. The characteristic value is limited to 300kN for the total width of the bridge.

Acceleration forces are assumed to have same characteristics as breaking forces, only with the amplitude in the other direction. The practical difference between braking and acceleration

forces is the sign indicating positive or negative value. During analysis, the value therefore must be considered as the most unfavourable of the positive or negative value.

Acceleration and braking forces should be taken into account as located along the axis of any lane. However, when not taking the effects of eccentricity into account, the force from breaking or accelerating may be simplified. Simplified, the forces are applied only to the centre line of the carriageway, and they are uniformly distributed over the loaded length.

When it comes to the centrifugal and transverse forces, no centrifugal effects are considered, due to there being no bend or curvature of the bridge in longitudinal direction. However, the transversal force acting laterally on the bridge deck must be considered due to acceleration and braking forces. The transversal force is simplified to 25% of the braking force, and like the braking force, the actual value in the analysis should be the most unfavourable of the positive and negative value. The forces in horizontal plane act simultaneously.

5.2.1.3 Groups of traffic loads

Considering the simultaneity of the vertical and horizontal forces, it is useful to categorize groups of relevant load models. Table 4.4a in the Eurocode 1-2 [13] states the relevant grouping of simultaneous loads. Since load models LM1 and LM2 are the relevant load factors, the groups gr.1a, gr.1b and gr.2 are the relevant groups. The contribution from LM1 in gr.2 is only frequent values, and not dominating, while in gr.1a it is the dominating component action. Therefore, the only combination relevant in the analysis is gr.1a.

However, the Handbooks [3] states that the combination of load models should only occur in two lanes at a time. No other traffic loads, except load on pedestrian sidewalks, should be considered acting on the bridge. This does not include the horizontal or lateral forces.

For the analysis of the bridge, the Handbooks are more relevant, with the Norwegian regulations. The loading will occur on two lanes, in 6 metres width of the carriageway.

Load type			CARRIAGEWAY						FOOTWAYS AND CYCLE TRACKS
			Vertical forces				**Horizontal forces**		**Vertical forces only**
Reference			4.3.2	4.3.3	4.3.4	4.3.5	4.4.1	4.4.2	5.3.2-(1)
Load system			LM1 (TS and UDL systems)	LM2 (Single axle)	LM3 (Special vehicles)	LM4 (Crowd loading)	Braking and acceleration forces	Centrifugal and transverse forces	Uniformly Distributed load
Groups of Loads	gr1a		Characteristic values				[a]	[a]	Combination value [b]
	gr1b			Characteristic value					
	gr2		Frequent values [b]				Characteristic value	Characteristic value	
	gr3 [d]								Characteristic value [c]
	Gr4					Characteristic value			Characteristic value [b]
	Gr5		See annex A		Characteristic value				

Dominant component action (designated as component associated with the group)

[a] May be defined in the National Annex.
[b] May be defined in the National Annex. The recommended value is 3 kN/m².
[c] See 5.3.2.1-(2). One footway only should be considered to be loaded if the effect is more unfavourable than the effect of two loaded footways.
[d] This group is irrelevant if gr4 is considered.

Figure 6.2: Table 4.4a from the Eurocode 1991-2 [13], describes the combination of different traffic groups.

5.2.2 Nature loads

Forces that are due to climatic influences, which vary in both time and endurance. For special circumstances where there exists a need for accurate measurements, they are derived independently.

Nature loads can be combined in two ways; either the nature loads in combination are assembled into one load in combination with the other loads, if the nature loads are considered to occur simultaneously. Loads that should be considered simultaneous are wind, current, wave and tidal loads. If they are not considered simultaneous, the interaction between these loads needs to be documented. When nature loads are not assumed simultaneous, they are to be combined individually with the other loads, i.e. assumed not to occur simultaneous with other nature loads.

Snow loads are considered to interact with traffic loads, and are therefore not relevant to this thesis. The snow load on the bridge will never become the dominant load component.

Wind load on the structure is derived from the handbook N400 [2] and Eurocode 1-1-4, as a bridge in class I. This thesis will not consider the dynamic load amplifications due to wind, instability, or forces due to the vortex shedding. The wind forces will not create any dominating load values for the capacity, and will therefore be neglected in the analysis.

Other nature load, such as ice load, loads from avalanches due to snow, floods or stones/soil, thermic loads or seismic loads will not be considered in this thesis. The thermic loads will not be substantial enough to be dominant when considering the alkaline reactions. In addition, the analysis will use the thermal representation on the model for the expansions due to the alkaline reactions.

5.3 Deformation loads

Non-direct influence from either deformation or skewed constructional parts are to consider as deformation loads, given either as permanent effect or live load.

Prestressing tendons, creep, relaxation, consolidation, friction or other deformations due to loads applied on the structure are examples of loads that can induce deformations on the construction. This thesis will not consider any of the above.

5.4 Accidental loads

Accidental loads on the structure comes from direct misuse, accidents or un-normal circumstances causing loads to occur. The handbook clearly states accidental loads that need to be considered:

- Loads from crashes; vehicles, ships or railway traffic
- Falling objects
- Fire with possible explosion
- Explosion with possible fire
- Loads caused by floods or landslides

Most of these are not relevant for Elgeseter Bridge, since neither railway traffic, ships nor any vehicles are able to crash with the bridge. Some would be considered relevant when designing such a bridge, such as vehicles crashing on the bridge. However, none of the listed loads will be considered in this thesis.

5.5 Interactions of loads

The handbook determines the interaction between nature loads as "two or more loads, dependent on time and location, or that often occurs within its maximum value at the same time, should be calculated as one load."

Loads that, with reasoning, are considered to occur at different time or periods of time, are not to be considered as one load.

Temperature loads, and loads caused by variation in the waters density, can both be assumed to not interact with any of the other nature loads. However, wind, current, wave and tidal loads are assumed to occur simultaneous. Where these loads are not considered as one simultaneous load, the interaction between these loads should be documented.

In the modelling, the interaction of forces depends on which software is in use. For the 3D modelling program, no forces will be interacting, since it is function is to represent the expansion due to the alkaline reactions only. For the 2D modelling program, the traffic loads interact with the loads due to the alkaline reactions. This is more thoroughly explained in *Chapter 6* and *7*.

5.6 Expansion forces

The alkaline reactions cause the concrete to expand, and tension and compression will occur in the cross sections. This is due to the reaction itself and the fact that the entire bridge deck and beams do not expand in the same rate. The reaction effects also material parameters such as compressive strength and Young's modulus. The exact effects on the material parameters are impossible to calculate, and therefore they are neglected in this thesis.

The expansion effect will be modelled in the 3D modelling program. Effects from the ASR will be distributed in the 2D model to see the effect during the analysis for traffic loads. The expansion "grows" equal in all direction where the expansive reaction occurs, even though the different amount of reinforcement will affect the actual elongation in each direction.

When modelling the expansion in the 3D software, the expansion is assumed equal in every direction. The effects due to different reinforcement amounts is not considered. The correct modelling of the expansive force is rather elaborate and exceptionally time consuming. For simplification, the load is created as a temperature loading occurring in the bridge deck or in interaction between both the bridge deck and external beams.

Calculation of the expansion is simplified, as either a homogenous or a composite bar. The expansion occurs in one material, where the elongation causes strain in the material. The strain is the basis for the temperature used for the heat expansion in Abaqus. The calculations for homogenous materials is to compare the strains if the bridge deck expands alone, or with the outer beams.

The elongation due to heat expansion is described by following equation.

$$\Delta_L = \alpha_c \cdot L_0 \cdot \Delta_T \qquad\qquad (Eq.\,5.6)$$

Where the elongation is described by Δ_L, the length of the structure before elongation is L_0, the heat difference is Δ_T, and the α_c is the heat expansion coefficient for concrete.

In the case for Elgeseter Bridge the elongation is known to be 100 mm. Therefore, the needed temperature to drive the expansion 100 mm can be calculated from *Equation 5.7*. The heat difference needed in order to drive the expansion is then modelled in Abaqus.

$$\Delta_T = {\Delta_L}/{(\alpha_c \cdot L_0)} \qquad\qquad (Eq.\,5.6)$$

5. 7 Loads in the analysis

The modelling of the structure and loads in 3D are in order to view the effect of the expansion on the entire structure. The intention is to model the entire bridge with a given expansion, and see how the structure reacts or behaves. When modelling all the relevant loads in the 3D-model, the analysis would be very time consuming to run with the evaluation for different load models. The simplified model in the 2D modelling program is sufficient for characterising the behaviour of the structure for each load model. The load models are less time consuming to create and evaluate during the modelling and analysis in the 2D-model.

The traffic loads and permanent loads will be added to the structure in the 2D-model in FAP-2D, in order to see the statically effects on the structure. The expansion load will be modelled in the 3D program, to see the effects from the different load methods on the structure. The effects of the expansion due to ASR on the structure will be modelled in the 2D-model.

6 Abaqus model

Abaqus is a program for finite element analysis, for predicting strength and deformations both in the linear and non-linear range. This thesis focuses on the expanding reactions in the 3D-model, while modelling the traffic loads and nature loads are done in the 2D-modelling program, FAP-2D.

6.1 Creating the model

When modelling the bridge for expansion due to the reaction in the concrete, the model needs to represent the whole structure. This because the structure is not symmetrical in the longitudinal direction. In Abaqus, the model representing Elgeseter Bridge has two *parts*. One part consisting of the bridge deck and beams, the other part represents the columns. The bridge deck and beams are cast together with the columns, therefore continuity between the parts is vital. To create the parts, the models cross-section is drawn first. Next step is setting the depth of the part (corresponding to the length of the structure). The bridge deck and the beams need to carry a property alone, in order to place the correct material properties. This is done by partitioning the parts from the bridge deck. The bridge deck is assigned one material, the two outer beams is assigned a second material, and the two inner beams are assigned to a third material. The columns are created separately, and are assigned to a fourth material. All materials have the same capacity for expansion.
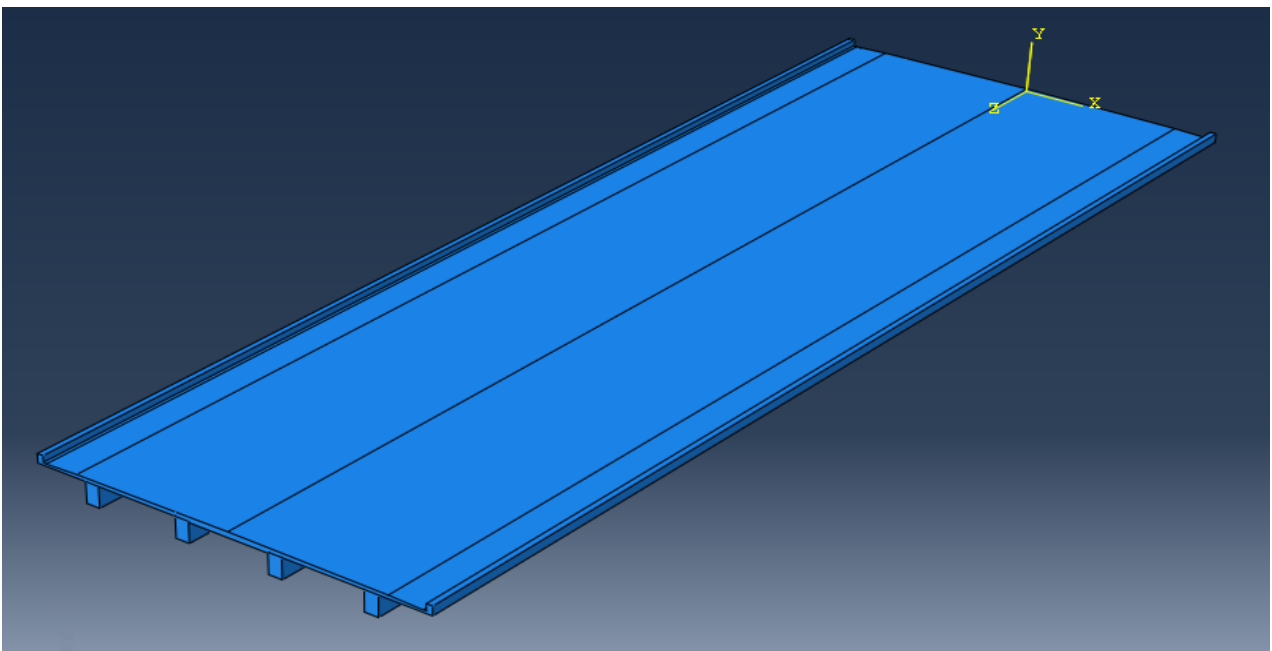
Figure 6.1: View of the model in Abaqus, where the origo is represented in the middle of the slab, in the centre of the width, at the south abutment.

When modelling the construction, in the section sketch, the input data for distances was meter. This has consequences for all other input data in the model. Material properties now need to be input in N (Newton, not kN or Pa) and m (metres).

Coordinate system in Abaqus is global X-Y-Z, where the section-sketch is drawn in the XY-plot. Therefore, the z-axis becomes the longitudinal direction. Local coordinate systems or datum points can be implemented. Displacements are described as U1, U2 and U3, corresponding to the displacement in each axis. Rotations are described as UR1, UR2 and UR3, which corresponds to the rotation about each axis.

$$U1 - Displacement\ in\ x - dir. \qquad UR1 - Rotation\ about\ x - axis$$
$$U2 - Displacement\ in\ y - dir \qquad UR2 - Rotation\ about\ y - axis$$
$$U3 - Displacement\ in\ z - dir \qquad UR3 - Rotation\ about\ z - axis$$

6.2 Materials and material properties

When constructed, the bridge deck and beams were cast together, with the same concrete, but over time the moist conditions and alkali-silica reactions have affected the constructional parts at different rates. The inner beams are the ones with severe cracks, but they have low or no effects by moisture exposure. The bridge deck is most likely exposed more to higher humidity, from rain or water on the top plate. Inspections under the bridge shows a clear distinction of the concrete exposed to higher moisture-levels, se *Figure 6.2*.
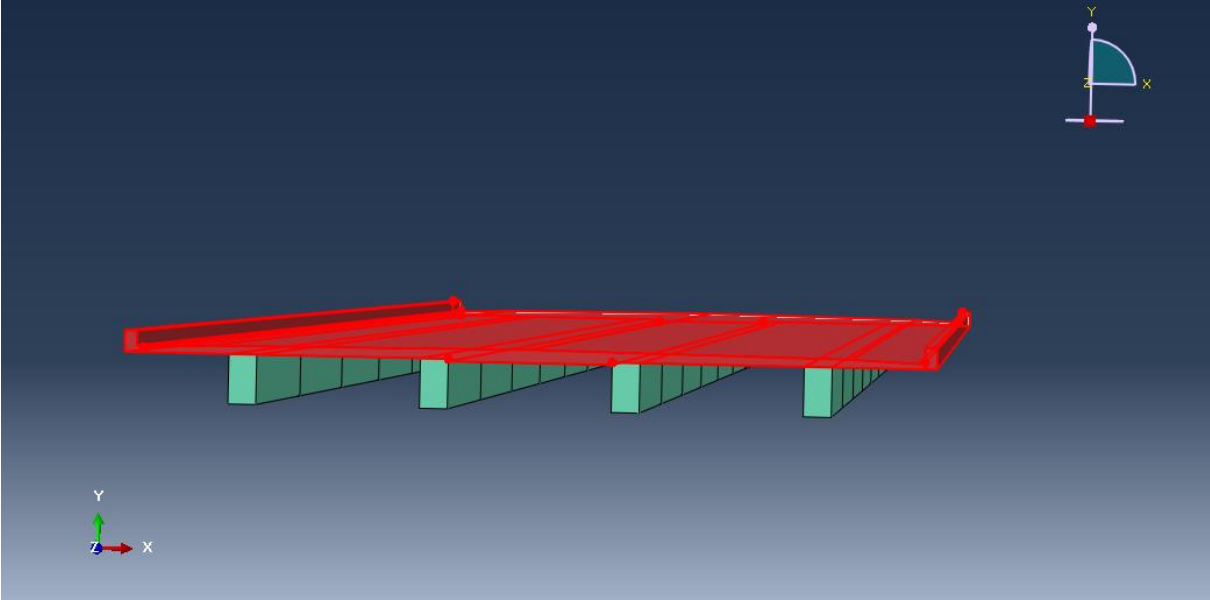
Figure 6.2: Illustration of the partitioned part, with the bridge deck marked in red.

To represent the different effects of ASR on each part, the parts are modelled with a material properties of their own. The bridge is divided into four different materials. The bridge deck as one, containing material properties to represent the part. The beams are divided into two, the

46

inner beams and the outer beams, with each having their own material. The fourth material is assigned to the columns, the concrete used for the columns has a different compressive concrete strength.

Figure 6.3: Visible moisture level differences on the bridge deck.

The inner beams are the constructional parts least affected by the moisture, but the expansion of the concrete has caused large cracks. Outer beams are the beams most affected by moisture and the ASR, but the expansion has not yielded as many critical cracks as for the inner beams. The bridge deck is most affected by moisture and most likely the most affected ASR part as well. In addition, it is affected by cracks, although not as severe cracks as for beams or columns, as well as superficial damage from casting. As described earlier, the input data to Abaqus needs to be in metres, which for the elasticity module for the concrete means that values in the order of 20 000 MPa now are described as $20\ 000 * 10^6$ N/m^2, $20 * 10^9$ N/m^2.

$$20\,000\ MPa\ =\ 20\,000\ N/mm^2 \qquad\qquad (Eq.\,6.1) 1\ N/mm^2$$

$$1\ N/mm^2\ =\ 1/10^{-6}\ N/m^2\ \rightarrow\ 1\ N/m^2 = 1\cdot 10^6\ N/mm^2 \qquad (Eq.\,6.2)$$

$$=\ 1/10^{-6}\ N/m^2\ \rightarrow\ 1\ N/m^2 = 1\cdot 10^6\ N/mm^2 \qquad (Eq.\,6.2)$$

The Poisson's ratio for the concrete is assumed 0.2 for all constructional elements in the simulation. For cracked concrete elements, the Poisson's ratio is recommended to be applied as zero. However, this analysis is simplified to the elastic part of the expansion. Therefore, the Poisson's ratio is defined equally to all the constructional elements.

The expansion is in reality free to develop in every direction, if the reinforcement or restraints are not considered. Modelling the expansion as heat expansion due to a change in temperature, the parts assigned the heat change will have the same expansion rate in every direction. The expansion is then only restrained by global restraints. The beams and bridge deck are all modelled with the same heat expansion coefficient, to ensure equal expansion.

The concrete compression strength is not required for any calculations during the analysis in Abaqus. The capacity and strength calculations and the corresponding calculations for the expansion and its effects on the strength and capacity requires different compressive strength for the different constructional parts. The materials in Abaqus describe the different elasticity modules and the heat expansion coefficient.

6.3 Elements, boundary conditions and constraints

Elements are created by meshing the parts. During the analysis, some elements can become distorted due to deformations. This easily happen when selected mesh elements are too large. To prevent this, the general settings for mesh, mesh sensitivity and general settings for verifying the mesh is used. The general settings is set with an approximate global size of the elements at 0.1 for the columns and 0.2 for the bridge deck and beams.

A correct description of the boundary conditions sustains a correct simulation of the structures behaviour in reality. Boundary conditions represent the withholding of the structure, by defining the restriction for the degrees of freedom at a given node. Boundary conditions applied on this structure represent the pinned support at the southern end, roller support at the northern end, as well as the fixed end of each column. The pinned support restricts any displacement, in either direction. The roller end restricts all displacement, except in the

longitudinal direction. The fixed end supports for the column ends restricts all displacement and rotation.
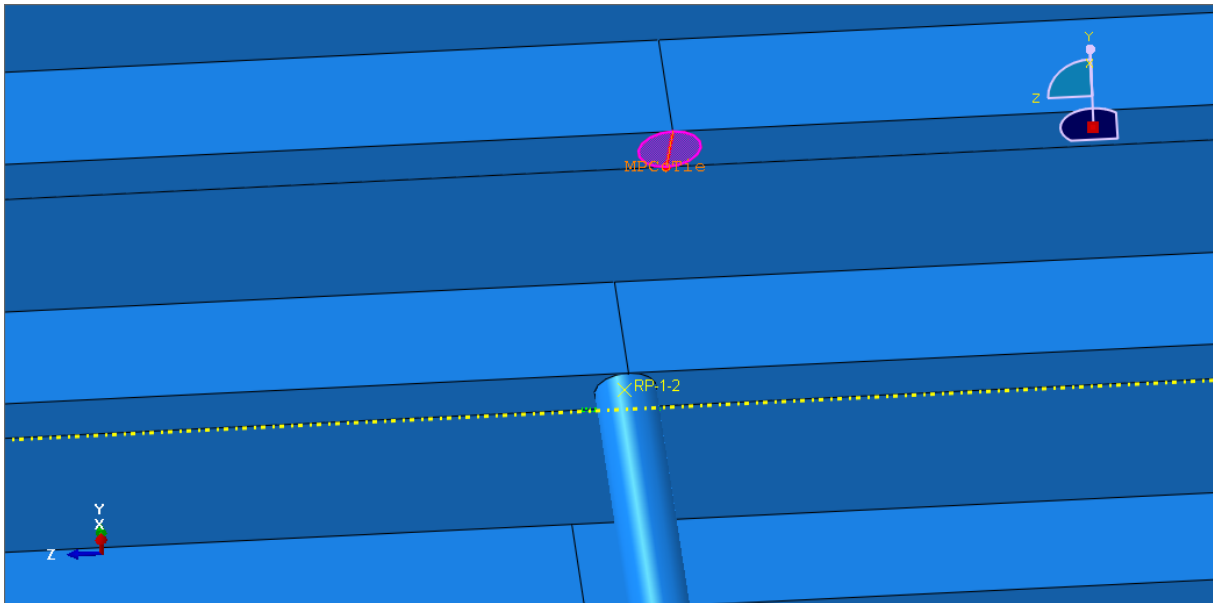
Figure 6.4: Illustration of the area the MPC constraint is connected to, with the tie link in the node MPC-Tie.

Constraints define the constraints for the degrees of freedom between regions of a model. You can also supress and resume constraints to vary the analysis model. In Abaqus, it is possible to create the following constraints: tie constraint, rigid body constraint, display body constraint, coupling constraint, adjust points constraint, MPC constraint, shell-to-solid coupling constraint, embedded region constraint and equation constraint. The necessary constraints in the case for the Elgeseter Bridge model are applied on the face between the column top and the face on the bottom of the beam, which is connected to the bridge deck.

In order to simulate the transferral of forces correctly through the beam and column, the model in Abaqus is assigned MPC constraints, specified to the MPC type of beam. Thus, by selecting the top face of the column as slave nodes, and connecting them to a control point, they are equal to the control point in each active degree of freedom. The bridge deck was cast simultaneously with the beams and columns, with reinforcement ensuring the force transferral, therefore the forces subjected to the beam must transfer to the columns also in the simulated model.

6.4 Modelling and parts

The first thing to determine when modelling in Abaqus is which type of model to use, Standard/Explicit Model, CFD Model or Electromagnetic model. CFD is an abbreviation for Computational Fluid Dynamics, and neither the CFD nor Electromagnetic Model is appropriate for modelling Elgeseter Bridge.

To model the bridge correctly, it is separated into two parts. The bridge deck and beams are modelled as one part while the columns are modelled as the other part. Separate column heights is the cause for several column parts. In order to create the part, one sketches the cross-section and specifies its depth. Each part can only be assigned one material, or composite, unless it is further partitioned, which is the case for the bridge deck and beams.

Modelling the entire span of the bridge, the correct number of columns in each respective height is assembled together with the bridge deck and beam part. The assembly tool in Abaqus gives the opportunity to assemble together different parts in the order of preference and with the required quantity. For the Elgeseter Bridge, one part of bridge deck and beams is assembled with eight parts of column rows.
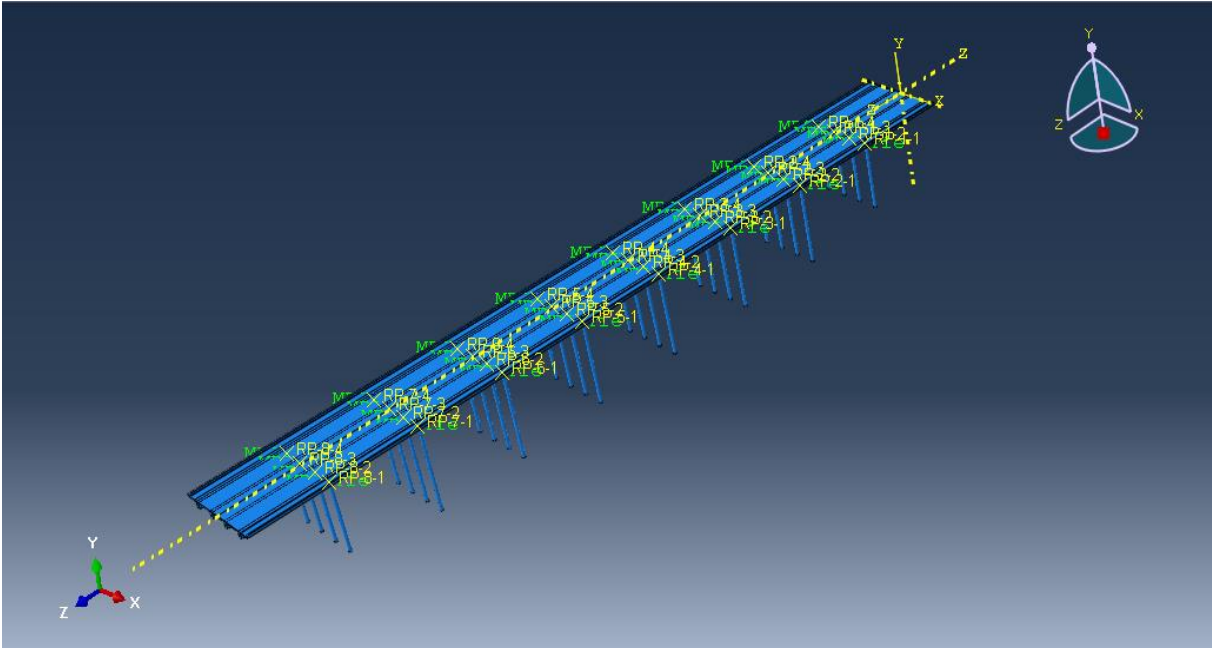
Figure 6.5: Elgeseter Bridge as modelled in Abaqus, bridge deck, beams and columns in the entire length of the bridge.

6.4.1 Bridge deck

The bridge deck is originally modelled as the same part as the beams. The bridge deck will be modelled with heat expansion. Since all the beams are not going to be assigned heat expansion, the bridge deck is partitioned from the beams. The partition separates the material properties for the bridge deck from the four beams. The material is called "Concrete – bridge deck". The section sketch is shown in *Figure 6.6*.
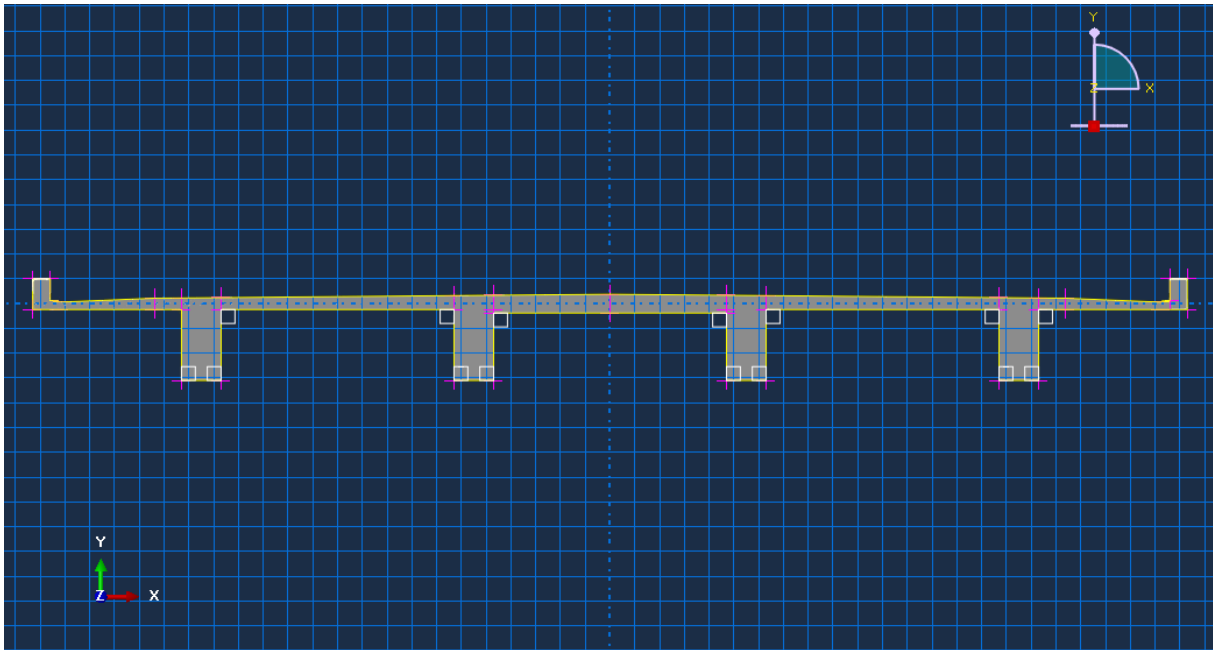
Figure 6.6: Cross-sectional view of the bridge deck and beams in Abaqus.

As shown in the section sketch, the thickness of the slab is thicker in the middle of the bridge. It varies from 380mm at the thickest, to as little as 150mm at the thinnest area. The thickness of the bridge deck varies. The original bridge was designed for a slope given the total decrease in height of the thickness of 8cm from the centre of the bridge to the end of the carriageway.

6.4.2 Beams

All the beams are modelled together with the bridge deck. They are also partitioned from the bridge deck, in order to assign different materials to the beams. All the four beams have the same rectangular cross-section, 1430 x 800 mm.
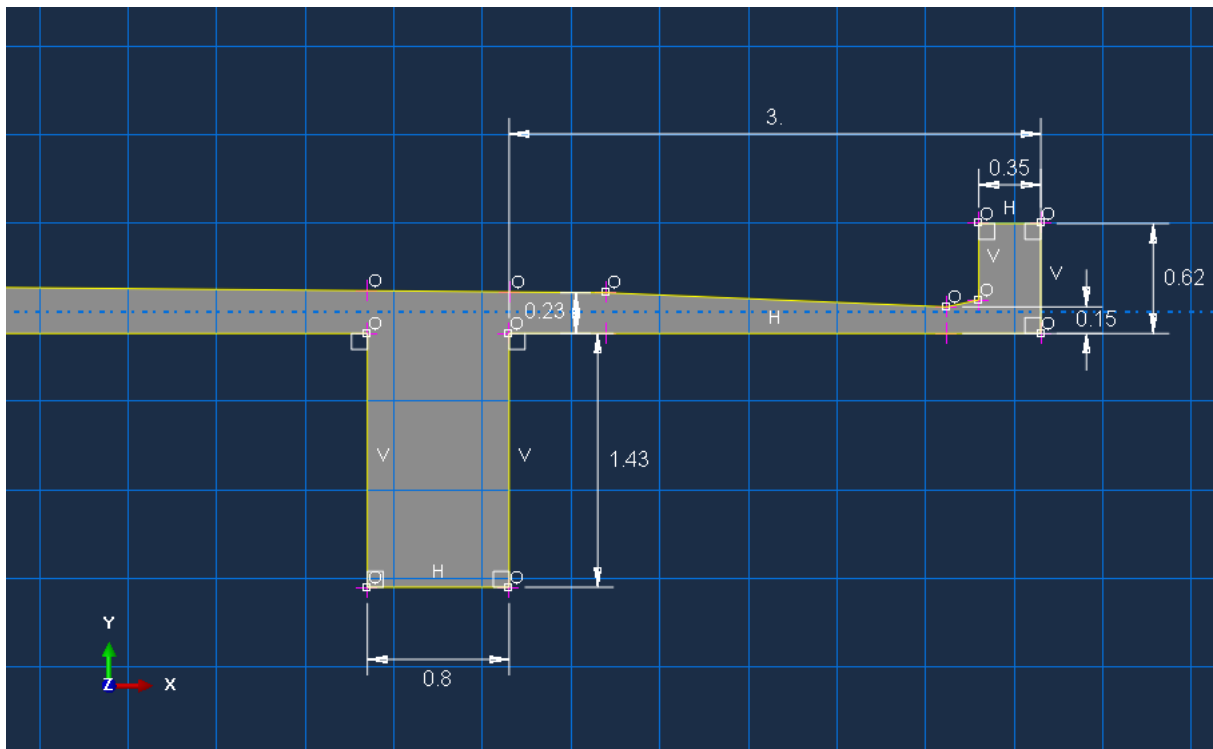
Figure 6.7: Section sketch for the outer part of the bridge deck, showing the correct measures for the beams.

The two mid beams are less exposed to the weather than the two outer beams. Weather conditions, such as heavy rain and snowfall, are relevant to the calculations for the alkali-silica reaction, where high relative humidity is a key factor. The two mid beams are the ones with the observed large cracks. The outer beams can be assumed to have a higher rate of ASR induced expansion, due to the high moisture levels. Considering this, the outer beams might be considered to expand with the bridge deck. One relevant load model in Abaqus might then be the expansion of the bridge deck and outer beams.

6.4.3 Columns

Columns are cast together with the beam and bridge deck. They are modelled as a separate part in order to draw the model correctly. There are three parts of columns needed, in order to assign the different height specifications. The height of the three parts of column row are as follows:

The eight column rows are assembled with two of the column rows with the highest length of 20m, 4 column rows with the height 19 m, and 2 column rows with the shortest length of 17 m. The columns are connected to the beams of the bridge deck as described in *Chapter 6.3*.

The circular cross section is equal for each column with a diameter of 800 mm, the same as the width of the beam.
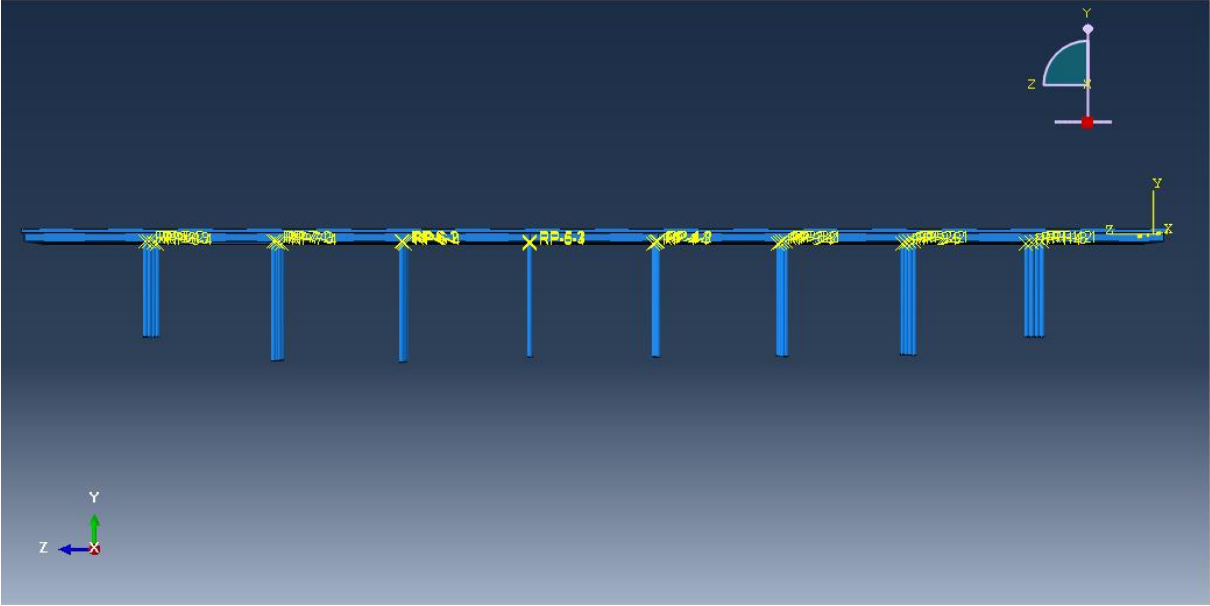
Figure 6.8: Elgeseter Bridge viewed from the side, showing all eight column rows.

The material for the columns is slightly different from the concrete in the bridge deck and beams. Thus, the Young's Modulus for the columns is different for the beams. The columns are relatively damaged by the alkali-silica reaction, but naturally not an equal reaction for each beam. A survey given by NORUT [14] shows different humidity and damage for each column, showing a tendency for higher moisture levels and more frequent cracks for the outer columns. The columns are continuously under observation, and currently under a test project. Therefore, the material properties given in Abaqus are not completely correct in order to represent reality. The focus on this thesis is not affected by a slightly incorrect modulation of the material properties of the columns.

6.5 Load modelling

Abaqus CAE* has not predefined a way of modelling the expansion. From this chemical reaction, the expansion grows in all directions. To replicate the effects of the chemical reaction, and expansion, the model is applied a thermal load to ensure equal expansion in all directions. The elongation of the bridge in longitudinal direction was 100 mm, measured in 2010 [5]. With a temperature expansion rate at $1*10^{-5}$ mm/K, the expansion from the chemical reaction is the equivalent of loading a temperature difference of 50 K (or Celsius). With the base from *Equation 5.6* in *Chapter 5,* we can calculate the needed temperature difference as in *Equation 6.3*.

$$\Delta_T = {100\ mm} \Big/ {\left(1 \cdot 10^{-5} \frac{1}{K} \cdot 200\ m\right)} \qquad (Eq.\,6.3a)$$

$$\Delta_T = 50\ K = 50°C \qquad (Eq.\,6.3b)$$

The chemical reaction occurring in the concrete will expand equally in all directions when the concrete is unreinforced. With a reinforced concrete slab, the reaction will try to expand in the confined area. Seeing that the expansion will be more active in the longitudinal direction, the modelling of the load is not completely correct. The forces affecting the columns in the transverse direction are over-represented by the current load model. This is considered as an acceptable modelling error in order to create the model and load reactions as close to reality as possible. However, the columns are currently under an independent study and rehabilitation process, so these will not be discussed thoroughly in this thesis.
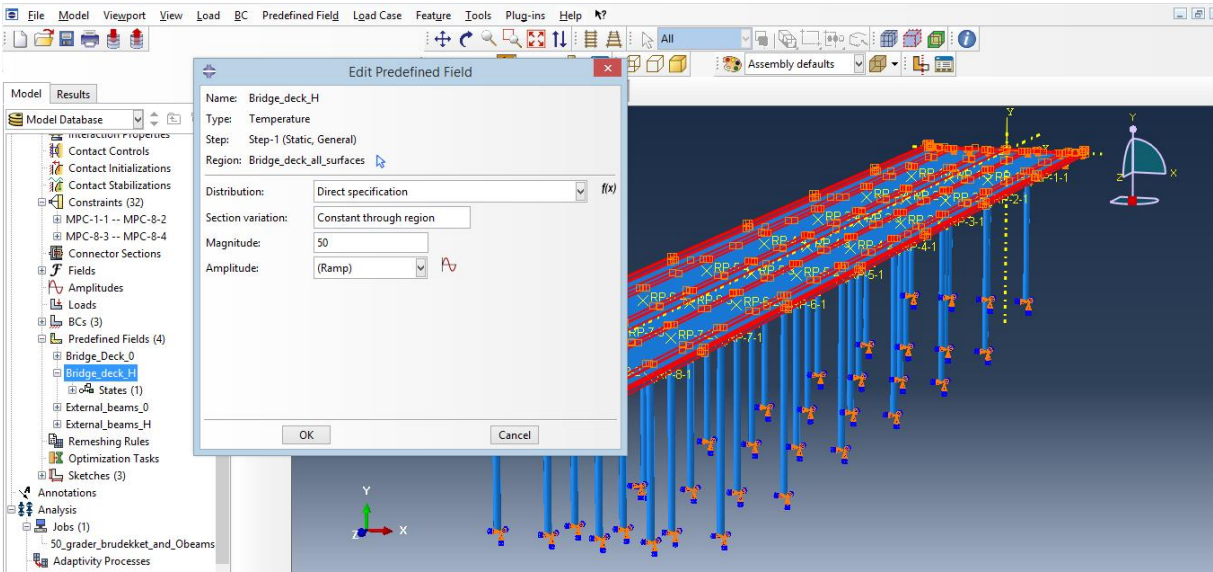
Figure 6.9: Dialogue box in Abaqus for selecting the areas defined with the heat expansion.

54

The model is described the heat expansion through *predefined fields* in Abaqus. These *predefined fields* are areas prescribed with a certain change, in this case the temperature difference. The change needs to be described, in this case as *constant through region*, and the areas needs to be selected. *Figure 6.9* shows the selection box and defined area for the heat expansion of the bridge deck.

The heat expansion is first modelled in only the bridge deck. The second modelling prescribes the heat difference, and expansion to occur in both the bridge deck and outer beams. Due to the high moisture level, this is the current case assumed for Elgeseter Bridge.

6.6 Extraction of results

In order to extract results from Abaqus, the History and Field output for the relevant sections or nodes has to be defined. When they are defined, and the job is completed successfully, the relevant values can be selected visualized or plotted in a chart. Displacement data can be plotted as XY-data from Abaqus, i.e. time on the x-axis and displacement on the y-axis. The extraction of the XY data can either be picked out individually for each set or node, or the average of a selection.
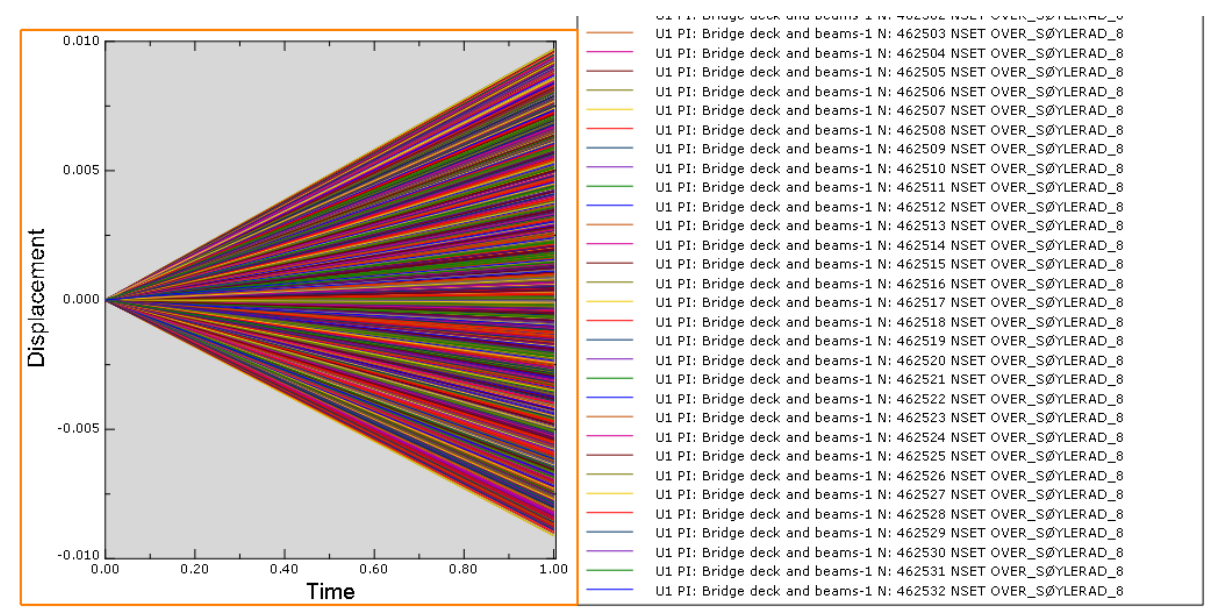
Figure 6.10: Illustration of the XY-plot by Abaqus, here illustrating the displacement in the U1 direction due to the heat expansion.

When the number of results grows larger, and the individual node set extraction becomes time consuming, the average or maximum values of one or several selections is a good method for extraction.

In the case for Elgeseter Bridge, this thesis will focus on the stress distribution on the visualized structure, in order to see the effects from the expansion.

6.6.1 Visualized results for Elgeseter Bridge

The visualization by Abaqus lets you see a plotted scale on each element on the structure. The plot can be scaled on the undeformed or deformed shape of the structure.
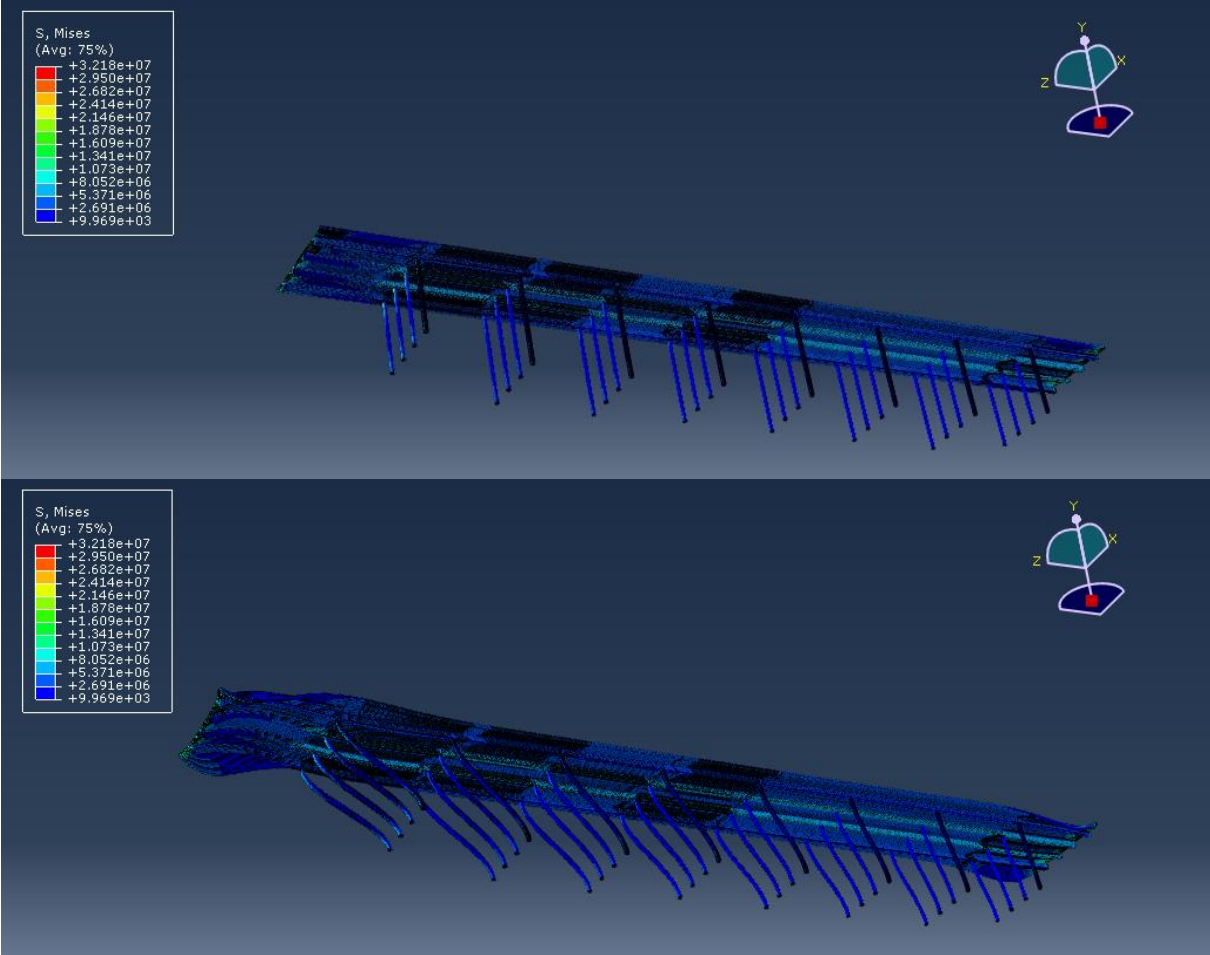
Figure 6.11: Illustration of the visualization on undeformed and deformed shape of Elgeseter Bridge.

The visualization is useful to see the different stress behaviour with different loads. The bridge is loaded with two cases. One case with the expansion occurring in the bridge deck alone. The other case with the expansion occurring in the bridge deck and the outer beams. The inner beams and columns are not prescribed with any expansion or heat load.

7 Frame model

FAP-2D is a two-dimensional analysis program for static and dynamic evaluation. The 2D frame structured model is to analyse the load cases caused from traffic. Which loads to analyse, is described in *Chapter 5*.
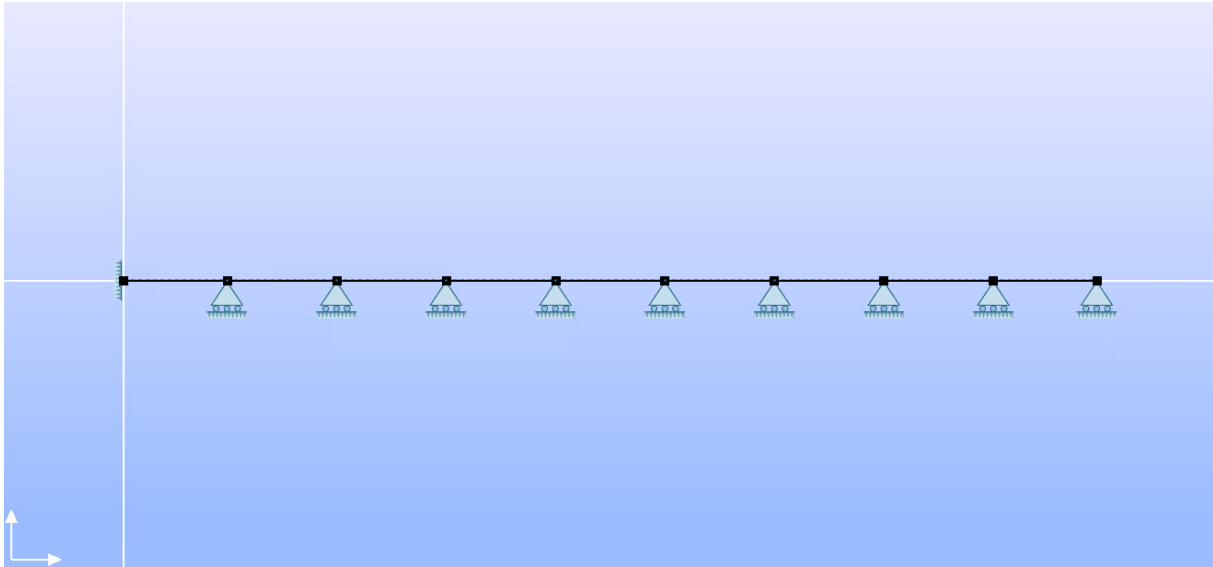
Figure 7.1: Simplified frame model of Elgeseter Bridge in FAP-2D.

7.1 Creating the model

The modelling of the traffic loads can be done either on the entire cross-sectional area of the bridge, or on each notional lane. For most of the loads, the notional lane is the most relevant load modelling method.

The general dimensions and symmetric evaluations of the structure is not relevant for the modelling of the frame model. The bridge deck and beams are modelled as one element across the entire length.

In simple terms, the program utilizes two separate parts. One part for the structural model, as the graphical user interface. The other part is the computational model, the part that derives the results. When using FAP-2D, the GUI (Graphical User Interface) is the only part that can be accessed or altered. The computational part is only influenced by the user through the structural model.

The structural model consists of members that are referred to the global coordinate system. The global coordinate system with X- and Z-axis. Cross-sectional properties are sectioned in a XY-coordinate system, but the model does not contain a Y-axis. The cross-section is specified

for each member, and each member is drawn in the global coordinate system. The Z-axis then becoming the longitudinal direction. Members are connected to each other either by joints or by internal joints. Internal joints creates sub members of an existing members, which are then called the host member.

The model uses standard SI units of kN and m, specified where necessary. A rectangular cross-section for instance, is drawn in units mm x mm, e.g. 500 mm x 1500 mm. Any results are specified in which unit they are, e.g. bending moments in kNm.

7.2 Materials and meshing

The material properties are pre-defined in the program when selecting the material, i.e. concrete for Elgeseter Bridge. These pre-defined materials cannot be altered in the GUI of FAP-2D. However, a new material can be created if necessary. The material properties are not that relevant for the computation of our beam. This because the material properties are only used in the calculation of displacement and capacities, which will not be computed in FAP-2D for this case. Concrete is the material selected in this model. The bridge deck and beams are assumed to react as a uniform material.

The computation of structural members are pre-defined with a set of elements. These elements are loaded by so-called "lumping" from the actual load. The load is specified to act in the end-node of each element, derived from the load acting on the entire member. The
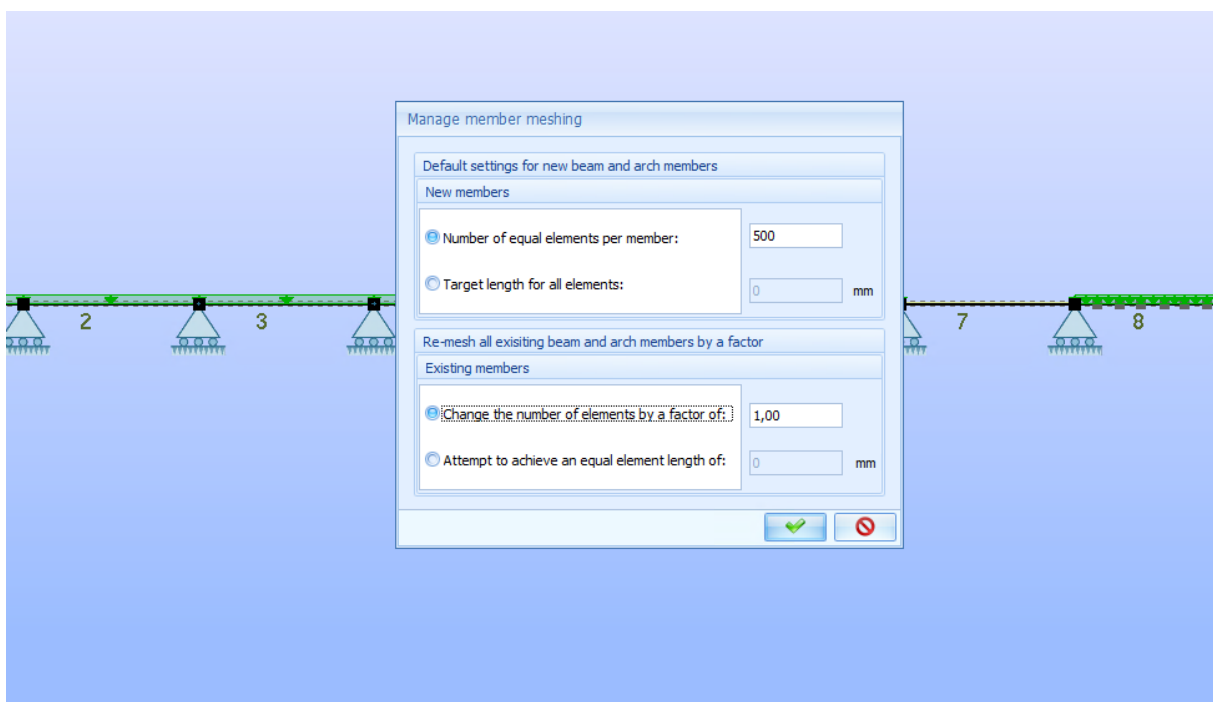
Figure 7.2: Mesh dialogue in FAP-2D.

elements are pre-defined as 50 elements per host member. For this analysis, the amount of elements are increased to the tenfold, i.e. 500 elements per member. If the amount of member are increased too much, the software may experience some numerical difficulties when running the analysis. That also depends on the cross-sectional size, and is not a relevant issue for these analyses.

7.3 Modelling and Parts

For the frame analysis, the different parts in the cross-section are modelled as one. Bridge deck and beams are assumed to work as one, due to that the concrete is cast together. The columns will not be modelled in the 2D analysis, and the different material properties are not necessary to consider.

The model is simplified to not consider the columns as a fixed connection to the bridge deck. The bridge deck is simply supported where the column rows stand.

Parts are modelled as members, where the centre of the cross-section is the line drawn. Each member has the same cross-section and material properties throughout the entire member. There is one exception where the cross-section differs over the member length, but that is for parametric cross-sections and is not relevant in this thesis. Members are connected by joints, and can be sub-divided into sub-members with internal joints. When sub-divided, the members inherit the properties from their host-member, i.e. cross-sectional and material properties.

7.4 Elements, boundary conditions and constraints

When modelling, the first thing that need to be selected is the material and cross-section. After that, the element type is selected. The possible member types to choose are straight beam members, curved beam members, straight bar members, straight cable members and straight strut members. Bar-, cable- and strut members are only loaded by axial tension or compression, or both. Curved beam members are also called arch members, these may have parabolic or circular shape of the beam. The latter, straight beam members, are just called beam members. These are the relevant members for modelling Elgeseter Bridge.

When the joints are defined, the beam members can be drawn and connected to each joint. All beam members will initially be rigidly connected in the joints. The joints can be released for rotation using the *Hinge-button,* as shown in *Figure 7.3 (<mark>REF</mark>)*.
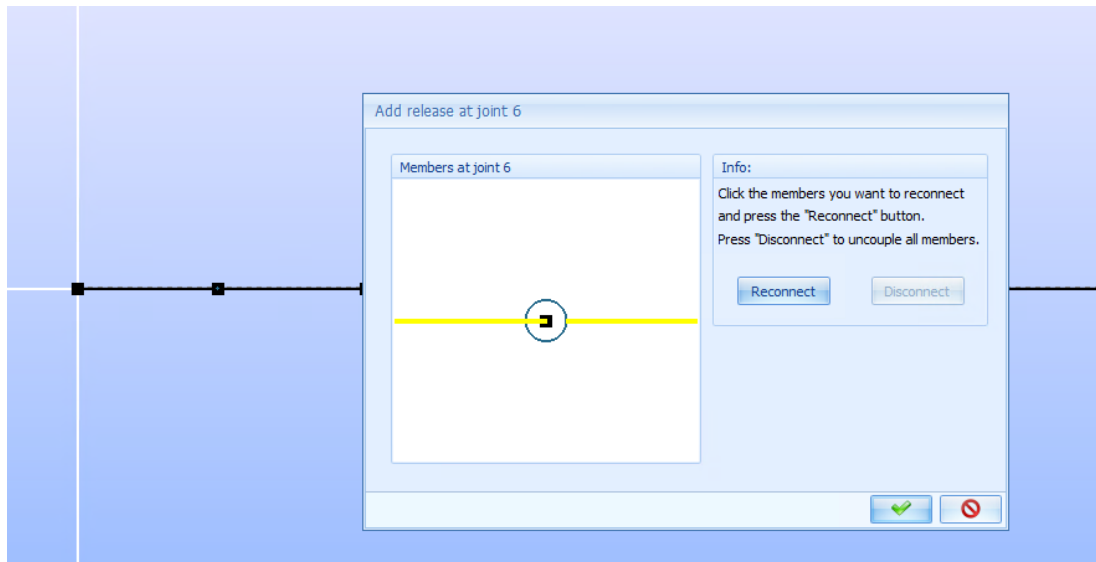
Figure 7.3: The dialog for releasing the rotation in a joint, also called the hinge-button.

The assumptions for the boundary conditions are the same as for the 3D modelling software, when defining the degrees of freedom. The only condition that is different for the 2D-model is the columns. They are not modelled at all, but the column rows are simplified and modelled as boundary conditions. The bridge deck and beams are then supported by eight rolling joints instead of column rows. This assumption does not take into consideration the eccentricity effects the expansion might have had to the columns.

When it is relevant to model a hinge in the span, the hinge can either be modelled before or after modelling the beam element. With the first alternative, the beam is drawn from one joint to the joint that will be the hinge, and then drawn from the hinge joint to the end joint. To make sure the joint resembles a hinge, the hinge-button shows how the joint is connected or disconnected with rotational degrees with the members.

7.5 Load modelling

The loads are either as a simple static load, working alone or in combination, or as a load train. Load trains, or influence lines, evaluate the response for the structural elements with one static force moving in X or Z-direction. The spacing between each separate point of the load train is given, and the entire length of its path is defined for each separate load train. Static

forces can be modelled as either a point load in either direction, distributed loads, defined displacement or strain state.

The loads are modelled one at a time, and placed in one specific point. For the evenly distributed loads, it is necessary to choose type of projection, e.g. horizontal or vertical projection. There are two types of loading that are relevant for this thesis, the point load and the vertically projected, evenly distributed load.

The most unfavourable placements of the point loads can be decided by defining a load train in the analysis. The load train needs to define a load path and load intensity as well as details about placement. The load train iterates a solution for each load placement continuously along the load path. With a load path equal to the total length of the structure, it becomes clear which placement is the most unfavourable.
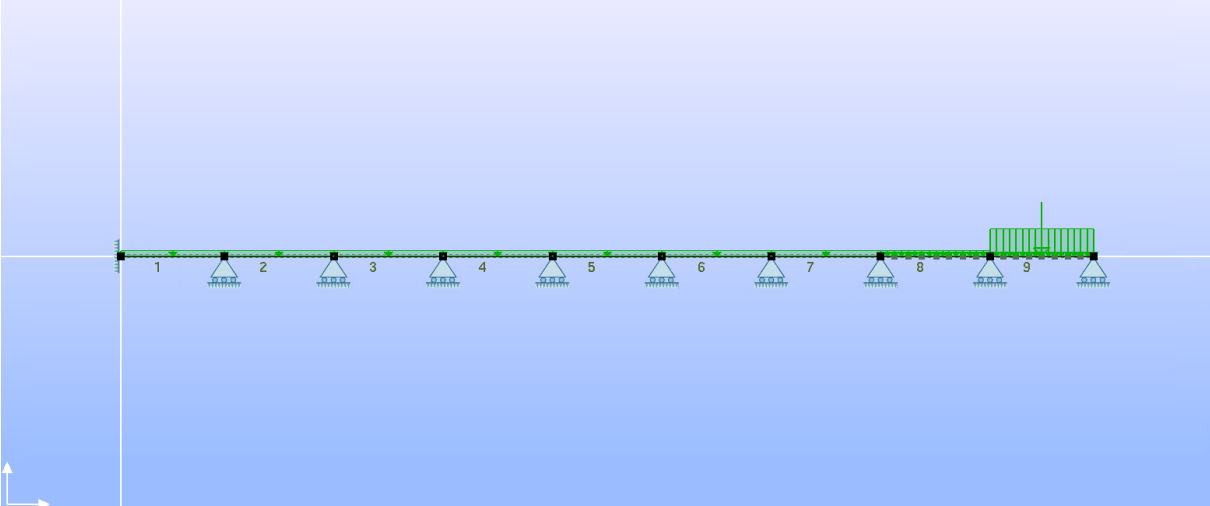
Figure 7.4: Illustration a load combination in FAP-2D.

The loads are combined by editing a Load Combination, LC. When combined, the loads are multiplied with a factor. The multiplication factor here can be utilized as the design factor for combination in ULS.

When the loads are modelled, the values are given for the width of one notional lane. The bridge has four driving lanes, but five notional lanes. The traffic loads are taken up by the cross-section, which is divided into four T-beams. The maximum effective width for a beam is 5.5 metres, which accounts for loads given by one plus 5/6 of a lane. In order to compare the loads with the capacities, they need to be recalculated for the width of a T-beam cross-section. *Equation 7.1* shows how the forces needs to be recalculated in order to be valid for the capacity calculations.

$$M_{d.T-beam} = M_{d.lane} \cdot \left(1 + \frac{5}{6}\right) \qquad (Eq.\,7.1a)$$

$$V_{d.T-beam} = V_{d.lane} \cdot \left(1 + \frac{5}{6}\right) \qquad (Eq.\,7.1b)$$

The Loads relevant to this thesis are the permanent loads given by the self-weight and the live loads given by the traffic loads. The forces due to ASR will be investigated, and the effect a plastic hinge will have on the structure will be analysed.

7.5.1 Traffic Load

The most unfavourable traffic load is the heaviest total vehicle load, with the included axle load and uniformly distributed load. The analysis is made to consider only one notional lane.

The point load is added as a Z-projected point load with the intensity of 40 kN, placed at the most unfavourable location. The evenly distributed load, p, is redistributed to cover the total width of the lane, since its original width is 2 metres. The total vehicle load is evenly distributed across the total vehicle length, which was 16 metres. Both evenly distributed loads are projected as vertical loads.

7.5.2 Self-weight

The self-weight is added as uniformly distributed load, projected vertically on the beams. The self-weight calculated is calculated for the entire bridge. For simplification, and to be quite on the safe side, the self-weight is considered to distribute over the carriageway width, and then recalculated to be valid for the width of a notional lane. The traffic loads relevant for the analysis in FAP-2D are all modelled for the case of one notional lane, i.e. width of 3 metres.

7.5.3 Combinations

The self-weight and traffic load analysis are completed both separately and combined. For the combined analysis, the characteristic traffic loads need to be multiplied with a safety factor of 1.5 in order to fulfil the ULS requirements by the Eurocode [15]. The self-weight needs to be multiplied with a safety factor of maximum 1.2, and minimum 1.0.

Figure 7.4 shows how the load combinations can be added to the structure in FAP-2D. Each load can be added with a different multiplication factor than the others.

7.6 Plastic hinge considerations

The effects due to ASR taken into account in the 2D modelling software, is the effect that will cause the formation of a plastic hinge. The plastic hinge is then modelled as a joint unable to carry bending moment. The joint is modelled where the large crack is observed. For simplification, only the large crack in span 8-9, between column row 7-8, is modelled in this thesis.

8 Designing loads and forces

The other factor important to the ULS is the occurring loads and subsequent forces acting in the relevant cross-sections. Different loads acting on different parts of the structure give different stress and strains. Load models are designed to use the one that gives the most unfavourable effect.

8.1 Self-weight

Table of how the self-weigh contributes to the construction. Designing self-weight is multiplied by a factor of 1.2 in accordance with the Eurocodes.

Self-weight	Over the support	In the span	Crack location
Mgd.max	4 763 kNm	3 200 kNm	365.2 kNm
Vgd	1 242 kN		643 kN

Table 8.1: Maximum design values caused by the self-weight.

The self-weight is recalculated to be valid for the width of a notional lane.

8.2 Traffic loads

How traffic loads are assumed is more thoroughly described in *Chapter 5*.

The most unfavourable traffic load has three systems. One axial load, located inside a vehicle area. One total vehicle load, spread over the vehicle area. And one Uniformly Distributed Load, UDL, outside the vehicle area. The axle load consists of two wheels with the magnitude of 20 kN per wheel. The most unfavourable effect of this load is obtained in two locations, in the span and over the support. Other traffic loads, such as braking forces, are designed in a combination with this load.

Calculations of the analysis are made per notional lane.

8.2.1 Bending moment

Following values are the designing values for bending moment occurring on the structure, due to the traffic loads. The calculations with the joint in the location of the crack will give a different distribution of the forces, and will create a larger bending moment over the support.

Bending moments	Traffic load *on normal structure*	Traffic load *on the hinged structure*
Over the support	1 140 kNm	2 123 kNm
In the span	1 707 kNm	1 500 kNm

Table 8.2: Designing bending moments acting on the structure.

The bending moments are calculated per notional lane.

8.2.2 Shear forces

Shear forces are most unfavourable over supports. The reinforcement drawings show an increased amount of shear reinforcement over the support, due to this. The Eurocode states that shear forces contributing over the support can be reduced to the shear force acting in the distance d, from the support.

Highest recorded shear force in the structure due to traffic loads are 722 kN. The reduced value being equal to 665 kN. For the self-weight the highest value is 1 242 kN, and the reduced value is 1 100 kN. Total contribution on the shear forces is shown in Table 8.X.

Shear forces due to	Over the support	Reduced value
Self-weight	1 242 kN	1 100 kN
Traffic load	465 kN	410 kN
Combination	1 707 kN	1 510 kN

Table 8.3: Designing shear forces acting on the structure.

The axle load creates shear forces in the span, but the design values are on the safe side of capacity.

When the structure is assumed with the plastic hinge, the maximum shear forces acting over the support is 587 kN. The crack experiences 426 kN for the same case. These values are designing values, i.e. the characteristic values multiplied by a factor of 1.5.

8.2.3 Axial forces

The following forces are only caused by the horizontal forces due to braking or acceleration. The designing forces for acceleration or braking are the characteristic values multiplied by the factor 1.5.

The only experienced axial force, N_{Ed}, is 30 kN either as compression or as tension.

8.3 Forces due to ASR

The expansion of the bridge deck that are to be designed for combination with the traffic loads. The combination of the ASR and the frame model are the plastic hinge considerations.

The direct effects from the expansion due to ASR is derived from Abaqus, where the stresses are plotted on the structure. This to see how the stress distributes over the different constructional parts when considering different load models of the temperature. There are two different load models relevant when modelling the expansion. The two relevant models are the bridge deck expanding alone, or bridge deck expanding with the external beams.

The effects ASR contributing to the FAP-2D model is the different load effects caused on the structure due to the formation of the plastic hinge. Calculations for the effects the plastic hinge will cause is further described in *Chapter 10.2*.

8.3.1 Stresses - Visualized results for Elgeseter Bridge

The first case of the heat distribution is the expansion of the bridge deck alone. The analysis of the stress distribution shows slightly increased stress-levels for the outer beams.
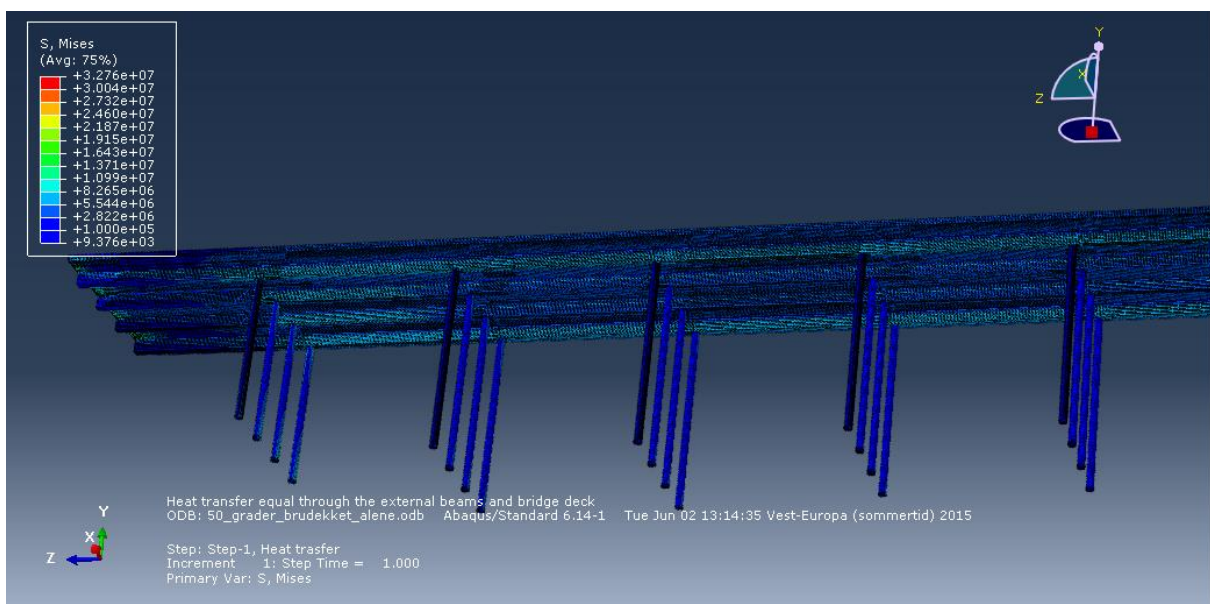
Figure 8.1: Stress distribution on the lower edge of the beam, when the expansion occurs in the bridge deck alone.

Figure 8.1 shows the stress distribution on the lower edge of the bridge deck for the northern end of the structure. The constraints and abutments will experience higher stresses, this due to the confinement of the expansion. The stresses on the outer beams are between 1-10 N/mm^2. The figure shows the inner beams in span 8-9 will also experience a slightly higher stress level than the other spans.

The supported ends will experience stresses in the range slightly over 30 N/mm^2 for both load cases. These stresses might not be realistic due to the uncertainties in modelling and load modelling. These stresses are not considered as critical in this thesis.

When modelling the other load case, the outer beams are given the exact same heat expansion as the bridge deck. Results show that the higher stress levels are now occurring mostly in the inner beams. The inner beams show a stress-distribution over the entire length as shown in *Figure 8.2*. Stresses are in the range between 2-10 N/mm^2.
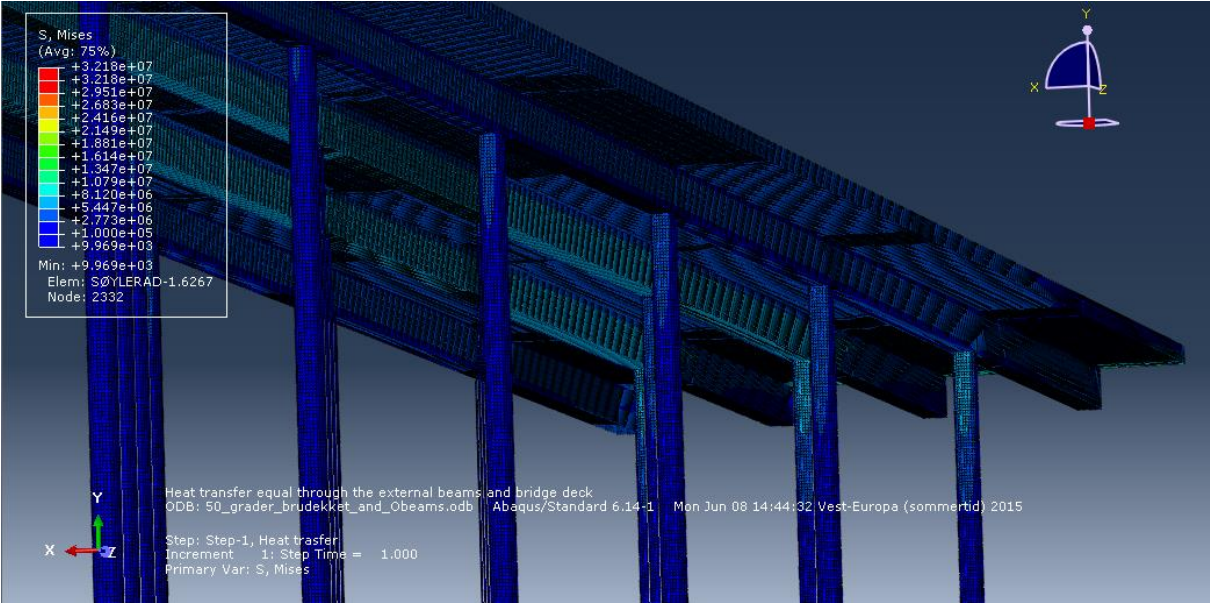
Figure 8.2: Stress distribution of the lower edge of the bridge, when loaded in the bridge deck and outer beams.

Figure 8.2 shows the stress distribution in the lower edge of the bridge for the north end. In this case, the temperature load was given to the bridge deck and outer beams, i.e. the inner beams are the only part not expanding. The brighter the colour, the more intense stress levels. The figure clearly shows that the inner beams are experiencing higher stress levels than the outer beams. In addition, the columns are experiencing stress levels on the south side. The columns with the brightest colours are the columns on the north end, which would be the

elongated end. The columns would experience some eccentricity due to the elongation, and that is the cause for the higher stress levels on the columns.

8.4 Combination of loads

In order to consider the load bearing forces and capacities the relevant loads that work in combination need to be considered in combination.

For the normal case, the traffic loads are combined with the self-weight to create the most unfavourable effects for bending moments and shear forces both in the span and over the supports. The combination and forces are shown in *table 8.4*.

Load	Self-weight	Traffic load	In combination
Bending mom. (sup)	4 763 kNm	1 140 kNm	5 903 kNm
Bending mom.(span)	3 200 kNm	1 707 kNm	5 006 kNm
Shear forces	1 100 kN	410kN	1 510 kN
Axial load	0	30 kN	30 kN

Table 8.4: Combination of traffic loads with self-weight in the normal situation.

For the case considering the effects of the ASR, the case consider the structure to have obtained a plastic hinge in the span 8-9. The plastic hinge affects the structure in such a manner that no bending moment can be carried through the hinge. This changes the static behaviour of the structure, and gives different values for the bending moment.

The self-weight is not relevant to use in this evaluation, so the traffic loads are only combined with each other.

Loads	Plastic hinge	Section in comparison
Bending moment (sup.)	2 123 kNm	1 130kNm
Bending moment (span)	1 500 kNm	1 395 kNm
Shear forces	501 kN	420 kN
Axial forces	30 kN	30 kN

Table 8.5: Design load occurring due to the statical change of the hinge.

Table 8.5 describes the designing loads in the support and span due to the change in static for the traffic loads. The section in comparison has been loaded in the span over the crack, to compare the structural effects.

The loads are calculated for the width of one notional lane, but each capacity is calculated for each T-beam. The maximum width for the T-beams are 5.5 metres, for the inner beams. The traffic loads must then be recalculated to fit the width of the T-beams. In addition, the loads are recalculated with the safety factors from the Aas-Jakobsen report. The capacity with both safety factors are shown in Table 8.6, calculated for the width of a T-beam cross-section.

Design Load effects	Designing load factor from the Eurocode		Designing load factors as stated in the report from Aas-Jakobsen(REF)	
	In the span	Over the support	In the span	Over the support
Bending moment	9 178 kNm	10 822 kNm	8 718 kNm	10 320 kNm
Shear forces		2 933 kN		2 635 kN

Table 8.6: Designing loads calculated for the width of a T-beam cross-section.

9 Ultimate Limit State - ULS

The Ultimate Limit State is defined in the Eurocodes to describe the limits to when a structure will not fulfil its design criteria. The uncertainties when it comes to combining different structural members, as well as loads and deformations. When the criterions for the ULS are fulfilled, the structure contains the necessary strength and stability during loading.

The ULS is the minimum requirement for the classification of bridges, according to the NPRA's handbook R412 [3]. When designing to the ULS, the two parameters most important for the requirements are the material properties with correlating material strength, and the design loads.

9.1 Capacities

The bridge deck with its connected beams can be viewed as one constructional element, simplified to a T-beam cross-section. When
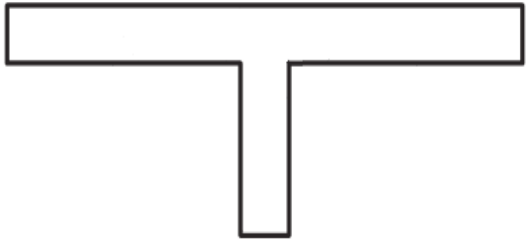
Figure 9.1:Cross-sectional view of a T-beam.

simplified, the total concrete area is equal, but the area is reformed into a perfect T-shaped cross-section, as showed in *Figure 9.1*. The entire width of the beam might not be able to redistribute the forces adequately, hence it is necessary to calculate the effective width of the cross section. *Figure 9.2* shows how the width of the flange is narrowed.
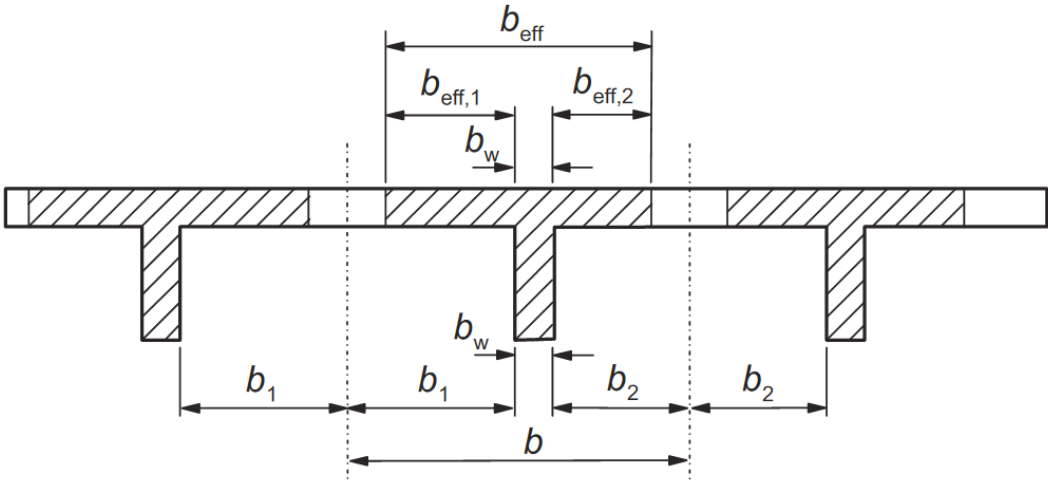
Figure 9.2: Effective width as described in Eurocode 2.

Effective width is dependent on the total width of the T-beam and the effective length, as shown in *Figure 4.8*, in *Chapter 4.6.1.1*. Cross-sectional values for the analysis are as follows:

- B_{max}=5 500 mm.
- Thickness of the flange: 280 mm.
- Height of beam: 1 420 mm.
- Width of beam: 800 mm.

The cross-sectional area is one of the deciding factors for the capacities. The effective width of the flange is calculated from formulas given in EC2 [12].

$$b_{eff} = (0.2 \cdot b) + (0.1 \cdot l_0) \qquad (Eq.\,9.1)$$

The material parameters are important for the calculations, and are as follows:

Material	Material parameter	Characteristic strength	Design strength
Concrete C25	γ_c=1.5, α_{cc}=0.85	16.8 N/mm^2	12 N/mm^2
Reinforcement st.52	γ_s=1.25	340 N/mm^2	272 N/mm^2
Reinforcement st.37	γ_s=1.25	230 N/mm^2	184 N/mm^2

Table 9.1: Material design value in relation to the characteristic value.

Other important parameters for the materials are the Young's modulus, described as follows:

Material	Young's modulus
Concrete	23 300 N/mm^2
Reinforcement st.52	210 000 N/mm^2
Reinforcement st.37	210 000 N/mm^2

Table 9.2: Elasticity modulus for each constructional element.

Capacity checks in the ultimate limit state include safety factors for the materials, in order to take account for the uncertainties.

9.1.1 Bending moment capacity

The bending moment capacity is derived for six different sections, due to different amounts of reinforcement or different statics. Three sections for a cross-section in the span of the beam, since the first and last span is shorter. The other three sections are over the supports, also due to the different length in the spans. The first (and last) support will be subjected to slightly higher loading than the other supports. The first and last span might be subjected to lower bending moments, due to the lower reinforcement amounts in the first and last span.

The six different cross sections are calculated slightly different, depending on which direction the bending moments are assumed to have, and the amount of reinforcement. Calculations are done according to the Eurocode 2 [12] and assessments made in Sørensen [16].

The bending moment capacity depends on the cross-sectional properties, amount and location of reinforcement, and material strength. Design capacity for bending moments in the span:

$$M_{Rd.span} = 0.8 \cdot \alpha_f \cdot (1 - 0.4\alpha_f) \cdot f_{cd} \cdot b_{eff} \cdot d_{eff}{}^2 \qquad (Eq.\,9.2)$$

Design capacity for bending moments over the supports is derived from a similar equation, but parameters are calculated slightly differently.

$$M_{Rd.support} = \left[0.8 \cdot \alpha_s \cdot (1 - 0.4\alpha_s) \cdot f_{cd} \cdot b_w \cdot d_{eff}{}^2 \right] + \left[A_{s.b} \cdot f_{yd} \cdot d \right] \qquad (Eq.\,9.3)$$

Capacities are calculated for two different types of locations. One over the supports, i.e. tension in the top part of the cross-section as well. The other situation is in the span, between the supports, experiencing only tension in the bottom. Each of these locations is then divided in to two more sections, due to variations in the amount of reinforcement. The first span is considered to experience slightly lower bending moments that the rest of the spans, due to the shorter length. The first spans are however assumed to experience higher bending moments, and therefore have more reinforcement than the later spans.

Situation I: Over supports			Situation II: In the span		
Section 1	Section 2	Section 3	Section 1	Section 2	Section 3
11 147 kNm	10 454 kNm	12 040 kNm	6 660 kNm	7 428 kNm	10 193 kNm

Table 9.3: Table of bending moment capacities.

Calculations for capacities are found in the *Appendix C*.

The bending moment acting over the support has tension in the bridge deck, while the bending moment acting over the span has tension in the lower part of the beam. The

maximum designing bending moments from self-weight and traffic loads are found in the last span and over the supports. The maximum bending moments occur in the span where the capacity is highest. The same happens for the bending moments over the span. The bending moments loaded to the structure is inside the capacity of the loaded cross-section.

9.1.2 Shear capacity

Shear capacity is calculated for the four situations, just like the bending moments. The sections in the span has few or no shear tendons to increase the capacity of shear. Thus, the shear capacity in the span is decided from the concrete capacity alone.

The section over the supports has the capacity of the shear tendons in addition. The shear tendons are placed in a 45-degree angle. *Figure 9.4* illustrates the design of shear forces.
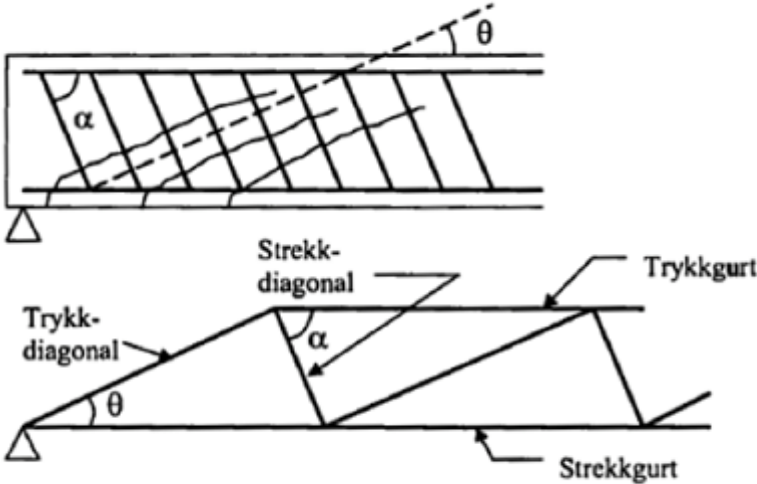
Figure 9.4: Strut-and-tie-model, to illustrate shear force. Sørensen [16].

Total shear capacity is calculated in *Appendix B*. Here also in the two situations, with the two sections each.

Situation I: In the span		Situation II: Over the support	
Section 1	Section 2	Section 1	Section 2
V_{Rd}= 1 434 kN	V_{Rd}= 1 455 kN	V_{Rd}= 2 658 kN	V_{Rd}= 2 817 kN

Table 9.4: Shear capacity in the different sections of the bridge.

Shear forces is not likely to occur in the middle of the spans, but the shear forces increases linearly closer to the supports. The shear tendons are mostly longitudinal reinforcement bent in a 45-degree angle. Some extra tendons are placed over the supports, as shown in the reinforcement drawings. The tendons with an angle is calculated separately from the vertical reinforcement tendons.

The calculated forces in the frame modelling program gives a designing shear force slightly higher than the shear capacity. This is due to the safety factors multiplied with the loads. If the load models are given the safety factors used in Aas-Jakobsen's report [5], the design values for shear forces are barely on the safe side of the capacity.

10 Discussion

As described in *Chapter 4.3* there are two large cracks observed in the inner beams. One crack is observed in the span between column row 7-8, the other crack is observed in the other inner beam between the column row 2-3. The crack in span 8-9 is shown in *Figure 10.1*.

Figure 10.1: Pictures of the large crack in span 8-9, taken by Aas-Jakobsen [9].

If the large cracks observed should be caused by pure bending moments, the cracks should continue in the bridge deck due to the large strains in the compression zone, which would be smaller than the plate thickness in this case.

The large cracks may then only be explained by the cross-section being rotated by the expansion forces and self-weight in the weakest cross-section in longitudinal direction, which happens to be where the cracks are located. The large cracks occurring when the reinforcement goes in the plastic stage.

Smaller cracks are observed in a great magnitude over the entire bridge. The cracks are not observed over the supports, which suggest that the reactions propogating the cracks are caused by a positive bending moment, i.e. tension in the lower edge. The distance between the smaller cracks are between 0.5-1.0 metres, the distance being smaller in the lower edge and larger at the top of the web.

The crack width varies with the reinforcement, and for a general span the average crack width is measured to be 0.5 mm.

10.1 ASR expansion

The expansion of Elgeseter Bridge is assumed to occur in the outer parts of the width, and not as much in the inner beams. This can be caused by several factors, such as the rain and wind causing higher RH on the outer parts. The drainage of the bridge is not functioning as specified may also cause a higher RH in the bridge deck and outer parts. In addition, the state of the membrane under the pedestrian footpath is unknown, and may have caused a higher RH in the outer parts.

If the outer beams and outer bridge deck is assumed to expand alone, then the cracks due to this phenomenon should be observed consistently throughout the entire height, even through the bridge deck. However, the observed cracks are only through the beam, and not the bridge deck. This kind of crack would not occur in such a magnitude (6mm) without the beam being independent from surrounding constructional parts expanding, and we have no current signs suggesting that.

The stress intensities, as shown in *Chapter 8.3*, also corresponds with the assumption. The stress levels observed during inspections coincides with the stress distribution for the case where the bridge deck and beams expand simultaneously.

10.2 Formation of a plastic hinge

The observation of large vertical cracks has occurred in two spans. One span between column row 2-3 and one between columns row 7-8. In these spans there are only observed one large, vertical crack on each inner beam. The crack width observed is up to about 6 mm. The weakest cross-section is in the area where the observed cracks occur. The formation of a plastic hinge is an acceptable assumption, since it will occur in the weakest cross-sectional area.

The longitudinal reinforcement in the span 8-9 (i.e. between column row 7-8), contains 20 Ø32 in the middle of the span. However, the longitudinal reinforcement is bent up in a 45-degree angle to form shear tendons closer to the support. In the area where the crack occurs, the longitudinal reinforcement contains only 3 Ø32, with a bend in the reinforcement just before. The area where the crack occurs is illustrated by the red circle in *Figure 10.2*.
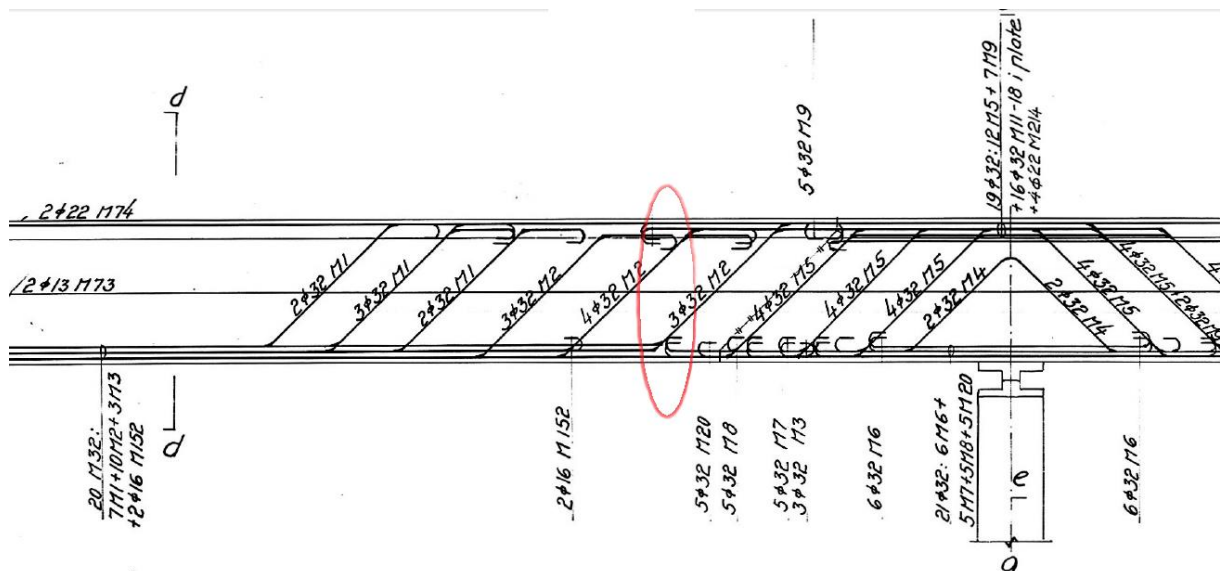
Figure 10.2: Illustration showing where the crack occurs on the reinforcement drawings.

The crack in the other span has similar preconditions with reinforcement amounts.

When a crack like that occurs, the concrete section cannot withstand external or internal loads, and the reinforcement is assumed the only bearer of tension.

It is necessary to consider the effects of yield in the reinforcement when assessing the large cracks. If the stresses in the reinforcement in this cross section reaches the plastic zone it will start to deform. When reaching the plastic zone of the cross-section, deformations are permanent. Given more loading in the plastic zone, yield limit will be reached. When the yield limit is reached, a plastic hinge will form in the cross-section. A plastic hinge will create a deformation of the cross-section and surrounding area.
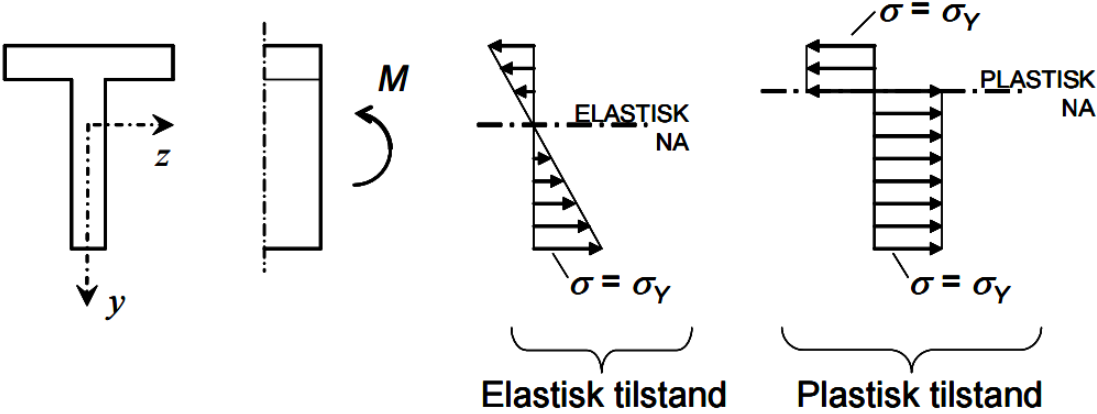
Figure 10.3: Illustration of the elastic and plastic stress distribution in a homogenous T-beam.

When considering a simply supported, straight beam, exposed to linear elongation and curvature, the effects of curvature will not create any withholding- or internal forces. When the beam is elongated, there will be no internal stresses, because the beam can simply curve and elongate without any withholding forces, as shown in *Figure 10.4*.
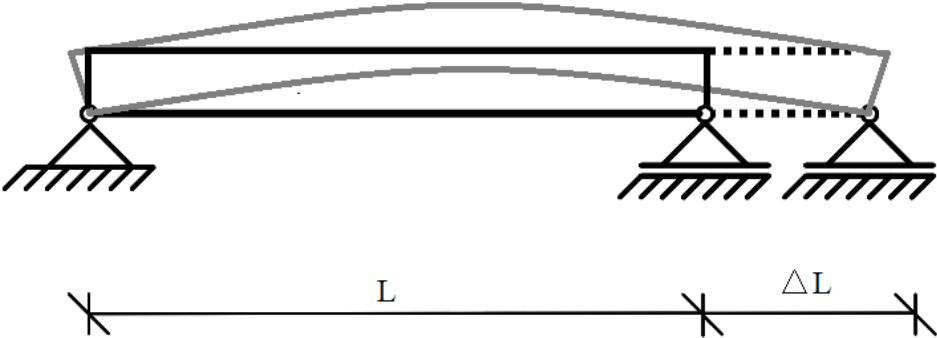
Figure 10.4: Illustration of the curvature and elongation of a simply supported beam.

Then, if we consider a beam fixed in both ends, it is prohibited to expand or rotate at the ends. The curvature expected to occur due to the expansion is then taken up in the supports and creates a restraining bending moment in the end supports. Bending moments in the end supports will create internal forces in the beam, and will affect the capacity of the cross-section. If the expansion is assumed to continuously regenerate and increase its force contribution, the beam will reach yield in a cross-section. When yield occurs, the cross-section forms a plastic hinge. With further expansion after this, the plastic hinge will just increase its displacement.
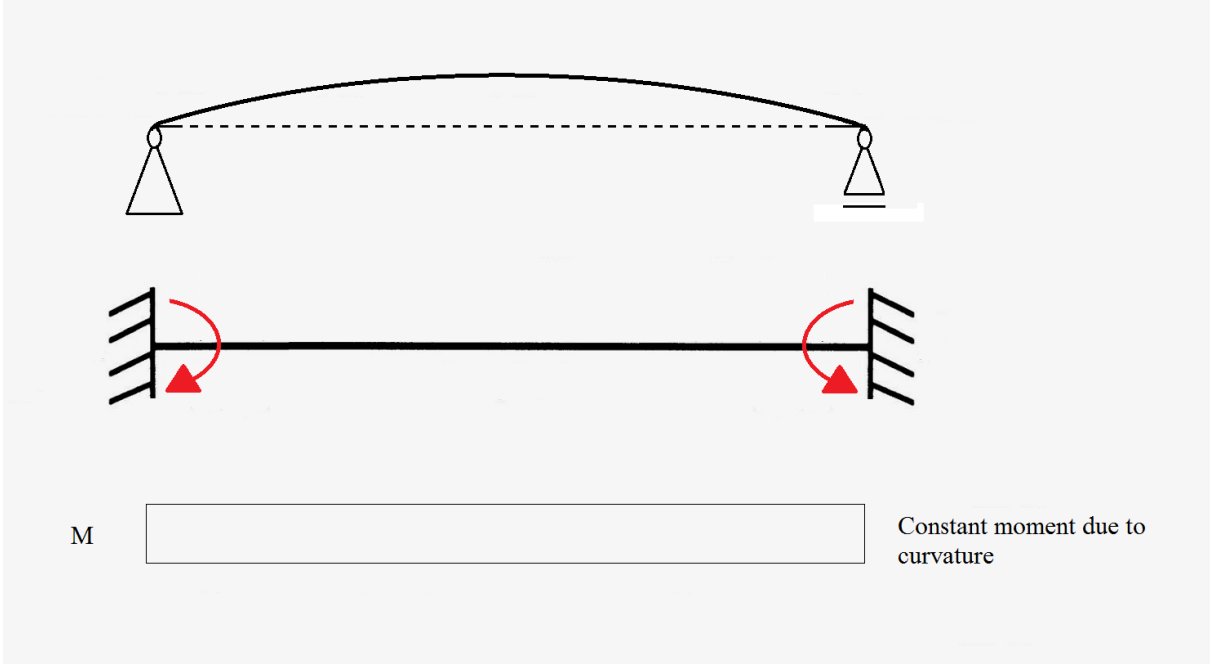
Figure 10.5: Figure illustrating the curvature effect prohibited by the fixed ends creating a constant moment.

Assuming the formed plastic hinge is driven from the forced due to ASR alone, the equation for the rotation would be:

$$\theta = \frac{M_{ASR}}{EI_I} \; (for\ uncracked\ concrete\ section) \qquad (Eq.\,10.1a)$$

$$\theta = \frac{M_{ASR}}{EI_{II}} \; (for\ cracked\ concrete\ section) \qquad (Eq.\,10.1b)$$

When the concrete section cracks, it is assumed that the reinforcement is the only load carrying constructional element. However, the entire structure is not cracked, and in between the cracks the concrete contributes to the load carrying. Therefore, the cracked section can be assumed with an increased capacity, which is more than just for the reinforcement alone.

If the assumed plastic hinge forms, it creates internal forces that exceed the yield-limit for the concrete and reinforcement. When the yield is reached for the concrete in tension, it will crack. When the yield-limit for the concrete is reached, it will lose its tensile strength and bend. If the cracked section, that has created a plastic hinge, is repaired, the concrete can again contribute somewhat to the tensile capacity of the section. In addition, a plastic hinge creates massive compressional forces in the top section of the beam. When the crack is repaired, no additional changes are made for the concrete in the top part of the cross-section. Therefore, the assumed high compression will not change.

Assuming the plastic hinge forms, the cross-sectional area creating the hinge will deform and no longer carry any bending moment. The crack width can be calculated from the strain applied on the structure and the angle of rotation. Likewise, the strain needed to propagate the crack can be derived from the same equations. The total rotation depends on the length and curvature, since the bending moment is constant. The crack width, described by w, can be calculated from the following equation:

$$w = \theta \cdot h' = \left[\left(\frac{\varepsilon_0}{h'} L_1 \right) + \left(\frac{\varepsilon_0}{h'} L_2 \right) \right] \cdot h' \qquad (Eq.\,10.2)$$

The necessary strain in order to propagate a crack of 6 millimetres is calculated to be 0.27 ‰. The height, h', is assumed as the height from the centre of the top plate to the bottom of the beam. The ASR could easily cause this amount of strain by expanding the structure locally. The global elongation of the structure is measured to about 100 mm, which in a straight bar element would cause a strain of 0.5 ‰ (Appendix C). However, the local strains due to the expansion are practically impossible to calculate theoretically. In addition, the actual boundary conditions for one span is not as simple as fixed end supports.

Assumptions made in the Aas-Jakobsen report [5] clearly state that the cracks caused by the expanding ASR will not decrease the capacity of the reinforcement tendons in tension. This is not correct, if one considers the plastic hinge effect. The report also states that the shear reinforcement will not be affected, with the assumption of the shear tendon being intact and effective even with the crack. The tendons for shear reinforcement are longitudinal reinforcement bars bent up in a 45-degree angle. If the crack occurs and the longitudinal reinforcement yields, it is likely that the reinforcement bars bent up might also be affected when creating the plastic hinge. Thus, shear reinforcement might be lacking in the actual section where the crack occurs.

10.2.1 Plastic bending moment

The bending moment needed to drive the reinforcement to yield can be calculated by the maximum capacity of the cross-section.

The relevant cross-section is only reinforced by three longitudinal reinforcement bars with the diameter of 32 millimetres. The reinforcement is in the steel quality st.52, as mentioned in *Chapter 4.6*. The total resistance against bending moment can then be calculated from the following equation to be 984 kNm.

$$M_{Rd} = f_{sd} \cdot A_{s,rel} \cdot \left(d_{rel} - \frac{t}{2} \right) = 983.74 \; kNm \qquad (Eq.\,10.3)$$

The bending moment from the self-weight, in the placement 5 metres out from the support where the crack occurs, is derived to be 365 kNm from the 2D modelling programme. That means the needed bending moment to occur from the ASR expansion and curvature would need to rise to 619 kNm.

When the plastic hinges occurs, even if the structure is loaded, there will be no bending forces occurring in the cross-section. Considering this fact, the traffic loads on the structure will then affect the structure differently. The traffic loads must then be reconsidered after modelling a joint where the crack occurs in the frame model, unable to distribute bending moments. The joint, or hinge, created will affect the bending moment distribution over the span and the support.

The self-weight and expansion load is assumed to propagate the crack, and is therefore not in the evaluation of the loads on the jointed structure. The traffic loads created on the jointed structure will give a larger maximum load for the support than the uncracked situation.

10.3 Consequences of forming a plastic hinge

The assumptions for the crack being caused by the formation of a plastic hinge is supported by several factors. The main factor is that there are two large vertical cracks exiting this behaviour, and these two cracks are in separate spans in separate beams. They occur in the inner beams that are assumed to have a lower rate of ASR occurring. They occur in one span near the North end, and the other occurring close to the South end. The ASR is assumed to have caused stability problems closer to the North end, but the ASR does not affect the surroundings closer to the South end in the same magnitude.

Due to the fact that the ASR occurs in greater magnitude seemingly at random, it is a logical explanation that the structure may be affected with the necessary intensity at local areas. The local intensity may arise to the level where the ASR can cause this plastic hinge to form.

10.3.1 Worst-case scenario

The worst-case scenario is when the plastic hinge is formed solely due to ASR and the self-weight. The reinforcement goes to yield in the three longitudinal reinforcement bars, and in the shear tendons that is occurring in the cross-section. This will mean that the bending moment distribution of traffic loads over the support is affected. In addition, the shear force capacity is affected close to the support, due to the missing capacities in the tendons that yields.

Furthermore, if the hinge is continuously loaded, it will simply displace and form a larger crack. Since both the cracks are injected and strengthened, the cross-section is now stronger and has more capacity for the expanding forces. However, the reinforcement has gone to yield, and will behave as a hinge none the less. The increased strength in the cross-section will only affect the capacity for the expansion forces.

This case may easily occur in any other span as well, given the conditions for ASR are in the same category.

10.3.2 Best-case scenario

If we consider the instability of the structure has contributed to the rotational angle for the crack, the magnitude of the expansive reaction is not as critical. The instability can be caused by the global elongation, in particular for the span between the 7th and 8th column row. Skewed foundations, or the like, can for instance cause the instability for the other span.

If this is the case, the reinforcement has still gone to yield, and the cross-section is not capable of carrying bending moments. The hinge is still formed, but not solely due to the expansion of the ASR. There might still be capacity in the section, but it is not possible to calculate or assume without further examination.

11 Conclusion

The conclusion for this thesis, considering the damages of Elgeseter Bridge, is that the large vertical cracks in the spans are caused by the Alkali-Silica Reaction (ASR) in combination with the self-weight. However, the magnitude of the expansion locally is unknown. Core samples taken on the bridge shows higher occurrence in the outer parts of the bridge deck.

The assumptions of the locations where ASR occurs are found to be valid, based on the findings in the modelling program. The visualizations in Abaqus confirm that if the outer beams expand with the bridge deck, the inner beams will then experience higher stress-levels. If the bridge deck were to expand alone, the outer beams would experience a larger stress-level in the lower edge of the beams, which is not the case for Elgeseter Bridge.

The large vertical cracks are propagated after the cross-sectional capacity for bending moment has reached its yield-limit. The cross-sectional capacity is reached by the adding the ASR effects to the effects of the self-weight. After the cross-section can no longer carry more bending moments, a plastic hinge is created. The formation of the joint in the span means the effects the traffic loads have on the bending moment needs to be redistributed. The shear force capacity might have reached yield in the cross-section where the crack occurs. Further monitoring of the crack location is recommended, even after strengthening the structure.

Calculations and modelling shows that the designing traffic load will be 20% higher over the support when the bending moments are redistributed due to the hinge. The calculations for capacities will be affected by this. Without taking the effects of the hinge into consideration, the occurring forces are lower than the capacities for the loaded cross-sections. The redistribution causes higher bending moments over the support that has the higher cross-sectional capacity. The increase of bending moment is critical for the capacity over the support, in particular for the crack that occurs in span 2-3. This is due to the capacity of the structure being slightly higher for the last spans. The redistributed traffic forces gives a larger bending moment than the capacity for either of the supports in span 2-3.

The designing shear forces are barely on the safe side of capacity. Due to low, or no, observations of shear cracks, the shear reinforcement is considered effective for the structure for the time being. However, inspections and monitoring over a longer period of time is recommended.

References

[1]   Lindegård, S. og Haugen, M. *TKT 4215 Concrete Technology 1 – Chapter 9: Concrete aggregates.* NTNU, institutt for konstruksjonsteknikk. 2005

[2]   Statens vegvesen. Håndbok N400 *Bruprosjektering, Prosjektering av bærende konstruksjoner for det offentlige vegnettet.* 2015

[3]   Statens vegvesen. Håndbok R412 *Bruklassifisering, Laster for klassifisering av bruer og fergekaier i det offentlige vegnett. 2014.*

[4]   Sørensen T.E. og Søraa T., *Historiske Trondheim.* Akademika 2013

[5]   Aas-Jakobsen, Bruer i Trondheim, inspeksjon og reparasjon. *Oppgave 2 Elgeseter Bru. Del 2 av 2.* 2014

[6]   Norsk betong og tilslagslaboratorium, Rapport *Elgeseter bru: Fukt og ekspansjonsmålinger intill24.oktober 2011.Vurdering av fukt, ekspansjon og overflatebehandlinger samt rissutvikling iubehandlede søyler.* Statens vegvesen 2011

[7]   Rambøll Norge AS, *Rapport fra hovedinspeksjon. 14-0406 Elgeseter bru.* Statens vegvesen 2011

[8]   SINTEF byggforsk, *Rehabilitering av brusøyler med alkalireaksjonsskaer*[sic]. *Feltforsøk på Elgeseter Bru. Sluttrapport.* Statens vegvesen 2012

[9]   Aas-Jakobsen, Bruer i Trondheim, inspeksjon og reparasjon. *Oppgave 2 Elgeseter Bru. Del 1 av 2.* 2014

[10]   Aas-Jakobsen, Elgeseter bru – Tilstandskontroll, statiske beregninger. Trondheim. Statens vegvesen 2001

[11]   Standard Norge. NS 3473 *Prosjektering av betongkonstruksjoner - Beregnings- og konstruksjonsregler.* 1998

[12]   Standard Norge. NS-EN 1992-1-1:2004+NA: 2003, *Eurokode 2: Prosjektering av betongkonstruksjoner.* 2008

[13]   Standard Norge. NS-EN 1991-2:2003+NA2010 *Eurokode 1: Laster på konstruksjoner – Del 2: Trafikklast på bruer.* 2010

[15]   Standard Norge. NS-EN 1990: 2002+NA:2008 *Eurokode: Grunnlag for prosjektering av konstruksjoner.* 2002

[16]   Sørensen S.I. *Betongkonstruksjoner - Dimensjonering etter NS 3473/1989.* Tapir Forlag. 1989

[17]   Bell K., A windows-based program for static and dynamic analysis of 2D-frame

structure, user's manual. 2014

[18]   Aas-Jakobsen, *Rapport fra spesialinspeksjon 2012. 16-0406 Elgeseter bru*. Statens vegvesen 2012.

[19]   Statens vegvesen, Region midt. *Rapport for rehabilitering av Elgeseter bru. 2014*

[20]   Øverli J.A. og Sørensen S.I. *TKT4222 Concrete Structures 3 – Compendium*, institutt for konstruksjonsteknikk. NTNU. 2013

[22]   Jensen V. Elgeseter Bridge: humidity and expansion measurements till 5 September 2002. Assessment of treatment with 3 types of monosilane on columns. NBTL report no. R02001; 2002

[23]   Johansen H. NTNU: *TKT6003 Prosjektering av bruer 1 - Praktisk prosjektering av etteroppspente betongbruer.* Statens vegvesen Vegdirektoratet. 2013

[24]   Jensen V. *Elgeseter Bridge in Trondheim Damaged by Alkali Silica Reactions: Microscopy, expansion and relative humidity measurements, treatments with mono silanes and repair.* NBTL 2003.

[25]   Dassault Systèmes, *Abaqus Analysis User's Manual* 2007.

[26]   Smeplass S. *TKT4215 Concrete Technology 1 - Kapittel 12: Strength of Concrete.* NTNU, institutt for konstruksjonsteknikk. 2003

[27]   Larsen P.K., Clausen A.H. og Aalberg A. *Stålkonstruksjoner - Profiler og formler.* Tapir akademisk forlag. 2003

[28]   Standard Norge. NS-EN 1991-1-1:2002+NA2008 *Eurokode 1: Laster på konstruksjoner Del 1-1: Allmenne laster - Tetthet, egenvekt og nyttelaster i bygninger.* 2008

[29]   Norsk betongforening, *Betongtavlen 2004*, Elgeseter bru og Vardåsen kirke. 2004
       http://www.betong.net/ikbViewer/Content/750395/Betongtavlen%2004-LR.pdf
       (hentet den 16.01.15)

[30]   Wisniewski M og Wojslaw K, *Nonlinear and Time Dependendt Analysis of a Concrete Bridge Suffering from Alkali-Silica Reaction.* Masteroppgave, NTNU, institutt for konstruksjonsteknikk. 2014

[31]   Larsen P.K. *Dimensjonering av stålkonstruksjoner*. Tapir akademisk forlag. 2010

Appendices

II

APPENDIX A

Calculations for Self-weight

IV

Egenvekt - Elgeseter Bru

$$l_{tot} := 220m$$

Total length of bridge: 220m. Total span equals 200m. Total width of the bridge 23.5m.

$$l_{span} := 200m$$

Largest thickness of bridge slab equals 380mm (in the centre of the bridge). Cross-sectional area taken from the design drawings og the bridge.

$$B_{tot} := 23.4m$$

1.1 Bridge deck and beams - Area:
Cross sectional properties

$$\gamma_c := 25\frac{kN}{m^3}$$

Slab of 150mm continously across entire width

$$A_1 := 150mm \cdot B_{tot}$$

"Triangles" at the edge part of slab

$$A_2 := 2\left[\left(\frac{50mm \cdot 180mm}{2}\right) + \left(\frac{80mm \cdot 2300mm}{2}\right)\right]$$

"Leftovers" of the bridge deck (inkl. tram rails)

$$A_3 := 2\cdot\left[(80mm \cdot 9000mm) + \left[\frac{(230mm - 80mm)\cdot 9000mm}{2}\right]\right]$$

$$A_3 = 2\cdot\left[(80mm \cdot 9000mm) + \left(\frac{150 \cdot mm \cdot 9000mm}{2}\right)\right]$$

Edges of the bridge deck

$$A_4 := [350mm(620mm - 150mm)]\cdot 2$$

Beams

$$A_5 := (800mm \cdot 1430mm)\cdot 4$$

$$A_{tot} := A_1 + A_2 + A_3 + A_4 + A_5 = 11.398\,m^2$$

Total Area of cast-in-place concrete

$$A_{tot} = 1.14 \times 10^7 \cdot mm^2$$

$$g_{c.1} := \gamma_c \cdot A_{tot} = 284.95\frac{kN}{m}$$

1.2 Selfweight due to cast-in-place concrete

Wear and tear layer varies in thickness acc. to the drawings. Also, there has been additions on the layer over the years.
Assumed value is from drawings/reports.

$$A_{w.1} := (150mm \cdot 9000mm)\cdot 2 = 2.7 \times 10^6 \cdot mm^2$$

$$A_{w.2} := (30mm \cdot 1900mm)\cdot 2 = 1.14 \times 10^5 \cdot mm^2$$

Pedestrian footpath concists of 6cm reinforced concrete plates, held up by two supports of 100mm x 350mm (350 as a mean of 300 and 400mm).

$$A_p := [(60mm \cdot 2000mm) + 2\cdot(100mm \cdot 350mm)]\cdot 2$$

$$A_{e.c.1} := (200mm \cdot 350mm)\cdot 2$$

Two types of "kantstein"

$$A_{e.c.2} := \left[(200mm \cdot 360mm) + (110 \cdot mm \cdot 60mm) + \left(\frac{60mm\frac{250mm}{2}}{2}\right)\right]\cdot 2$$

Total area of wear surfaces: $A_w := A_{w.1} + A_{w.2} + A_p + A_{e.c.1} + A_{e.c.2} = 3.499 \times 10^6 \cdot mm^2$

Wear surfaces are not all the same materials, but the material properties for each is not wildly different from each other when it comes to selfweight.

$$\gamma_w := \gamma_c = 25 \cdot \frac{kN}{m^3} \qquad\qquad g_w := \gamma_w \cdot A_w = 87.468 \frac{kN}{m}$$

Railings: 0.5 kN/m

$$g_r := 0.5 \frac{kN}{m}$$

Added weight from N400 (brubelegning)

Footpath = 7 metres

$$W_{add1} := 2.0 \frac{kN}{m^2} \qquad g_{a.1} := W_{add1} \cdot 7m = 14 \frac{kN}{m}$$

Carriageway = 16.5 metres

$$W_{add2} := 3.50 \frac{kN}{m^2} \qquad g_{a.2} := W_{add2} \cdot 16.5m = 57.75 \frac{kN}{m}$$

1.3 Line load placed on structure

$$g_{1.k} := g_{c.1} + g_w + g_r + g_{a.2} = 430.668 \frac{kN}{m}$$

1.4 Surface load placed on structure

Load carrying surfaces of the selfweight, is modelled to be the top surface of the bridge deck. To ensure correct load, the line load is divided by the width of the load carrying surfaces.

$$b_{brubane.tot} := 23.5m \qquad\qquad G_{1.k} := \frac{g_{1.k}}{b_{brubane.tot}} = 18.326 \frac{kN}{m^2}$$

1.5 Line load placed on notinal lane

Loads occuring in the notional lane, derived from the line load calculated for the entire bridge deck. One notional lane is designed with the width of 3 metres, the total line load for one notional lane of the structure then becomes:

$$w_1 := 3m \qquad\qquad b_t := 5.5m \cdot 4$$

$$\frac{g_{1.k}}{b_t} = 19.576 \frac{kN}{m^2} \qquad g_{lane.k} := \frac{g_{1.k}}{b_t} \cdot w_1 = 58.727 \frac{kN}{m} \qquad g_{lane.d} := g_{lane.k} \cdot 1.2 = 70.473 \frac{kN}{m}$$

APPENDIX B

Cross-sectional parameters and capacities.

VIII

B.1 Kapasiteter - T-bjelke tversnitt

Krav og regulations er hentet fra NS-EN 1992-1-1,

$$\gamma_c := 1.4 \qquad \gamma_s := 1.25$$

Tverrsnittet av brudekket er ikke kontinuerlig, og det ytterste delen av dekket er det tynneste. Ved bruk av t-bjelke metoden antaes det samme tverrsnittsareal, men bredden tilpasses da slik at den er kontinuerlig over flensbredden.

$$f_{ck} := 16.8 \, \frac{N}{mm^2} \quad f_{cd} := 12 \, \frac{N}{mm^2} \qquad f_{yk.32} := 343 \, \frac{N}{mm^2} \quad f_{yd.32} := \frac{f_{yk.32}}{\gamma_s} = 274.4 \cdot \frac{N}{mm^2}$$

$$h_{tot} := 1700mm \quad b_{tot} := 5500mm \qquad b_{beam} := 800mm \qquad h_{deck} := 280mm \qquad\qquad t_f := h_{deck}$$

$$h_{beam} := h_{tot} - h_{deck} = 1420 \cdot mm \qquad f_{yk.22} := 230 \, \frac{N}{mm^2} \qquad\qquad f_{yd.22} := \frac{f_{yk.22}}{\gamma_s} = 184 \cdot \frac{N}{mm^2}$$

Bjelketversnitt forenkles som en t-bjelke med platetykkelse 280mm, flensbredder som totalt tilsvarer en bredde på 5500mm, og høyde på bjelke som utgjør 1700mm fra topp av plate til bunn av bjelke. Bjelkebredden er 800mm, som i modellen.

Flytegrensen til stålet avhenger av hvilke ståltype. Fastheter til stål er derfor notert med enten 32 eller 22, som henviser til kvaliteten for armeringsjern med diameter hhv Ø32 og Ø22. Som forklart i oppgaven, er stålkvaliteten for armeringsjern med diameter Ø32 *St.52*, og for armeringsjern med diameter Ø32 er stålkvaliteten *St.37*.

B.1.1 Effektiv flensbredde:

For bestemmelsen av effektiv flensbredde, bestemmes avstanden L_0 for hvert enkelt snitt som er av betydning i lengderetning. Det er tre snitt som blir bestemmende for den effektive flensbredden.

Snitt 1 - Over første (og siste) opplager og spen.
Snitt 2 - Over opplager (søyler)
Snitt 3 - Mellom opplager (søyler)

Snitt 1
$$l_{1.1} := 21.25\,m \qquad l_{0.1} := 0.85 \cdot l_{1.1} = 18.063\,m$$

Snitt 2
$$l_{1.2} := 21.25\,m \quad l_{2.2} := 22.5\,m \qquad l_{0.2} := 0.15 \cdot \left(l_{1.2} + l_{2.2}\right) = 6.563\,m$$
$$l_{1.2.2} := 22.5\,m \quad l_{2.2.2} := 22.5\,m \qquad l_{0.2.2} := 0.15 \cdot \left(l_{1.2.2} + l_{2.2.2}\right) = 6.75\,m$$

$$l_{2.3} := 22.5\,m \qquad l_{0.3} := 0.7 \cdot l_{2.2} = 15.75\,m$$

Snitt 1
$$b_w := b_{beam} \qquad b_1 := \frac{b_{tot} - b_{beam}}{2} = 2.35\,m \qquad b_2 := b_1$$

Snitt 3
$$b_{eff.1.1} := \left(0.2 \cdot b_1\right) + 0.1 \cdot l_{0.1} = 2.276\,m \quad < \quad 0.2 \cdot l_{0.1} = 3.613\,m \qquad OK!$$

$$b_{eff.2.1} := \left(0.2 \cdot b_2\right) + 0.1 \cdot l_{0.1} = 2.276\,m \quad < \quad 0.2 \cdot l_{0.1} = 3.613\,m \qquad OK!$$

$$b_{eff.1} := b_{eff.1.1} + b_{eff.2.1} = 4.553\,m \quad < \quad b_{tot} = 5.5\,m \qquad OK!$$

Snitt 2
$$b_w = 1 \cdot b_{beam} \qquad b_1 = 1 \cdot \frac{b_{tot} - b_{beam}}{2} \qquad\qquad b_2 = 1 \cdot b_1$$

$$b_{eff.1.2} := \left(0.2 \cdot b_1\right) + 0.1 \cdot l_{0.2} = 1.126\,m \quad < \quad 0.2 \cdot l_{0.2} = 1.313\,m \qquad OK!$$

$$b_{eff.2.2} := \left(0.2 \cdot b_2\right) + 0.1 \cdot l_{0.2} = 1.126\,m \quad < \quad 0.2 \cdot l_{0.2} = 1.313\,m \qquad OK!$$

$$b_{eff.2} := b_{eff.1.2} + b_{eff.2.2} = 2.252\,m \quad < \quad b_{tot} = 5.5\,m \qquad OK!$$

Snitt 3
$$b_w = 1 \cdot b_{beam} \qquad b_1 = 1 \cdot \frac{b_{tot} - b_{beam}}{2} \qquad\qquad b_2 = 1 \cdot b_1$$

$$b_{eff.1.3} := \left(0.2 \cdot b_1\right) + 0.1 \cdot l_{0.3} = 2.045\,m \quad < \quad 0.2 \cdot l_{0.3} = 3.15\,m \qquad OK!$$

$$b_{eff.2.3} := \left(0.2 \cdot b_2\right) + 0.1 \cdot l_{0.3} = 2.045\,m \quad < \quad 0.2 \cdot l_{0.3} = 3.15\,m \qquad OK!$$

$$b_{eff.3} := b_{eff.1.3} + b_{eff.2.3} = 4.09\,m \quad < \quad b_{tot} = 5.5\,m \qquad OK!$$

B.1.2 Effektive flensbredder og armering:

Pga forskjellig armeringsmengde i lengderetning, må de tre hovedsnittene deles opp ytterligere. Det snittet som er dimensjonerende brukes videre i kapasitetsberegningene. $B_{eff.2}$ og $B_{eff.3}$ er konservative beregninger for de første og siste spenn og støtter.

X

B.1.3 Beregning av nøytralakse, ser kun på betongbidraget:

$$x_1 := \frac{h_{deck}}{2} = 140 \cdot mm \qquad x_2 := \frac{h_{beam}}{2} = 710 \cdot mm \qquad A_2 := x_2 \cdot b_{beam} = 568 \cdot 10^3 mm^2$$

Snitt 1 $\qquad A_{1.1} := x_1 \cdot b_{eff.1} = 637.35 \cdot 10^3 mm^2 \qquad A_{tot.1} := A_2 + A_{1.1} = 1205.35 \cdot 10^3 mm^2$

Snitt 2 $\qquad A_{1.2} := x_1 \cdot b_{eff.2} = 315.35 \cdot 10^3 mm^2 \qquad A_{tot.2} := A_2 + A_{1.2} = 883.35 \cdot 10^3 mm^2$

Snitt 3 $\qquad A_{1.3} := x_1 \cdot b_{eff.3} = 572.6 \cdot 10^3 mm^2 \qquad A_{tot.3} := A_2 + A_{1.3} = 1140.6 \cdot 10^3 mm^2$

Snitt 1 $\qquad x_{na.1} := \dfrac{(x_1 \cdot A_{1.1}) + [(x_2 + h_{deck}) \cdot A_2]}{A_{tot.1}} = 540.548 \cdot mm$

Snitt 2 $\qquad x_{na.2} := \dfrac{(x_1 \cdot A_{1.2}) + [(x_2 + h_{deck}) \cdot A_2]}{A_{tot.2}} = 686.556 \cdot mm$

Snitt 3 $\qquad x_{na.3} := \dfrac{(x_1 \cdot A_{1.3}) + [(x_2 + h_{deck}) \cdot A_2]}{A_{tot.3}} = 563.286 \cdot mm$

B.1.4 Annet arealmoment

$$I_z := \Sigma \cdot \frac{b_i \cdot h_i^3}{12} + \Sigma \cdot A_i \cdot (x_i - x_{na})^2$$

Snitt 1 $\qquad\qquad\qquad\qquad\qquad I_{1.1} := \frac{1}{12} b_{eff.1} \cdot h_{deck}^3 = 8.328 \times 10^9 \cdot mm^4$

$\qquad\qquad\qquad\qquad\qquad\qquad I_2 := \frac{1}{12} \cdot b_{beam} \cdot h_{beam}^3 = 1.909 \times 10^{11} \cdot mm^4$

$$I_{z.1} := I_{1.1} + [A_{1.1} \cdot (x_{na.1} - x_1)^2] + I_2 + [A_2 \cdot [(x_2 + h_{deck}) - x_{na.1}]^2] = 4.162 \times 10^{11} \cdot mm^4$$

Snitt 2 $\qquad\qquad\qquad\qquad\qquad I_{1.2} := \frac{1}{12} b_{eff.2} \cdot h_{deck}^3 = 4.121 \times 10^9 \cdot mm^4$

$$I_{z.2} := I_{1.2} + [A_{1.2} \cdot (x_{na.2} - x_1)^2] + I_2 + [A_2 \cdot [(x_2 + h_{deck}) - x_{na.2}]^2] = 3.415 \times 10^{11} \cdot mm^4$$

Snitt 3 $\qquad\qquad\qquad\qquad\qquad I_{1.3} := \frac{1}{12} b_{eff.3} \cdot h_{deck}^3 = 7.482 \times 10^9 \cdot mm^4$

$$I_{z.3} := I_{1.3} + [A_{1.3} \cdot (x_{na.3} - x_1)^2] + I_2 + [A_2 \cdot [(x_2 + h_{deck}) - x_{na.3}]^2] = 4.044 \times 10^{11} \cdot mm^4$$

B.2 Bøyemomentkapasitet:

B.2.1: Over støtter er det tre forskjellige armeringsmengder, j.fr. tegninger.

De to svakeste sees på her:

$h := 1750mm$ $\qquad$ $\emptyset32 := 32mm$ $\qquad$ $\emptyset22 := 22mm$ $\qquad$ $b_{eff.2} = 2252.5 \cdot mm$

$b_w = 800 \cdot mm$ $\qquad$ $c_{nom.1} := 55mm$ $\qquad$ $c_{nom.2} := 90mm$

$n_{top.1.\emptyset32} := 30$ $\qquad$ $n_{top.1.\emptyset22} := 3$ $\qquad$ $n_{b.1.\emptyset32} := 13$ $\qquad$ $n_{tot} := 30 + 3 + 13 = 46$

$$A_{s.tot.1} := \left[\pi \left(\frac{\emptyset32}{2}\right)^2 \cdot \left(n_{top.1.\emptyset32} + n_{b.1.\emptyset32}\right)\right] + \left[\pi \cdot \left(\frac{\emptyset22}{2}\right)^2 \cdot n_{top.1.\emptyset22}\right] \quad A_{32} := A_{\emptyset32} \qquad A_{22} := A_{\emptyset32}$$

$$A_{s.tot.1} = 35.723 \cdot 10^3 \cdot mm^2 \qquad A_{\emptyset32} := \pi \cdot \left(\frac{\emptyset32}{2}\right)^2 = 804.248 \cdot mm^2 \qquad A_{\emptyset22} := \pi \cdot \left(\frac{\emptyset22}{2}\right)^2$$

$$d_{x.1} := \frac{\left[A_{32} \cdot f_{yd.32} \cdot \left[\left(x_{2.1} \cdot 8\right) + \left(x_{2.2} \cdot 6\right) + \left(x_{2.3} \cdot 6\right) + \left(x_{2.4} \cdot 8\right) + \left(x_{2.5} \cdot 2\right)\right]\right] + \left(A_{22} \cdot f_{yd.22} \cdot x_{2.6} \cdot 3\right)}{\left(43 \cdot A_{\emptyset32} \cdot f_{yd.32}\right) + \left(3 \cdot A_{\emptyset22} \cdot f_{yd.22}\right)}$$

$$A_{s.bunn.1} := \left[\pi \cdot \left(\frac{\emptyset32}{2}\right)^2 \cdot n_{b.1.\emptyset32}\right] = 10.455 \cdot 10^3 \cdot mm^2$$

$x_{2.1} := 71mm$ $\qquad$ $n_{x.1} := 8$ $\qquad$ $x_{2.2} := 106mm$ $\qquad$ $n_{x.2} := 6$ $\qquad$ $x_{2.3} := 132mm$ $\qquad$ $n_{x.3} := 6$

$x_{2.4} := 136mm$ $\qquad$ $n_{x.4} := 8$ $\qquad$ $x_{2.5} := 516mm$ $\qquad$ $n_{x.5} := 2$ $\qquad$ $x_{2.6} := 291mm$ $\qquad$ $n_{x.6} := 3$

$$b_x := \frac{[5 \cdot (71mm + 65mm)] + (8 \cdot 71mm)}{13} = 96 \cdot mm$$

$d_{x.1} = 106.969 \cdot mm$ $\qquad$ $d_{mean.1} := h - d_{x.1} = 1643.031 \cdot mm$

$d_{b.x} := h - b_x = 1.654\ m$

Underarmert tverrsnitt:

$$\alpha_s := \frac{\left(f_{yd.32} \cdot 33 \cdot A_{\emptyset32}\right) + \left(f_{yd.22} \cdot 2 \cdot A_{\emptyset22}\right) - \left(A_{s.bunn.1} \cdot f_{yd.32}\right)}{0.8 \cdot f_{cd} \cdot b_w \cdot d_{mean.1}} = 0.361$$

Kapasitetskontroll

$$M_{Rd.1} := \left[0.8 \cdot \alpha_s \cdot \left[1 - \left(0.4 \cdot \alpha_s\right)\right] \cdot f_{cd} \cdot b_w \cdot d_{mean.1}^2\right] + \left(A_{s.bunn.1} \cdot f_{yd.32} \cdot d_{b.x}\right) = 11.147 \cdot 10^3 \cdot kN \cdot m$$

B.2.2 Snitt 2:

$n_{top.2.\varnothing 32} := 28$ $n_{top.2.\varnothing 22} := 5$ $n_{b.2.\varnothing 32} := 17$ $n_{tot.2} := 28 + 5 + 17 = 50$

$A_{s.top.\varnothing 32} := n_{top.2.\varnothing 32} \cdot A_{\varnothing 32}$ $A_{s.top.\varnothing 22} := n_{top.2.\varnothing 22} \cdot A_{\varnothing 22}$ $A_{s.b.2} := n_{b.2.\varnothing 32} \cdot A_{\varnothing 32}$

$A_{s.tot.2} := A_{s.top.\varnothing 32} + A_{s.top.\varnothing 22} + A_{s.b.2} = 38.092 \cdot 10^3 \cdot mm^2$

$A_{s.tot.1} = 35.723 \cdot 10^3 \cdot mm^2$ $A_{s.strekk.2} := A_{s.b.2} = 1.367 \times 10^4 \cdot mm^2$

$x_{\varnothing 32\_1} := 71\,mm$ $n_{x\_1} := 6$ $x_{\varnothing 32\_2} := 106\,mm$ $n_{x\_2} := 16$ $x_{\varnothing 32\_3} := 136\,mm$ $n_{x\_3} := 6$

$x_{\varnothing 22\_4} := 66\,mm$ $n_{x\_4} := 2$ $x_{\varnothing 22\_5} := 291\,mm$ $n_{x\_5} := 3$

$$x_{top\_1} := \frac{\left[A_{32} \cdot f_{yd.32} \cdot \left[\left(x_{\varnothing 32\_1} \cdot 6\right) + \left(x_{\varnothing 32\_2} \cdot 16\right) + x_{\varnothing 32\_3} \cdot 6\right]\right] + \left(A_{22} \cdot f_{yd.22} \cdot x_{\varnothing 22\_5} \cdot 3\right)}{\left[\left(A_{s.top.\varnothing 32} + A_{s.b.2}\right) \cdot f_{yd.32}\right] + \left(A_{s.top.\varnothing 22} \cdot f_{yd.22}\right)}$$

$x_{top\_1} = 75.634 \cdot mm$ $d_{mean.2} := h - x_{top\_1} = 1674.366 \cdot mm$

$d_{b.x} = 1.654\,m$

Underarmert tverrsnitt:

$$\alpha_{.s} := \frac{f_{yd.32} \cdot \left(A_{s.top.\varnothing 32} - A_{s.b.2}\right) + f_{yd.22} \cdot 5 \cdot A_{\varnothing 22}}{0.8 \cdot f_{cd} \cdot b_w \cdot d_{mean.2}} = 0.216$$

Kapasitetskontroll

$$M_{Rd.2} := \left[0.8 \cdot \alpha_{.s} \cdot \left[1 - \left(0.4 \cdot \alpha_{.s}\right)\right] \cdot f_{cd} \cdot b_w \cdot d_{mean.2}^2\right] + \left(A_{s.b.2} \cdot f_{yd.32} \cdot d_{b.x}\right) = 10.454 \cdot 10^3 \cdot kN \cdot m$$

Over støttene er det første snittet dimensjonerende, for resterende snitt vil kapasiteten være noe høyere (men ikke mye).

B.2.3: Snitt 3.1

Bøyemomentkapasitet i felt, mellom støtter og opplager, dvs. snitt 3. Snitt3 har tre forskjellige armeringsmengder mellom støttene, j.fr. tegningene. Her ser vi på de forskjellig armeringsmengde mellom første(og siste) felt i fht til resterende felt.

Første felt: $b_{eff.3} = 4090 \cdot mm$

$h = 1750 \cdot mm$ $\emptyset 32 = 32 \cdot mm$ $\emptyset 22 = 22 \cdot mm$ $b_{eff.2} = 2252.5 \cdot mm$

$b_w = 800 \cdot mm$ $c_{nom.1} = 55 \cdot mm$

$n_{\emptyset 32.1} := 19$ $n_{\emptyset 22.1} := 0$ $n_{tot.1} := n_{\emptyset 32.1} + n_{\emptyset 22.1} = 19$

$A_{\emptyset 32} = 804.248 \cdot mm^2$ $A_{\emptyset 22} = 380.133 \cdot mm^2$

$A_{.s.tot.1} := \left(n_{\emptyset 32.1} \cdot A_{\emptyset 32} \right) + \left(n_{\emptyset 22.1} \cdot A_{\emptyset 22} \right) = 15.281 \cdot 10^3 \cdot mm^2$

$d_{\emptyset 32.1} := 71 mm$ $n_{d.1} := 8$ $d_{\emptyset 32.2} := 136 mm$ $n_{d.2} := 8$ $d_{\emptyset 32.3} := 201 mm$ $n_{d.3} := 3$

$$d_1 := \frac{A_{\emptyset 32} \cdot \left[\left(d_{\emptyset 32.1} \cdot n_{d.1} \right) + \left(d_{\emptyset 32.2} \cdot n_{d.2} \right) + \left(d_{\emptyset 32.3} \cdot n_{d.3} \right) \right]}{A_{.s.tot.1}} = 118.895 \cdot mm$$

$d_{.1} := h - d_1 = 1631.105 \cdot mm$

Underarmert tverrsnitt, og tykk flens:

Krav for å regne flensen som tynn.

$\alpha_{f.1} := \dfrac{f_{yd.32} \cdot A_{.s.tot.1}}{0.8 \cdot f_{cd} \cdot b_{eff.3} \cdot d_{.1}} = 0.065$ $0.8 \cdot \alpha_{f.1} \cdot d_{.1} = 85.432 \cdot mm$

Vår flens er tykkere - OK!

Kapasitetskontroll

$M_{3.Rd.1} := 0.8 \cdot \alpha_{f.1} \cdot \left[1 - \left(0.4 \cdot \alpha_{f.1} \right) \right] \cdot f_{cd} \cdot b_{eff.3} \cdot d_{.1}^2 = 6.66 \cdot 10^3 \cdot kN \cdot m$

B.2.4: Snitt 3.2

Bøyemomentkapasitet i felt mellom støtter, dvs snitt 3:

Snitt 2: $\qquad b_{eff.3} = 4090 \cdot mm$

$h = 1750 \cdot mm \qquad \emptyset 32 = 32 \cdot mm \qquad \emptyset 22 = 22 \cdot mm \qquad b_{eff.2} = 2252.5 \cdot mm$

$b_w = 800 \cdot mm \qquad c_{nom.1} = 55 \cdot mm$

$n_{\emptyset 32.2} := 20 \qquad n_{\emptyset 22.2} := 2 \qquad n_{tot.II} := n_{\emptyset 32.2} + n_{\emptyset 22.2} = 22$

$A_{\emptyset 32} = 804.248 \cdot mm^2 \qquad A_{\emptyset 22} = 380.133 \cdot mm^2$

$A_{.s.tot.2} := \left(n_{\emptyset 32.2} \cdot A_{\emptyset 32} \right) + \left(n_{\emptyset 22.2} \cdot A_{\emptyset 22} \right) = 16.845 \cdot 10^3 \cdot mm^2$

$d_{\emptyset 32.I} := 71mm \qquad n_{d.I} := 8 \qquad d_{\emptyset 32.II} := 136mm \qquad n_{d.II} := 8 \qquad d_{\emptyset 32.III} := 201mm \qquad n_{d.III} := 6$

$d_{\emptyset 22.IV} := 136mm \qquad n_{d.IV} := 2$

$$d_I := \frac{\left[A_{\emptyset 32} \cdot f_{yd.32} \cdot \left[\left(d_{\emptyset 32.I} \cdot 8 \right) + \left(d_{\emptyset 32.II} \cdot 8 \right) + \left(d_{\emptyset 32.III} \cdot 6 \right) \right] \right] + \left(A_{\emptyset 22} \cdot d_{\emptyset 22.IV} \cdot 2 \cdot f_{yd.22} \right)}{\left(n_{\emptyset 32.2} \cdot A_{\emptyset 32} \cdot f_{yd.32} \right) + \left(n_{\emptyset 22.2} \cdot A_{\emptyset 22} \cdot f_{yd.22} \right)}$$

$d_I = 142.882 \cdot mm \qquad d_{mean.I} := h - d_I = 1607.118 \cdot mm$

Underarmert tverrsnitt, og tykk flens:

$$\alpha_{f.2} := \frac{\left[\left(f_{yd.32} \cdot n_{\emptyset 32.2} \cdot A_{\emptyset 32} \right) + \left(f_{yd.22} \cdot n_{\emptyset 22.2} \cdot A_{\emptyset 22} \right) \right]}{0.8 \cdot f_{cd} \cdot b_{eff.3} \cdot d_{mean.I}} = 0.072$$

Krav for å regne flensen som tynn.

$0.8 \cdot \alpha_{f.2} \cdot d_I = 8.249 \cdot mm$

Kapasitetskontroll :

Vår flens er tykkere - OK!

$$M_{3.Rd.2} := 0.8 \cdot \alpha_{f.2} \cdot \left[1 - \left(0.4 \cdot \alpha_{f.2} \right) \right] \cdot f_{cd} \cdot b_{eff.3} \cdot d_{mean.1}^2 = 7.428 \cdot 10^3 \cdot kN \cdot m$$

Det første snittet er dimensjonerende, men midt idet første (og siste) feltet er det også mindre påkjenninger. Begge verdier er relevante for videre analyse.

B.2.5: Snitt 3.3

Bøyemomentkapasitet i siste felt mellom støtter, dvs snitt 3:

Snitt 3: $\quad\quad\quad\quad b_{eff.3} = 4090 \cdot mm$

$h = 1750 \cdot mm \quad\quad \emptyset 32 = 32 \cdot mm \quad\quad \emptyset 22 = 22 \cdot mm \quad\quad b_{eff.2} = 2252.5 \cdot mm$

$b_w = 800 \cdot mm \quad\quad c_{nom.1} = 55 \cdot mm$

$n_{\emptyset 32.3} := 30 \quad\quad\quad n_{\emptyset 22.3} := 0 \quad\quad\quad\quad n_{tot.III} := n_{\emptyset 32.3} + n_{\emptyset 22.3} = 30$

$A_{\emptyset 32} = 804.248 \cdot mm^2 \quad\quad A_{\emptyset 22} = 380.133 \cdot mm^2$

$A_{.s.tot.3} := \left(n_{\emptyset 32.3} \cdot A_{\emptyset 32} \right) + \left(n_{\emptyset 22.3} \cdot A_{\emptyset 22} \right) = 24.127 \cdot 10^3 \cdot mm^2$

$d_{\emptyset 32.I} = 71 \cdot mm \quad n_{d.I.} := 8 \quad d_{\emptyset 32.II} = 136 \cdot mm \quad n_{d.II.} := 8 \quad d_{\emptyset 32.III} = 201 \cdot mm \quad n_{d.III.} := 8$

$d_{\emptyset 32.IV} := 266 mm \quad\quad n_{d.IV.} := 26$

$$d_{I.} := \frac{A_{\emptyset 32} \cdot f_{yd.32} \cdot \left[\left(d_{\emptyset 32.I} \cdot 8 \right) + \left(d_{\emptyset 32.II} \cdot 8 \right) + \left(d_{\emptyset 32.III} \cdot 8 \right) + \left(d_{\emptyset 32.IV} \cdot 6 \right) \right]}{\left(n_{\emptyset 32.2} \cdot A_{\emptyset 32} \cdot f_{yd.32} \right) + \left(n_{\emptyset 22.2} \cdot A_{\emptyset 22} \cdot f_{yd.22} \right)} = 235.535 \cdot mm$$

$d_{I.} = 235.535 \cdot mm \quad\quad d_{mean.I.} := h - d_I = 1607.118 \cdot mm$

Underarmert tverrsnitt, og tykk flens:

$$\alpha_{f.3} := \frac{\left[\left(f_{yd.32} \cdot n_{\emptyset 32.3} \cdot A_{\emptyset 32} \right) + \left(f_{yd.22} \cdot n_{\emptyset 22.3} \cdot A_{\emptyset 22} \right) \right]}{0.8 \cdot f_{cd} \cdot b_{eff.3} \cdot d_{mean.I.}} = 0.105$$

Krav for å regne flensen som tynn.

$0.8 \cdot \alpha_{f.2} \cdot d_{I.} = 13.597 \cdot mm$

Kapasitetskontroll:

Vår flens er tykkere - OK!

$$M_{3.Rd.3} := 0.8 \cdot \alpha_{f.3} \cdot \left[1 - \left(0.4 \cdot \alpha_{f.3} \right) \right] \cdot f_{cd} \cdot b_{eff.3} \cdot \left(d_{mean.I.} \right)^2 = 10.193 \cdot 10^3 \cdot kN \cdot m$$

B.3 Skjærkraft / Skjærarmering (Shear)

Tegninger angir total mengde skjærarmering:

Ved beregning av skjærkraftkapasitet tas hensyn til alle lastvirkninger i tverrsnittet; MEd, NEd og VEd. I eurokode 2 er det to betraktninger. Man har i hht. pkt. 6.2.2 "*konstruksjonsdeler uten beregningsmessig behov for skjærarmering*". Også har man ihht. pkt. 6.2.3 "*konstruksjonsdeler med beregningsmessig behov for skjærarmering*".

Det bør i hht. pkt. 6.2.1(4) velges en minste skjærarmering etter pkt. 9.2.2.

Bøyle $\emptyset 32$ og $\emptyset 22$

B.3.1 Snitt 3.2

$$A_{c.3} := \left(b_{eff.3} \cdot t_f\right) + \left[\left(h - t_f\right) \cdot b_w\right] = 2.321 \times 10^6 \cdot mm^2$$

$$k_{2.1} := 1 + \sqrt{\frac{200\,mm}{d_{mean.1}}} = 1.349 \qquad k_{3.1} := 1 + \sqrt{\frac{200\,mm}{d_{.1}}} = 1.35 \qquad \text{Alle er under 2}$$

$$k_{2.2} := 1 + \sqrt{\frac{200\,mm}{d_{mean.2}}} = 1.346 \qquad k_{3.2} := 1 + \sqrt{\frac{200\,mm}{d_{mean.I}}} = 1.353 \qquad < 2 = OK!$$

$$\rho_{l.2} := \frac{A_{.s.tot.2}}{b_w \cdot d_{mean.I}} = 0.013 \qquad < 0.02 = OK \qquad\qquad k_1 := 0.15 \qquad k_2 := 0.18 \qquad C_{Rd.c} := 0.12$$

Her vil det være konservativt å ta med trykk krefter:

$$N_{Ed} := 0 \qquad \sigma_{cp} := \frac{N_{Ed}}{A_{c.3}} = 0 \qquad < \qquad 0.2 \cdot f_{cd} = 2.4 \cdot \frac{N}{mm^2}$$

Kapasitetskontroll

$$V_{3.2Rd.c} := \left[\left[\frac{N}{mm^2} \cdot C_{Rd.c} \cdot k_{3.2} \cdot \left(100 \cdot \rho_{l.2} \cdot \frac{f_{ck}}{\frac{N}{mm^2}}\right)^{\frac{1}{3}}\right] + \left(k_1 \cdot \sigma_{cp}\right)\right] \cdot b_w \cdot d_{mean.I}$$

$$V_{3.2Rd.c} = 584.914 \cdot kN$$

$$v_{min.2} := 0.035 \cdot \left(k_{3.2}\right)^{\frac{3}{2}} \cdot \left(\frac{f_{ck}}{\frac{N}{mm^2}}\right)^{\frac{1}{2}} \cdot \frac{N}{mm^2} = 0.226 \cdot \frac{N}{mm^2}$$

$$V_{3.2Rd.c.min} := \left[v_{min.2} + \left(k_1 \cdot \sigma_{cp}\right)\right] \cdot b_w \cdot d_{mean.I} = 290.199 \cdot kN$$

$$V_{3.Rd.c} := max\left(V_{3.2Rd.c}, V_{3.2Rd.c.min}\right) = 584.914 \cdot kN$$

B.3.2 Snitt 3.1:

$A_{c.3} = 2.321 \times 10^6 \cdot \text{mm}^2$

$k_{2.1} = 1.349$ $k_{3.1} = 1.35$

$k_{2.2} = 1.346$ $k_{3.2} = 1.353$

$\rho_{l.1} := \dfrac{A_{.s.tot.1}}{b_w \cdot d_{mean.I}} = 0.012$ $< 0.02 = \text{OK}$ $k_1 = 0.15$ $k_2 = 0.18$ $C_{Rd.c} = 0.12$

$N_{Ed} = 0$ $\sigma_{cp} = 0$ $<$ $0.2 \cdot f_{cd} = 2.4 \cdot \dfrac{N}{\text{mm}^2}$

Kapasitetskontroll

$$V_{3.1Rd.c} := \left[\left[\frac{N}{\text{mm}^2} \cdot C_{Rd.c} \cdot k_{3.2} \cdot \left(100 \cdot \rho_{l.2} \cdot \frac{f_{ck}}{\frac{N}{\text{mm}^2}} \right)^{\frac{1}{3}} \right] + \left(k_1 \cdot \sigma_{cp} \right) \right] \cdot b_w \cdot d_{.1}$$

$V_{3.1Rd.c} = 593.644 \cdot \text{kN}$

$$v_{min.1} := 0.035 \cdot \left(k_{3.1} \right)^{\frac{3}{2}} \cdot \left(\frac{f_{ck}}{\frac{N}{\text{mm}^2}} \right)^{\frac{1}{2}} \cdot \frac{N}{\text{mm}^2} = 0.225 \cdot \frac{N}{\text{mm}^2}$$

$V_{3.1Rd.c.min} := \left[v_{min.1} + \left(k_1 \cdot \sigma_{cp} \right) \right] \cdot b_w \cdot d_{.1} = 293.681 \cdot \text{kN}$

$V_{3.1.Rd.c} := \max\left(V_{3.1Rd.c} , V_{3.1Rd.c.min} \right) = 1 \cdot V_{3.1Rd.c}$

XX

B.3.3 Snitt 2.1

$$A_{c.2} := \left(b_{eff.2} \cdot t_f\right) + \left[\left(h - t_f\right) \cdot b_w\right] = 1.807 \times 10^6 \cdot mm^2$$

$$k_{2.1} = 1.349 \qquad\qquad k_{3.1} = 1.35$$

$$k_{2.2} = 1.346 \qquad\qquad k_{3.2} = 1.353$$

$$\rho_{l.l} := \frac{A_{s.bunn.1}}{b_w \cdot d_1} = 0.11 \qquad\qquad < 0.02 = OK!$$

$$k_1 = 0.15 \qquad k_2 = 0.18 \qquad C_{Rd.c} = 0.12$$

$$N_{Ed} = 0 \qquad \sigma_{cp} = 0 \qquad < \qquad 0.2 \cdot f_{cd} = 2.4 \cdot \frac{N}{mm^2}$$

Kapasitetskontroll

$$V_{2.1Rd.c} := \left[\left[\left[\frac{N}{mm^2} \cdot C_{Rd.c} \cdot k_{2.1} \cdot \left(100 \cdot \rho_{l.l} \cdot \frac{f_{ck}}{\frac{N}{mm^2}}\right)^{\frac{1}{3}}\right] + \left(k_1 \cdot \sigma_{cp}\right)\right] \cdot b_w \cdot d_{mean.1}$$

$$V_{2.1Rd.c} = 1211.595 \cdot kN$$

$$v_{min.2.1} := 0.035 \cdot \left(k_{2.1}\right)^{\frac{3}{2}} \cdot \left(\frac{f_{ck}}{\frac{N}{mm^2}}\right)^{\frac{1}{2}} \cdot \frac{N}{mm^2} = 0.225 \cdot \frac{N}{mm^2}$$

$$V_{2.1Rd.c.min} := \left[v_{min.2.1} + \left(k_1 \cdot \sigma_{cp}\right)\right] \cdot b_w \cdot d_{mean.1} = 295.41 \cdot kN$$

$$V_{2.1.Rd.c} := max\left(V_{2.1Rd.c}, V_{2.1Rd.c.min}\right) = 1 \cdot V_{2.1Rd.c}$$

B.3.4 Snitt 2.2

$A_{c.2} = 1.807 \times 10^6 \cdot mm^2$

$k_{2.1} = 1.349$ $k_{3.1} = 1.35$

$k_{2.2} = 1.346$ $k_{3.2} = 1.353$

$\rho_{I.II} := \dfrac{A_{s.strekk.2}}{b_w \cdot d_1} = 0.144$ $< 0.02 = OK!$

$k_1 = 0.15$ $k_2 = 0.18$ $C_{Rd.c} = 0.12$

$N_{Ed} = 0$ $\sigma_{cp} = 0$ $<$ $0.2 \cdot f_{cd} = 2.4 \cdot \dfrac{N}{mm^2}$

Kapasitetskontroll

$$V_{2.2Rd.c} := \left[\left[\frac{N}{mm^2} \cdot C_{Rd.c} \cdot k_{2.2} \cdot \left(100 \cdot \rho_{I.II} \cdot \frac{f_{ck}}{\frac{N}{mm^2}}\right)^{\frac{1}{3}}\right] + \left(k_1 \cdot \sigma_{cp}\right)\right] \cdot b_w \cdot d_{mean.2}$$

$V_{2.2Rd.c} = 1346.915 \cdot kN$

$$v_{min.2.2} := 0.035 \cdot \left(k_{2.2}\right)^{\frac{3}{2}} \cdot \left(\frac{f_{ck}}{\frac{N}{mm^2}}\right)^{\frac{1}{2}} \cdot \frac{N}{mm^2} = 0.224 \cdot \frac{N}{mm^2}$$

$V_{2.2Rd.c.min} := \left[v_{min.2.2} + \left(k_1 \cdot \sigma_{cp}\right)\right] \cdot b_w \cdot d_{mean.2} = 299.946 \cdot kN$

$V_{2.2.Rd.c} := max\left(V_{2.2Rd.c}, V_{2.2Rd.c.min}\right) = 1 \cdot V_{2.2Rd.c}$

B.3.5 Skjærkapasitet med *skrå* skjærarmering, snitt 2.1:

$$V_{Rd.s} := \frac{A_{sv}}{s} \cdot z \cdot f_{ywd} \cdot (\cot(\theta) + \cot(\alpha)) \cdot \sin(\alpha) \qquad \text{Eq(6.13)}$$

$$A_{sv.2.1} := 2412 \, mm^2 \qquad s_{2.1} := 1000 \, mm \qquad z_{2.1} := 0.9 \cdot d_{mean.1} = 1478.728 \cdot mm$$

$$\theta_{2.1} := 60 \, deg \qquad \alpha_{2.1} := 45 \, deg \qquad f_{ywd} := f_{yd.32} = 274.4 \cdot \frac{N}{mm^2}$$

$$V_{Rd.s.2.1} := \frac{A_{sv.2.1}}{s_{2.1}} \cdot z_{2.1} \cdot f_{ywd} \cdot \left(\cot\left(\theta_{2.1}\right) + \cot\left(\alpha_{2.1}\right)\right) \cdot \sin\left(\alpha_{2.1}\right) = 1091.598 \cdot kN$$

Ekstra bøyler over støtter, med Ø13 bidrar:

$$A_{sw} := 2 \cdot \pi \cdot \left(\frac{13mm}{2}\right)^2 = 265.465 \cdot mm^2 \qquad s_{13} := 175 \, mm \qquad z_{2.1} = 1478.728 \cdot mm$$

$$V_{Rd.s.\varnothing 13} := \frac{A_{sw}}{s_{13}} \cdot z_{2.1} \cdot f_{ywd} \cdot \cot\left(\theta_{2.1}\right) = 355.37 \cdot kN$$

$$V_{Rd.tot.2.1} := V_{2.1.Rd.c} + V_{Rd.s.2.1} + V_{Rd.s.\varnothing 13} = 2658.563 \cdot kN$$
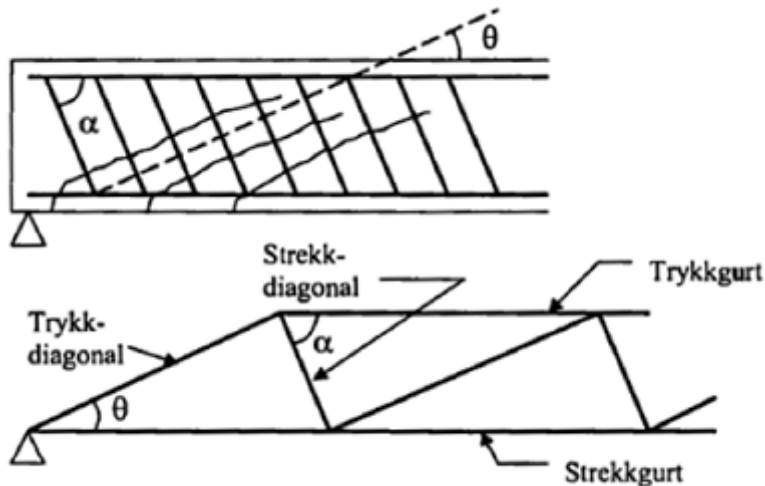

Figure B.1: Illustration of the strut-and-tie model for shear links, from Sørensen(2011)

B.3.6 Skjærkapasitet med *skrå* skjærarmering, snitt 2.2:

$A_{sv.2.2} := 2412\,mm^2$ $s_{2.2} := 1000\,mm$ $z_{2.2} := 0.9 \cdot d_{mean.2} = 1506.929 \cdot mm$

$\theta_{2.2} := 60\,deg$ $\alpha_{2.2} := 45\,deg$ $f_{ywd} = 274.4 \cdot \dfrac{N}{mm^2}$

$V_{Rd.s.2.2} := \dfrac{A_{sv.2.2}}{s_{2.2}} \cdot z_{2.2} \cdot f_{ywd} \cdot \left(\cot(\theta_{2.2}) + \cot(\alpha_{2.2})\right) \cdot \sin(\alpha_{2.2}) = 1112.417 \cdot kN$

Ekstra bøyler over støtter, med Ø13 bidrar: $A_{sw} = 265.465 \cdot mm^2$ $s_{13} = 175 \cdot mm$

$z_{2.2} = 1506.929 \cdot mm$ $V_{Rd.s.\emptyset 13} = 355.37 \cdot kN$

$V_{Rd.tot.2.2} := V_{2.2.Rd.c} + V_{Rd.s.2.2} + V_{Rd.s.\emptyset 13} = 2814.701 \cdot kN$

B.3.7 Max skjærkraftkapasitet

$\alpha_{c.w} := 1 + \left(\dfrac{\sigma_{cp}}{f_{cd}}\right) = 1$ $b_w = 800 \cdot mm$ $z_{2.1} = 1478.728 \cdot mm$ $\nu_1 := 0.6$

$V_{Rd.max.13} := \alpha_{c.w} \cdot b_w \cdot z_{2.1} \cdot \nu_1 \cdot \dfrac{f_{cd}}{\left(\cot(\theta_{2.1}) + \tan(\theta_{2.1})\right)} = 3688.173 \cdot kN$

$V_{Rd.max} := \alpha_{c.w} \cdot b_w \cdot z_{2.1} \cdot \nu_1 \cdot f_{cd} \cdot \dfrac{\left(\cot(\theta_{2.1}) + \cot(\alpha_{2.1})\right)}{\left[1 + \left(\cot(\theta_{2.1})\right)^2\right]} = 10.076 \cdot 10^3 \cdot kN$

B.3.8 Skjærkraftkapasitet uten bidrag fra betongtverrsnittet

$V_{Rd.red.1} := V_{Rd.s.2.1} + V_{Rd.s.\emptyset 13} = 1446.967 \cdot kN$

$V_{Rd.red.2} := V_{Rd.s.2.2} + V_{Rd.s.\emptyset 13} = 1467.786 \cdot kN$

B.4 Capacities over the critical section

Taking the effective width of the flanges for the T-beam section over the supports.

$b_{eff.support} := 2252\,mm$ $b_w = 800 \cdot mm$ $h_{plate} := 280\,mm$ $h_{beams} := 1430\,mm$

$h := h_{plate} + h_{beams} = 1710 \cdot mm$ $c_{nom} := 55mm + \dfrac{32}{2}mm = 71 \cdot mm$

$d_{crack} := h - c_{nom} = 1.639\,m$ $f_{cd} = 12 \cdot \dfrac{N}{mm^2}$ $f_{yd} := \dfrac{f_{yk.32}}{1.25} = 274.4 \cdot \dfrac{N}{mm^2}$

Over the cracked section, the reinforcement drawing shows a longitudinal reinforcement of 3 Ø32 bars in the lower edge of the beam.

$A_{Ø32} = 804.248 \cdot mm^2$ $A_{s.crack} := 3 \cdot A_{Ø32} = 2412.743 \cdot mm^2$

$t := h_{plate}$

$M_{Rd} := f_{yd} \cdot A_{s.crack} \cdot \left(d_{crack} - \dfrac{t}{2}\right) = 992.423 \cdot kN \cdot m$

Over the support closest to the cracked section, the last column-row on the north side.

$A_{s.tension} := 30428\,mm^2$ $A_{s.compression} := 15276\,mm^2$

$d := 1600\,mm$ $d_c := 1500\,mm$

$\alpha_c := \dfrac{\left(A_{s.tension} \cdot f_{yd}\right) - \left(A_{s.compression} \cdot f_{yd}\right)}{0.8 \cdot b_w \cdot d \cdot f_{cd}} = 0.338$

$M_{Rd.cr} := \left[0.8 \cdot \alpha_c \cdot \left[1 - \left(0.4 \cdot \alpha_c\right)\right] \cdot f_{cd} \cdot b_w \cdot d^2\right] + \left(A_{s.compression} \cdot f_{yd} \cdot d_c\right) = 12.04 \cdot 10^3 \cdot kN \cdot m$

Higher capacity than the other supports.

APPENDIX C

Expansion strains and temperature

XXVIII

C Elongation due to temperature

The coeffisient for linear temperature expansion α_T is taken from the Eurocode 2

[NS-EN 1992-1-1 Section 3.1.3(5)].

For Elgeseter Bridge, the elongation of the bridge deck is known, and the formulas are therefore altered to give the temperature needed for the elongation for the analysis.
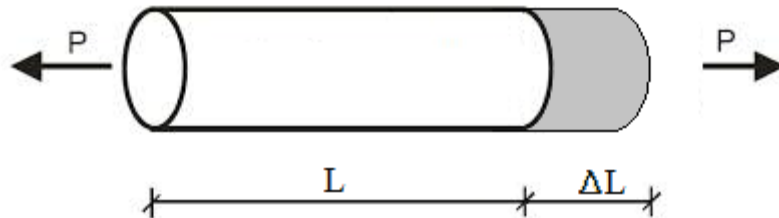

Figure C.1: Elongation of a homogenous bar.

$$\sigma_t := E_{c.l} \cdot \varepsilon_t \blacksquare \qquad \text{pga temperatur:} \quad \Delta_L := \alpha_c \cdot L_0 \cdot \Delta_T \blacksquare \qquad \varepsilon_t := \frac{\Delta_L}{L_0 + \Delta_L} = \blacksquare \cdot \frac{\alpha_c \cdot L_0 \cdot \Delta_T}{L_0 + \left(\alpha_c \cdot L_0 \cdot \Delta_T\right)} \blacksquare$$

$$\Delta_L := 100mm \qquad \alpha_c := 10\frac{m}{m \cdot K} \cdot 10^{-6} \qquad L_0 := 200m \qquad \Delta_T := \frac{\Delta_L}{\alpha_c \cdot L_0} = 50K$$

$$\varepsilon_t := \frac{\Delta_L}{L_0 + \Delta_L} = 0.5 \cdot 10^{-3}$$

Stresses: $\qquad \sigma_c := \frac{F_t}{A_c} = \blacksquare \cdot E_{c.l} \cdot \varepsilon_t \qquad$ And forces: $\qquad F_t := E_{c.l} \cdot \varepsilon_t \cdot A_c \blacksquare$

The formulas for elongation are for the basic situation of elongating a single element. Elgeseter Bridge has several constraints, both in longitudinal and horizontal direction, which would make the calculation quite elaborate and detailed. The elongation and expansion values are not accurate to the extent that these equations would render the accurate answer. The elongation of the bridge is therefore simplified to give an estimate that is accurate enough.

C.1 Elongation due to temperature

Equation for equilibrium with expansion force is as follows:

$$\sigma_1 \cdot A_1 + \sigma_2 \cdot A_2 = \blacksquare \cdot 0^\blacksquare \qquad N := 0$$

$$E_1 \left(\varepsilon - \alpha_T \cdot \Delta T \right) \cdot A_1 + \varepsilon \cdot E_2 \cdot A_2 = \blacksquare \cdot 0^\blacksquare$$

$$E_1 \cdot \varepsilon \cdot A_1 - \left(E_1 \cdot \alpha_T \cdot \Delta T \cdot A_1 \right) + \varepsilon \cdot E_2 \cdot A_2 = \blacksquare \cdot 0^\blacksquare$$

$$\varepsilon := \frac{E_1 \cdot A_1 \cdot \alpha_T \cdot \Delta T}{E_1 \cdot A_1 + E_2 \cdot A_2}^\blacksquare$$

$$\sigma_1 := E_1 \cdot \left[\varepsilon - \left(\alpha_T \cdot \Delta T \right) \right]^\blacksquare \qquad \sigma_2 := E_2 \cdot \varepsilon_2^\blacksquare$$

For the ability to look at the bridge deck to expand alone, or the bridge deck and external beams to expand (but not the inner beams), it is necessary to divide the materials with each separate measures of area and elasticity (Young's modulus).

The cross-sectional area of the bridge deck and beams are already calculated, when deriving the self-weight of the construction.

$$A_{bridge.deck} := 6.822 \cdot 10^6 \, mm^2 \qquad A_{beam} := 800 \cdot 1430 \, mm^2 \qquad A_{4beams} := 4 \cdot A_{beam} = 4.576 \times 10^6 \cdot mm^2$$

$$A_{external.beams} := 2 \cdot A_{beam} = 2.288 \times 10^6 \cdot mm^2 \qquad A_{inner.beams} := 2 \cdot A_{beam} = 2.288 \times 10^6 \cdot mm^2$$

Ratio between the area of the bridge deck and beams

$$\frac{A_{bridge.deck}}{A_{4beams}} = 1.491 \qquad \frac{A_{bridge.deck} + A_{external.beams}}{A_{inner.beams}} = 3.982$$

The Young's modulus is dependent on the material factors for the concrete in the elements. Bridge deck and beams are all made from the same concrete mix, and will have the same characteristics of material parameters.

$$E_{ck.bridge} := 9500 \cdot (20)^{0.3} \frac{N}{mm^2} = 23.336 \, 10^3 \frac{N}{mm^2}$$

$$E_{c.long.term} := \frac{E_{cm}}{1 + \varphi}^\blacksquare \qquad E_{c.long.term} := \frac{E_{ck.bridge}}{1 + 2} = 7778.777 \frac{N}{mm^2}$$

XXX

APPENDIX D

Crack width estimations, plastic bending moment and hinge calculations.

D.1 Crack width estimations

The crack occurs due to self weight and strain from the ASR.

Firstly, the assumptions for the crack width is calculated.

If the crack is propogated from the ASRs effect on the concrete, the strain experienced by the elongation kan be seen in connection with the angle of rotation. The expansion being considered as a temperatur gradient, with the top having greater expansion.

$$h_{beam} := 1430 mm \qquad h_{plate} := 280 mm \qquad h_{tot} := h_{beam} + h_{plate} = 1.71 m$$

$$L_{span} := 22.5 m \qquad L_{crack} := 5m \qquad L_1 := L_{span} - L_{crack} = 17.5 m \qquad L_2 := L_{crack} = 5 m$$

Curvature $\qquad \kappa := \dfrac{\varepsilon_0}{h}^{\blacksquare} \qquad$ Curvature equal for each side of the crack.

The calculations are simplified to look at the one specific span that is relevant.

The length of span is 22.5 metres. The longest length from one support to the crack is L_1, and the shortest length is L_2.

$$\theta_1 := \left(\frac{\varepsilon_0}{h} \cdot L_1 \right) + \left(\frac{\varepsilon_0}{h} \cdot L_2 \right) = \blacksquare \cdot \varepsilon_0 \cdot \left(\frac{L_1}{h} + \frac{L_2}{h} \right)^{\blacksquare}$$

The angle of rotation can be defined by:

Crack width: $\qquad w := \theta \cdot h = \blacksquare \cdot \left[\left(\frac{\varepsilon_0}{h} \cdot L_1 \right) + \left(\frac{\varepsilon_0}{h} \cdot L_2 \right) \right]^{\blacksquare} \cdot h \qquad w := \varepsilon_0 \cdot \left(L_1 + L_2 \right)^{\blacksquare}$

The crack can be described by the geometric assumptions which leads to: $w = \theta * h$

The crack width for the relevant section is known, inspections from the bridge shows crack width of up to 6 mm (Rapp., Aas-J.), which would yield following strains:

$$w := 6 mm \qquad h := h_{beam} + \frac{h_{plate}}{2}$$

$$\varepsilon_{0.} := \frac{w}{\left(L_1 + L_2 \right)} = 0.267 \cdot 10^{-3} \qquad \qquad \text{The strains need to be 0.267‰ in order to drive the reaction to this crack width.}$$

D.2 Plastic hinge estimation

The assumptions for the plastic hinge situation, is that only self-weight and the strains from the expansion due to ASR has propagated the yield situation.

The self-weight generates 365 kNm on the area where the crack occurs, i.e. 5 metres out from the support. The moment due to the curvature can be assessed by looking at the yield situation. When the concrete cracks and the plastic hinge forms, the only load bearing capacity comes from the reinforcement.

$$M_{Rd.s} := f_{sd} \cdot A_{S.rel} \cdot \left(d_{rel} - \frac{t}{2} \right)^{\blacksquare}$$

In the location of the crack, there is only 3 reinforcement bars in longitudinal direction.

$$\varnothing_{32} := \pi \cdot \left(\frac{32}{2} mm \right)^2 = 804.248\,mm^2 \qquad A_{S.rel} := 3 \cdot \varnothing_{32} = 2412.743 \cdot mm^2$$

$$f_{sd} := \frac{343 \dfrac{N}{mm^2}}{1.25} = 274.4 \dfrac{N}{mm^2} \qquad d_{rel} := h_{tot} - \left(55mm + \frac{32mm}{2} \right) = 1.639m$$

Assuming the three reinforcement bars left are in the lowest positioning in the cross-section. (C_{nom}= 55 mm)

$$t := h_{plate}$$

$$M_p := f_{sd} \cdot A_{S.rel} \cdot \left(d_{rel} - \frac{t}{2} \right) = 992.423\,kN \cdot m$$

Bending moment due to self-weight is calculated in the frame model, to be:

$$M_{g.d} := 365kN \cdot m$$

The bending moments needed to occur due to the ASR, in order to form the plastic hinge is then:

$$M_{nødv} := M_p - M_{g.d} = 627.423\,kN \cdot m \qquad M := \theta \cdot EI^{\blacksquare}$$

$$M_{nødv} := \theta_{nødv} EI_{II}^{\blacksquare} \qquad \theta_{nødv} := \frac{EI_{II}^{\blacksquare}}{M_{nødv}}$$

XXXIV